

The role of specific microbial communities in the biological carbon pump

Dissertation
Zur Erlangung des Grades eines
Doktors der Naturwissenschaften
- Dr. rer. nat. -

Dem Fachbereich Biologie/ Chemie
der Universität Bremen

vorgelegt von

Stefan Thiele

Bremen, April 2013

Die vorliegende Arbeit wurde von November 2009 bis April 2013 am Max-Planck-Institut für marine Mikrobiologie in Bremen angefertigt.

1. Gutachter: Prof. Dr. Rudolf I. Amann
2. Gutachter: Prof. Dr. V. Smetacek

1. Prüfer: PD Dr. Bernhard M. Fuchs
2. Prüfer: Prof. Dr. Ulrich Fischer

Tag des Promotionskolloquiums: 16.5.2013

“Give me a half tanker of iron, and I will give you an ice age”

John Martin

Abstract

Oceans cover ~70% of the Earth's surface and are the second largest global carbon reservoir. Major processes in marine carbon cycling are summarized in the biological carbon pump. Within the biological carbon pump, pivotal stages are the microbial loop and aggregate related processes. Within the surface layer and on aggregates, carbon is channelled within a complex food web based on microbial processes. These processes counteract the biological carbon pump, showing the importance of the microbial loop for carbon sequestration.

During the iron fertilization experiment LOHAFEX, a phytoplankton bloom of nano- and picoplankton was induced in the South Atlantic. We used catalyzed reporter deposition fluorescence *in situ* hybridization (CARD FISH) and 454 tag pyrosequencing to investigate the bacterial and archaeal community response to this bloom. The bacterial and archaeal community was stable over the course of the experiment and only members of the SAR11 and SAR86 clades showed elevated cell numbers. This led to the hypothesis of a top-down control exerted by a community of nano- and picoplankton grazers. Consequently, we used the same techniques to investigate the nano- and picoplankton community during the LOHAFEX experiment. We discovered a stable community with high but constant abundance of *Phaeocystis*, the major bloom forming organism, and a short peak of *Micromonas* and *Pelagophyceae* after the second iron fertilization. This again led to the hypothesis of a strong top-down control and a tight coupling of the microbial loop.

We investigated the bacterial community on aggregates at different depth from the Canary Current Upwelling system. A free drifting sediment trap was used to sample aggregates *in situ* at 100 m and 400 m depth. We used a three dimensional FISH approach to quantify the bacterial community. *Synechococcus* dominated the bacterial community on marine snow at both depths, while *Bacteroidetes* and *Alteromonas* abundance significantly decreased with depth. We hypothesize a change in the bacterial community due to a combined effect of changes in nutrient quality due to degradation processes, grazing, decreasing temperature and increasing pressure.

In summary, a strong top-down control was exerted on the bacterial and archaeal, and the nano- and picoplankton community, indicating a tight coupling of the microbial loop during the iron fertilizing experiment LOHAFEX. Marine snow investigations off Cape Blanc showed that *Bacteroidetes* and *Alteromonas* dominated the bacterial community but decreased with depth, indicating a nutrient quality, grazer, pressure and temperature dependent community composition.

Zusammenfassung

Ozeane bedecken ~70% der Erdoberfläche und sind das weltweit zweitgrößte Kohlenstoffreservoir. Grundlegende Prozesse im marinen Kohlenstoffzyklus sind zusammengefasst als „Biologische Kohlenstoffpumpe“. Die zentralen Abschnitte innerhalb dieses Systems sind der „Mikrobielle Kreislauf“ und Prozesse in Verbindung mit Aggregaten. Im Oberflächenwasser wird Kohlenstoff, in einem auf mikrobiologischen Prozessen beruhenden Nahrungsnetz zirkuliert. Diese Prozesse wirken antagonistisch zu der Biologischen Kohlenstoffpumpe und deuten auf die Wichtigkeit des Mikrobiellen Kreislaufs bei der Kohlenstoffsequestrierung hin.

Während des Eisendüngungsexperiments LOHAFEX wurde im Südatlantik eine Phytoplanktonblüte, bestehend aus Nano- und Picoplankton, erzeugt. Wir verwendeten Fluoreszenz *in situ* Hybridisierung mit enzymatisch markierten Oligonukleotiden und Tyramidsignalverstärkung (CARD FISH) und 454 Pyrosequenzierung um das Verhalten der bakteriellen und archaeellen Gemeinschaft auf die Phytoplanktonblüte zu untersuchen.

Die Gemeinschaft war konstant während der gesamten Dauer des Experiments und nur Angehörige der SAR11 und SAR86 Gruppen zeigten erhöhte Zellzahlen. Das führte zu der Hypothese einer übergeordneten Kontrolle durch eine Gemeinschaft von Nano- und Picoplankton Prädatoren. In der Folge benutzten wir die gleichen Techniken, um die Nano- und Picoplankton Gemeinschaft während des LOHAFEX Experiments zu untersuchen. Wir entdeckten eine konstante Gemeinschaft mit hoher, aber gleichförmiger Abundanz des Hauptblütenbildners *Phaeocystis* und ein kurzes Maximum von *Micromonas* und *Pelagophyceae* nach der zweiten Eisendüngung. Dies führte wiederum zu der Hypothese einer starken übergeordneten Kontrolle und einer engen Koppelung des Mikrobiellen Kreislaufs.

Wir untersuchten die bakterielle Gemeinschaft auf marinem Schnee in verschiedenen Tiefen im Kanarischen Auftriebssystem. Eine frei treibende Sedimentfalle wurde benutzt um die Aggregate *in situ* auf 100 m und 400 m Tiefe zu sammeln. Wir benutzten eine dreidimensionale FISH Methode um die bakterielle Gemeinschaft auf den Aggregaten zu quantifizieren. *Synechococcus* dominierte die bakterielle Gemeinschaft auf marinem Schnee in beiden Tiefen, während die Abundanz von *Bacteroidetes* und *Alteromonas* signifikant mit der Tiefe abnahmen. Wir vermuten, dass die Veränderung der bakteriellen Gemeinschaft durch die Veränderung der Nährstoffqualität durch Abbauprozesse, Predation, steigendem Druck und sinkenden Temperaturen ausgelöst wird.

Zusammenfassend wurde eine starke übergeordnete Kontrolle sowohl auf die bakterielle und archaeelle Gemeinschaft, als auch auf die Nano- und Picoplankton Gemeinschaft ausgeübt, welche auf eine starke Kupplung des Mikrobiellen Kreislaufs während des Eisendüngungs-experiments LOHAFEX hinweist. Untersuchungen des marinen Schnees vor Cape Blanc zeigten das *Bacteroidetes* und *Alteromonas* die bakterielle Gemeinschaft dominierten, aber in der Tiefe abnehmen, was eine Veränderung der Gemeinschaft abhängig von der Nährstoffqualität, Prädation, Druck und Temperatur andeutet.

Abbreviations

ACMEtool	Automated cell measuring and enumeration tool
ANME	Anaerobic methanotroph
ARISA	Automated ribosomal intergenic spacer analyses
ATP	Adenosine-5'-triphosphate
CARD	Catalyzed reporter deposition
CLSM	Confocal laser scanning microscopy
DGGE	Denaturing gradient gel electrophoresis
DIC	Dissolved inorganic carbon
DMSP	Dimethylsulfoniopropionate
DOC	Dissolved organic carbon
DOM	Dissolved organic matter
EBUS	Eastern boundary upwelling system
EisenEx	Eisendüngungsexperiment (Iron fertilization experiment)
EPS	Exopolymeric substances
FACS	Fluorescence-activated cell sorting
FeX	Iron fertilization experiment
FISH	Fluorescence <i>in situ</i> hybridization
FRRF	Fast repetition rate fluorometry
FT-ICR-MS	Fourier-transform ion cyclotron resonance mass spectrometer
GC-MS	Gas chromatography - mass spectrometry
HISH	Halogen <i>in situ</i> hybridization
HNLC	High nutrient low chlorophyll
HSi	High silicate
LOHAFEX	Loha = iron (Hindi) fertilization experiment
LSi	Low silicate
PHLIP	Phobia laser scanning microscopy imaging processor
POC	Particulate organic carbon
POM	Particulate organic matter
RCA	<i>Roseobacter</i> clade affiliated
rRNA	Ribosomal ribonucleic acid

ROV	Remotely operated vehicle
SAGE	The SOLAS air gas exchange experiment
SEEDS	Subarctic Pacific iron experiment for ecosystem dynamics study
SERIES	Subarctic ecosystem response to iron enrichment study
SEM	Scanning electron microscopy
SIMS	Secondary ion mass spectrometry
SOFeX	Southern Ocean iron experiments
SOIREE	Southern Ocean iron release experiment
SSU	Small subunit
TCC	Total cell count
TEP	Transparent exopolymeric particles
T-RFLP	Terminal restriction fragment length polymorphism

Table of Content

1. Introduction1

1.1. The carbon-cycle1

1.2. The marine carbon cycle.....2

 1.2.1. Methane2

 1.2.2. Carbon dioxide3

1.3. The biological carbon pump.....4

1.4. Surface layer processes5

1.5. The microbial loop6

 1.5.1. Microbial loop vs. classical food chain6

 1.5.2. Additional phototrophic bacteria.....7

 1.5.3. Grazing and viral lysis – short cuts in the microbial loop.....7

1.6. Aggregation formation.....9

 1.6.1. Aggregate size and abundance9

 1.6.2. Physical factors mediate particle collision9

 1.6.3. Chemical factors of aggregate formation10

 1.6.4. Biological mediated aggregate formation11

 1.6.5. Aggregate composition11

1.7. Aggregate colonization.....12

 1.7.1. Factors of colonization12

 1.7.2. Bacterial abundance and community structure13

 1.7.2. Eukaryotic communities on aggregates.....14

1.8. Aggregate degradation.....14

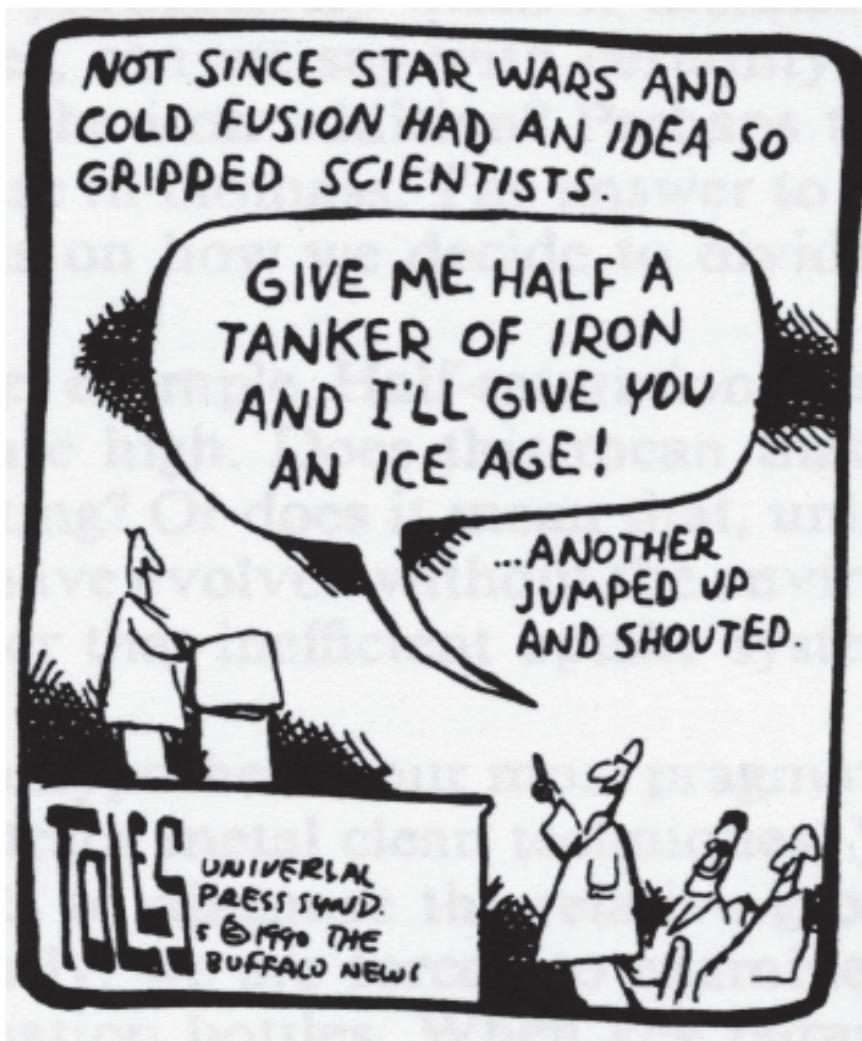
1.9. Sinking velocities and the efficiency of the biological carbon pump16

Table of Content

1.10. Phytoplankton blooms	17
1.10.1. Bloom forming organisms.....	17
1.10.2. Nano- and picoplankton communities during phytoplankton blooms	18
1.10.3. Bacterial and archaeal community response during phytoplankton blooms	20
1.11. Iron fertilization experiments	21
1.11.1. Iron – limiting factor in the open ocean	21
1.11.2. Iron fertilization experiments	21
1.11.3. The role of silicate.....	22
1.11.4. Bacterial and archaeal response to iron fertilization	23
1.11.5. Thesis project I – Investigation of the bacterial and archaeal community response to iron fertilization during LOHAFEX.....	24
1.11.6. Thesis project II – Investigation of the nano- and picoplankton community response to iron fertilization during LOHAFEX.....	25
1.12. The bacterial community of sinking aggregates.....	25
1.12.1. The Eastern Boundary Upwelling Systems (EBUS).....	26
1.12.2. Changes of the aggregate attached bacterial community with depth	26
1.12.3. Thesis project III – Investigation of the bacterial community on marine snow aggregates and TEP structures at two different depths from the Canary Current Upwelling.....	27
2. Methods	29
3. Aims	31
3.1. General objective.....	31
3.2. Specific objectives.....	31
4. Manuscripts	33
Manuscript I	35

Manuscript II	39
Manuscript III	72
5. General discussion	116
5.1. The microbial loop during the LOHAFEX experiment	116
5.1.1. Assessment of molecular tools for nano- and picoplankton analyses	118
5.2. The bacterial community on marine snow aggregates at different depth	120
5.2.1. A novel approach to investigate bacterial communities on aggregates.....	121
5.3. Implications for the carbon pump	123
6. Outlook	124
6.1. Next generation iron fertilization	124
6.2. Experimental setting	125
6.2.1 The microbial loop in a nano- and picoplankton bloom	126
6.2.2. Investigation of POC in a diatom bloom.....	129
6.3. Future perspectives in iron fertilization	131
7. References	134
Appendix	166
Appendix A	168
Appendix B	172
Appendix C	176
Acknowledgement	180

And so it all began...



John Martin, 1988

1. Introduction

1.1. The carbon-cycle

The major reservoir of carbon is the Earth's interior, where >75,000,000 Gt of carbon are stored (FIG 1; Falkowski et al. 2000). By geological activities annually about 0.13 to 0.44 Gt carbon dioxide (CO₂) are released into the atmosphere (Gerlach 1991, 2011; Marty and Tolstikhin 1998). The atmosphere is a relatively small reservoir for carbon, holding about 750 Gt (FIG 1; Falkowski et al. 2000). Here, carbon is present mainly in the form of CO₂ and methane (CH₄) and methane is converted into CO₂ by hydroxyl radicals (Bekki et al. 1994). The atmospheric CO₂ can solve in water, such as rain drops but also the oceans (Sarmiento and Quéré 1996; Broecker 1997), or can be converted into biomass by photosynthesis.

Within the terrestrial biosphere between 600 – 1000 Gt carbon are in the living biomass and about 1200 Gt in dead biomass (FIG 1; Falkowski et al. 2000). Most of the biomass can be found in the soil, such as soil fauna and flora, but also fossil fuels. Carbon is released into the atmosphere mainly by respiration processes. This release is in near equilibrium with the uptake and storage of carbon. Since the beginning of the industrial age anthropogenic activities, like fossil fuel combustion, cement production, deforestation, and the burning of biomass led to an additional release of CO₂ into the atmosphere (Andreae and Merlet 2001; Houghton 2003; van der Werf et al. 2004; Forster et al. 2007). This additional release was estimated to 7.8 Gt CO₂ per year in 2005 (Forster et al. 2007). This anthropogenic CO₂ release influences the carbon cycle by increasing the atmospheric CO₂ concentration from 220 ppm in the pre industrial age (Sage 1995) to 395.1 ppm in January 2013 (NOAA, Mauna Loa recent global CO₂ data, 10th April 2013). The resulting disequilibrium will increase the global greenhouse effect and lead to an acceleration of global warming (Cox et al. 2000).

Due to the size of the oceans and their carbon storage capacity, the marine carbon cycle is of pivotal importance in global warming discussions. An estimated of 38,400 Gt of carbon are stored in the ocean (FIG 1; Falkowski et al. 2000), a major part of it (~97%) in an inorganic state, as dissolved inorganic carbon (DIC). A smaller fraction of the oceanic carbon is assimilated via photosynthesis into biomass and can form dissolved organic carbon (DOC).

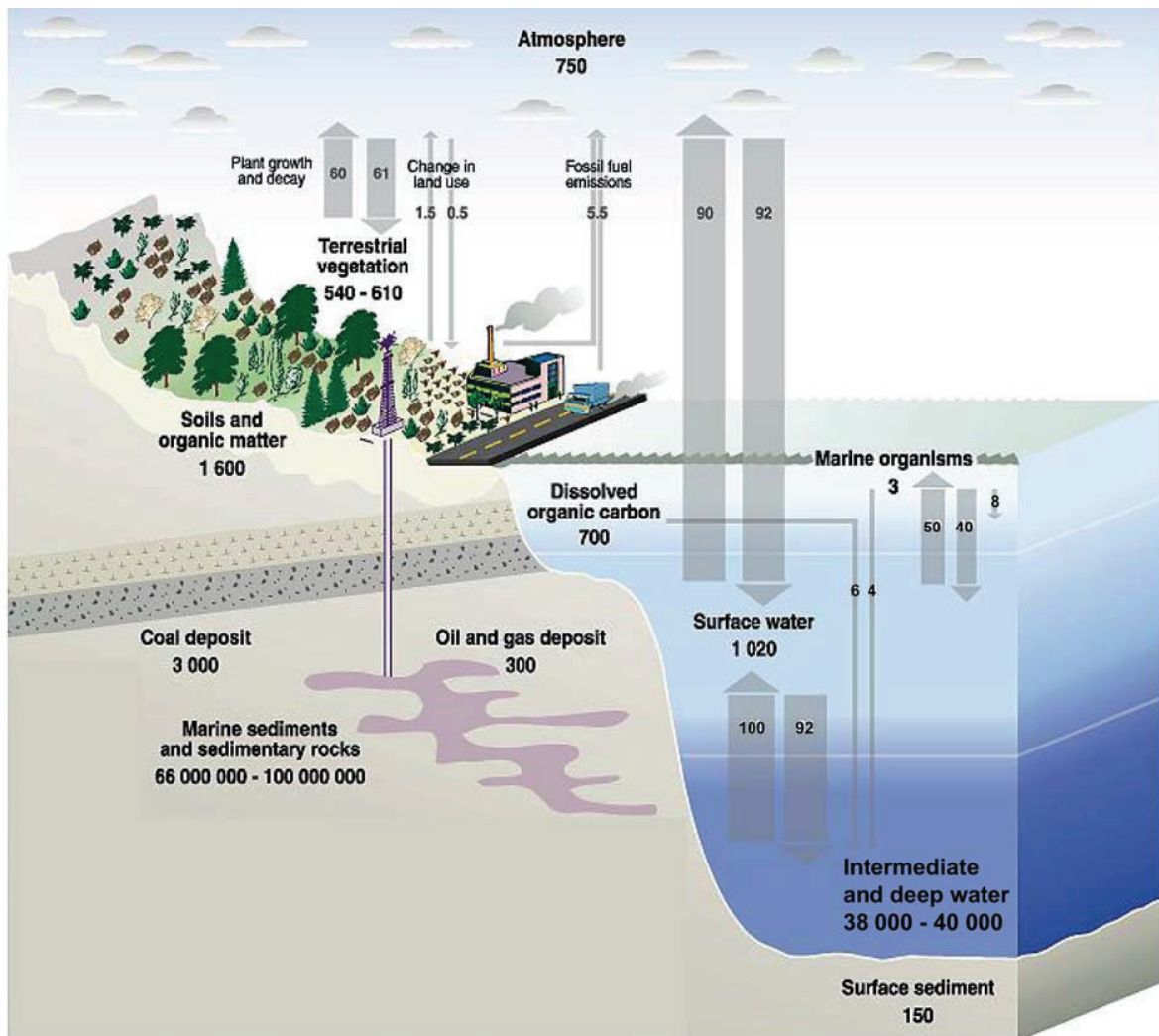


FIG 1: The global carbon cycle, including carbon fluxes in Gt carbon year⁻¹ (numbers in arrows) and reservoirs in Gt carbon (modified by Rekacewicz after Schimel et al. 1995). Values are estimations by Schimel et al (Schimel et al. 1995) and may differ from more recent estimations.

1.2. The marine carbon cycle

1.2.1. Methane

Methane, an important green house gas, is produced and consumed mainly in anoxic sediments in the marine realm. Methane production occurs only under anoxic conditions and methanogenesis is solely performed by *Archaea* belonging to a phylogenetically diverse group of the *Euryarchaea*. The annual methane production is estimated at 0.085 - 0.3 Gt (Reeburgh 2007).

About 90% of the produced methane is consumed directly in the sediment by *Archaea*, enforcing anaerobic oxidation of methane (Reeburgh 2007). The main archaeal group involved in methane consumption is the ANME-group, the anaerobic methanotrophic *Archaea*. Habitats of the bacterial-archaeal communities, in which ANME *Archaea* mainly occur, are cold seeps, hydrothermal vents, and the sulfate-methane-transition zones in sediments (Knittel and Boetius 2009). Due to the high consumption rates in the sediments, only minor amounts are released into the ocean. See reviews by Thauer, Reeburgh, and Knittel and Boetius (Reeburgh 2007; Thauer et al. 2008; Knittel and Boetius 2009).

1.2.2. Carbon dioxide

In contrast to methane, CO₂ plays a major role in ocean carbon cycling. Due to 50-fold higher CO₂ concentrations in the ocean, the atmospheric CO₂ concentrations are controlled by the ocean and not vice versa. The oceanic uptake of CO₂ is about 92 Gt C year⁻¹, while 90 Gt C year⁻¹ are emitted from the ocean into the atmosphere (FIG 1; Schimel et al. 1995). An annual net conversion of 1-2 Gt carbon from the atmosphere to the oceans was measured at high latitudes due to the lower water temperature and the subsequently higher solubility of CO₂. A net emission of 0.5 Gt carbon from the ocean into the atmosphere was measured at lower latitudes (Raven and Falkowski 1999; Takahashi et al. 2002). This results in a net uptake of ~1 Gt carbon year⁻¹ by the ocean. Within the ocean solved CO₂ is converted into several compounds in equilibrium (e.g. HCO₃⁻ and CO₃²⁻), which are summarized as dissolved inorganic carbon (DIC). These processes are summarized in the “solubility pump” and are dependent on several factors such as temperature, alkalinity and salinity of the surface water (Sarmiento and Quéré 1996; Broecker 1997).

The main factor driving the solubility pump is the biological uptake of DIC during photosynthesis. This process leads to a depletion of DIC in the surface waters and can subsequently lead to an export of carbon into deeper water layers. Here, microbial respiration again increases the DIC concentration. DIC is converged within the ocean and thus the concentration is higher in the deeper layers, where DIC can be hold for centuries (DeVries et al. in press). This convergence process, called the biological carbon pump (Volk and Hoffert 1985), produces a DIC gradient from low concentrations at the surface to high concentrations at depth and thus promotes the uptake of atmospheric CO₂ at the surface.

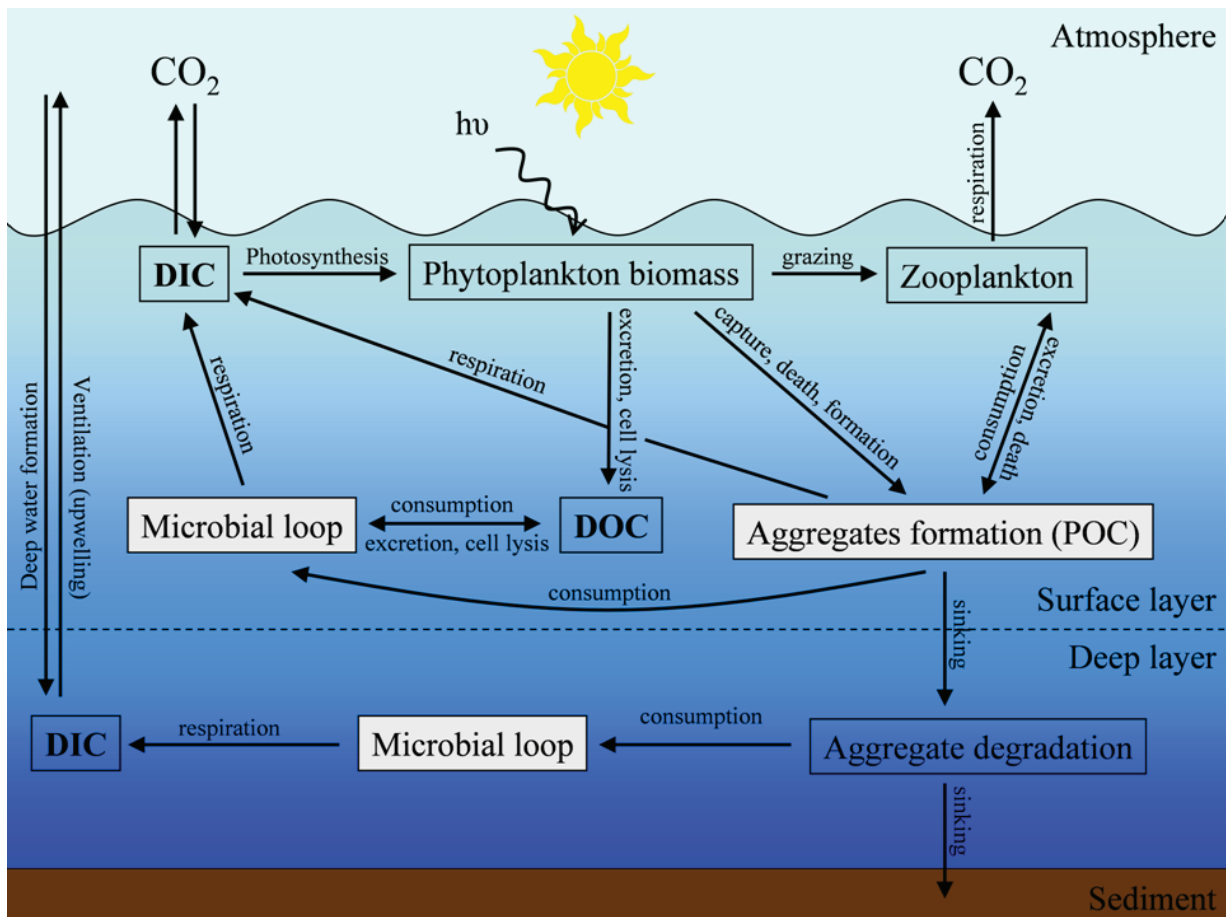


FIG 2: Schematic view of the biological carbon pump with major processes in grey boxes. Arrows mark carbon fluxes. The viral shunt and interaction from zooplankton and bacteria are omitted for simplicity (modified after Ducklow 2001).

1.3. The biological carbon pump

The biological carbon pump summarizes many processes of carbon cycling in the pelagic realm of the ocean (FIG 2; Volk and Hoffert 1985). About 50 Gt carbon are annually transferred into the ocean and converted into biomass by photosynthesis (Field et al. 1998). The biomass is subsequently cycled in the surface layer. These cycling processes are diverse and reach from grazing by zooplankton, to phytoplankton cell death by viral lysis, and bacterial respiration within the microbial loop. Respiration causes an estimated emission of 41-77 Gt of carbon per year (Del Giorgio and Duarte 2002). The remaining biomass is transformed into dissolved organic carbon (DOC) and particulate organic carbon (POC; FIG 2), such as phytoplankton detritus, transparent exopolymeric particles (TEP) structures, or fecal pellets (Simon et al. 2002;

Turner 2002). In this study I refer to living “POC” as biomass, while I use POC for dead organic matter. These aggregates export carbon from the surface and sink to the sea floor, where carbon might be residual for millennia (FIG 2; Middelburg and Meysman 2007). During the sinking process, degradation by bacteria, feeding by zooplankton and higher animals, and physical degradation may counteract the export process. Therefore, the biological carbon pump has an estimated export efficiency from the surface to the sea floor as low as 1% to 3%, which equals about 0.5 – 1.5 Gt carbon (Ducklow et al. 2001). Despite the low export efficiency, the transport of surface bound DIC into deeper layers (as POC) and the subsequent depletion of the DIC pool from the atmosphere is the major driving force of the biological carbon pump.

1.4. Surface layer processes

The initial step in the biological carbon pump is the conversion of CO₂ into biomass by photosynthesis. The surface waters possess low CO₂ concentrations which are determined by fluctuations in surface water temperature, mixing with deeper water layers, and photosynthesis rates. They vary between 5-25 μM (Burkhardt et al. 2001).

A variety of marine organisms are capable of photosynthesis, ranging from *Cyanobacteria*, to small *Eukarya*, dinoflagellates, diatoms up to macroalgae, which together constitute for about half of the global primary production (Falkowski et al. 1998; Field et al. 1998). Unicellular *Cyanobacteria*, like *Synechococcus* and *Prochlorococcus*, are ubiquitous and responsible for 80% of the oceans photosynthesis (Field et al. 1998; Scanlan 2003). Other photosynthetic organisms, like diatoms, dinoflagellates and sometimes even nanoplankton form local phytoplankton blooms. Within these blooms, primary production rates are high and phytoplankton biomass accumulates. This biomass then enters the pool of organic carbon in the surface layers.

Ultimately the phytoplankton biomass is converted into DOC or POC, by excretion of exopolymeric substances (EPS), viral lysis, bacterial interactions or sloppy feeding of zooplankton cells. POC can commence the sinking process and transport carbon into deeper water layers, as depicted in chapter 1.9., or is released into the DOC pool and DIC pool by bacterial degradation. The DIC pool is again available for primary producers. DOC can also be incorporated by various organisms and transformed into biomass. These cycling processes of

carbon in the surface layer, known as the microbial loop, are mainly mediated by microorganisms including all domains of life.

1.5. The microbial loop

1.5.1. Microbial loop vs. classical food chain

In 1983, Azam and co-workers found evidence for a tight coupling of the marine food web on the scale of microorganisms and coined the term “microbial loop” (FIG 3; Azam et al. 1983). This loop includes the cycling of carbon within the microbial food web and the channelling of carbon into the classical marine food chain. Even though, POC is important for the initiation of the microbial loop, the microbial loop dominates rather oligotrophic water bodies with low POC concentrations, due to the advantages small organisms have in competition for dissolved nutrients. In nutrient rich waters, such as upwelling systems, vast phytoplankton blooms form and thus the classical marine food chain is dominant (Kjørboe 1993). Both, the microbial loop and the classic food chain, are dependent on carbon fixation and biomass formation by photosynthetic organisms. In the classic food chain, these organisms are consumed by primary predators, such as dinoflagellates, ciliates or copepods. These predators are again consumed by higher level predators like copepods, amphipods and ultimately fish. In that way, the carbon is channelled towards the top predator of the system. Thus, the classic food chain can be referred to as a “carbon link”, channelling carbon to the highest trophic level.

In contrast, the microbial loop is a “carbon sink”, because most of the carbon is lost due to respiration processes during carbon channelling between the different trophic levels (reviewed in Fenchel 2008). Within the first version of the microbial loop, DOC formation by phototrophic eukaryotes, as well as the abundance of POC in the water, are the initial step, igniting a complex food web (FIG 3; Azam et al. 1983). Both, POC and DOC, are remineralised by heterotrophic bacteria. The DOC pool is of particular importance, since it is almost exclusively available for bacteria (FIG 3; Azam et al. 1983; Ducklow and Carlson 1992). The CO₂ emitted due to respiration is transferred into the DIC pool, while the bacterial biomass is consumed by predatory nanoflagellates, which again are preyed upon by higher predators. Thereby, the carbon is channelled into the classical food chain (FIG 3). These predators may also prey upon the primary producer, inserting a short cut into the microbial loop.

1.5.2. Additional phototrophic bacteria

During the three decades since the proposal of the microbial loop, many additional ways of carbon channelling have been added, supporting the role as a carbon sink (FIG 3; Fenchel 2008). One major discovery was the finding of autotrophic bacteria in the ocean, which add to the primary production and thus to the DOC pool. *Synechococcus* and *Prochlorococcus* are major primary producer in marine systems, especially in areas with nutrient concentrations too low to support phytoplankton blooms (Waterbury et al. 1979; Chisholm et al. 1988). These bacteria contribute significantly to the biomass production and are readily consumed by protozoan predators (e.g. Christaki et al. 1999; Hirose et al. 2008).

In addition to photoautotrophic bacteria, also photoheterotrophic bacteria, e.g. the members of the *Roseobacter* clade, were discovered. Photoheterotrophy is not based on CO₂ as primary carbon sources, carbon compounds come mainly from the DOC pool. This carbon metabolism is supplemented by the use of light as energy source. The light driven proton pump bacteriorhodopsin enables the establishment of a proton gradient, which is used for transport and adenosine-5'-triphosphate (ATP) production (Béjà et al. 2000). In this way photoheterotrophs remineralise DOC, incorporate also limited amounts of DIC, and produce DIC by respiration (FIG 3). Another CO₂ fixation pathway is the fixation CO₂ by anaerobic reactions to replenish the intermediates of the tricarboxylic acid cycle used by most aerobic organisms (Tang et al. 2011 and references therein).

1.5.3. Grazing and viral lysis – short cuts in the microbial loop

One major control mechanism of the bacterioplankton is the grazing by heterotrophic nanoplankton, dinoflagellates and ciliates (Pernthaler 2005). Initially, grazing by heterotrophic protozoa was assumed to be the major mortality factor of microorganisms, including autotrophic eukaryotes, auto- and heterotrophic bacteria, and archaea. This paradigm was changed with the discovery of marine viruses. Viruses were found in abundances of about 15- to 100-fold the abundance of bacteria and archaea and it is assumed that most bacterial and archaeal species in the ocean have at least one specific viral adversary (Bergh et al. 1989; Proctor and Fuhrman 1990; Suttle et al. 1990; Suttle 2005). Hence, viral lysis is another major factor of microbial mortality,

Introduction

exerting control on the bacterial and archaeal populations. Moreover, it represents another shortcut in the microbial loop, converting living biomass into DOC and detrital POC by cell lysis. This shortcut is known as viral shunt (Wilhelm and Suttle 1999).

Another discovery, adding to the complexity of the microbial loop, was the finding of eukaryotic cells which use photosynthesis as energy source and supplement photosynthesis with nutrients from ingested microbial cells (e.g. Zubkov and Tarran 2008; Frias-Lopez et al. 2009). These mixotrophic eukaryotes add to the DOC and POC pool in two ways. On one hand, carbon is converted by photosynthesis; on the other hand microorganisms are digested, leading both to an increase of biomass (FIG 3).

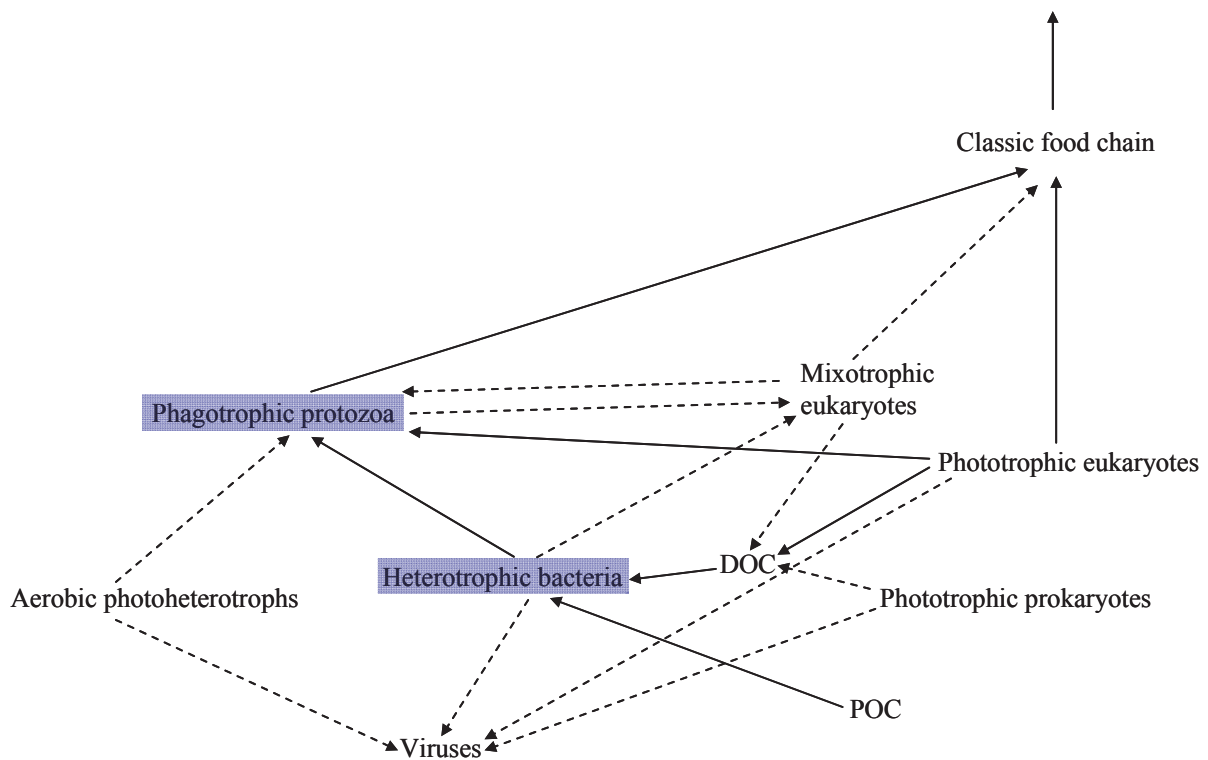


FIG 3: The microbial loop. Solid arrows mark the microbial loop as described by Azam and co-workers (Azam et al. 1983), dashed arrows are later additions (adapted from Fenchel 2008). Main groups of organisms addressed in this study are boxed.

1.6. Aggregation formation

1.6.1. Aggregate size and abundance

The second pivotal stage in the biological carbon pump is the formation of aggregates, which subsequently sink and transport carbon to deeper water layers, and may sediment on the sea floor. Upon sedimentation, carbon can be stored for centuries to millennia in the bathypelagic realm (Middelburg and Meysman 2007). These export processes are mainly due to macroscopic aggregates which often occur in high numbers during and at the end of phytoplankton blooms.

After the transformation of DIC into biomass by primary production, this biomass can be transformed into aggregates by various processes at different levels of the food web (FIG 2). Aggregates occur in many aquatic systems, including lakes, estuaries, coastal systems, open ocean, and rivers. The size of these aggregates ranges from $<1 \mu\text{m}$ to $>10 \text{ cm}$, covering more than 6 orders of magnitude (Simon et al. 2002). In rare occasions even larger aggregates were found, e.g. aggregates $>1 \text{ m}$ in the Northern Adriatic Sea (Herndl et al. 1999) or the very recent discovery of aggregates of sizes up to 50 cm in diameter on the Arctic sea floor (Boetius et al. 2013). The abundance of aggregates is dependent on environmental factors, like aeolian dust import, and the productivity of the ecosystem. The abundance of aggregates ranges from $<1 \text{ l}^{-1}$ to $>10^8 \text{ l}^{-1}$ and abundance is inversely related to aggregate size (Simon et al. 2002).

1.6.2. Physical factors mediate particle collision

The term marine, lake or river snow aggregates summarizes a vast variety of different aggregate types $>500 \mu\text{m}$ and often aggregates are combinations of different aggregate types. The formation of these marine snow and smaller aggregates is complex and depends on several controlling factors. The concentration, density, shape and size distribution of the source material must be sufficient to allow aggregate formation (Simon et al. 2002). Shear forces have to be low enough to avoid aggregate disruption, but also high enough to allow collision of source material and aggregates (Alldredge et al. 1990; Jackson 1990; Riebesell 1991, 1992; Macintyre et al. 1995). The settling velocities of larger aggregates must be high enough to allow the scavenging of source material from the water column during vertical transport (Jackson 1990). Another important factor of aggregate formation is the probability of particles sticking together after

collision. This stickiness is often mediated by TEP structures, which were found to increase the sticking coefficient of diatoms and organic particles (Alldredge et al. 1993).

A vast variety of mechanisms leads to the collision of source particles and might consequently lead to aggregate formation. A brief description of the mechanisms will be given, along the lines of Simon and co-workers (Simon et al. 2002). For small particles below 8 μm , Brownian motion has been characterized as a major factor for aggregate formation. These particles are largely controlled by their laminar flow and diffusion processes (Eisma 1993). Particles larger than 8 μm can be dependent on shear forces, as mentioned above. These mechanisms play a major role at discontinuity layers, bottom nepheloid layers, tidal currents, shallow seas, and also in pelagic systems (Alldredge et al. 1990; Jackson 1990; Riebesell 1991, 1992; Macintyre et al. 1995). Furthermore, settling particles can scavenge smaller particles during the sinking process (Jackson 1990). This mechanism is important in pelagic realms, shallow waters and estuaries and is dependent on the size of the scavenging aggregate. A special case of scavenging might be the filtration of small particles, and also dissolved nutrients, from the water column by highly porous aggregates (Jackson 1990; Kepkay 1994; Jannasch et al. 1996). Furthermore, filtration of particles from the water column or active feeding by zooplankton may result in particle collision and aggregate formation.

1.6.3. Chemical factors of aggregate formation

The success of the initial particle collision for the formation of aggregates is then influenced by several factors. A major factor in aggregate formation is the chemical surface property of the aggregate. Particles can be charged negatively by carboxylic and hydroxylic compounds (Gibbs 1983) or have positively charged residuals which act as bridging agents (Eisma 1993). DOC, consisting of humic acids, may attach to particles and form a negative coating, which might not only support aggregate formation with positive particles, but in high concentrations have a negative effect on aggregation due to the repulsion of negatively charged particles (Gerritsen and Bradley 1987; Eisma 1993). On the other hand, low DOC concentrations can enhance the aggregation of inorganic particles (Gibbs 1983). High concentrations of DOC, such as EPS, produced by diatoms, can enhance aggregate formation, due to the enhancement of particle stickiness (Simon et al. 2002). These DOC compounds may also attach to the surface of gas bubbles and form aggregate subsequent to the collapse of the bubbles (e.g. Eisma 1993; Zhou et

al. 1998; Mari 1999). In addition to the bubble aided formation of DOC aggregates, spontaneous coagulation may result in aggregates, such as TEP (Passow 2000).

1.6.4. Biological mediated aggregate formation

The discarding of houses from *Larvacea*, solitary marine tunicates, directly form aggregates (Alldredge and Silver 1988; Silver et al. 1998). Net feeding pteropods may also discard their nets when these become clogged, and thus create aggregates (Simon et al. 2002). The most obvious biological aggregate formation is the excretion of fecal pellets from zooplankton. These pellets are densely packed aggregates enclosed by a peritrophic membrane (Lampitt et al. 1990; Bochdansky and Herndl 1992; Turner 2002). Fecal pellets have high sinking velocities and thus contribute largely to carbon sequestration (Yoon et al. 2001 and references therein).

Aggregate attached bacteria may play a pivotal role during aggregate formation (Smith et al. 1995; Grossart et al. 2006; Alderkamp et al. 2007; Gärdes et al. 2011). Besides increased TEP production, bacteria can utilize low molecular weight DOC to produce fibrils, which lead to aggregate stabilization (Heissenberger et al. 1996). EPS are excreted from a vast variety of eukaryotic cells, such as diatoms or *Phaeocystis*, which leads to TEP production (e.g. Chin et al. 2004; Tsuyoshi Fukao 2012). TEP production was also found in bacteria, which can directly form TEP structures or indirectly assist aggregate formation by increasing of particle stickiness (Cambon-Bonavita et al. 2002; Klochko et al. 2012). In fact, TEP might be the major biological factor mediating aggregate formation (Simon et al. 2002).

1.6.5. Aggregate composition

The resulting aggregates are compositions of a vast variety of components, such as living, senescent and dead macro algae, diatoms, coccolithophorids, dinoflagellates, nano- and picoplankton, cysts of thecate dinoflagellates, cyanobacteria, phytoplankton detritus, diatom frustules, bacteria and archaea, zooplankton molts and carcasses, abandoned larvacaeen houses, pteropod feeding webs, fecal pellets, TEP structures and colloids, clay and silt minerals, calcite, and other particles abundant in the water column (Simon et al. 2002 and references therein). This might even include nano scale plastic particles, which are found frequently in the ocean (Law et al. 2010). For simplification, I will categorize all these described aggregate types in three groups

i) fecal pellets excreted from zooplankton, ii) transparent exopolymeric particles (TEP) formed from excreted EPS, and iii) detritus aggregates, that include all forms of planktonic detritus and will be referred to as marine snow aggregates. This shows the complexity of aggregate formation, in particular when considered that several processes can appear simultaneously and are mutually dependent on each other.

1.7. Aggregate colonization

1.7.1. Factors of colonization

Bacteria have been identified to be the main colonizing group on almost all types of aggregates, while *Archaea* play only a minor role in the microbial communities. Although, I focus here on the heterotrophic bacteria, members of the *Cyanobacteria* were found in marine snow aggregates in abundance (Alldredge et al. 1986, 1990; Ploug et al. 1999). However, the abundance of phototrophic organisms on particles sinking into the dark ocean is counterintuitive. The higher nutrient (especially nitrate and ammonia) concentrations within aggregates may attract the phototrophic bacteria (Willey and Waterbury 1989; Vanucci et al. 2001) which are then trapped by the aggregate and transported into the deeper layers.

The colonization of aggregates is complex and occurs in several steps. Fast swimming bacteria will encounter an aggregate in about <1 day (Kjørboe et al. 2002), but also non-motile bacteria collide with aggregates in lower frequency. In an initial phase, bacteria will attach loosely to the aggregate from where they still can detach again (Kjørboe et al. 2002). After short time the bacteria attachment gradually increases until cells are permanently attached and growth rates dominate over attachment (Grossart et al. 2003). Subsequently the total cell numbers on the aggregate increase and the bacterial community becomes established.

During the colonization process, bacteria were found to excrete antagonistic molecules to inhibit the colonization by other bacteria. *Alteromonas*, *Vibrionales*, and *Actinobacteria* produced large amounts of inhibiting molecules, while *Bacteroidetes* showed the strongest response and the least production (Long and Azam 2001; Grossart et al. 2004). This leads to the hypothesis of two colonization strategies. *Alteromonas*, *Vibrionales*, and *Actinobacteria* may initially attach to the aggregate and prevents further colonization of bacteria from other groups by antagonist excretion, before increasing growth rates lead to the formation of a stable biofilm. *Bacteroidetes* on the

contrary will outcompete other attaching bacteria by high growth rates and fast colonization (Grossart et al. 2004).

1.7.2. Bacterial abundance and community structure

The bacterial cell numbers are correlated to the size of the aggregate and range from <100 cells per aggregate on small microaggregates, to 10^8 or 10^9 cells ml^{-1} on large aggregates. Small aggregates and aggregates formed from minerals can also be uncolonized (Alldredge et al. 1986; Simon et al. 2002 and references therein). The cell abundance correlates positively with aggregate size, but not with the volume of the aggregate (Ploug et al. 1999; Ploug and Grossart 2000). As compared to the free living community, cell numbers of attached living bacteria are usually enriched (Alldredge et al. 1986; Ploug and Grossart 2000; Ploug et al. 2002). The distribution of bacteria on aggregates is often uneven, due to microcolonies and filamentous structures (Grossart and Simon 1998; Grossart and Ploug 2000).

Organisms belonging to the *Betaproteobacteria* and *Bacteroidetes* are dominating lake and river snow aggregates (Grossart and Simon 1998; Böckelmann et al. 2000; Schweitzer et al. 2001). This changes towards the rivers estuary in correlation with increasing salinity, where a shift in the community structure from *Beta-* to *Gammaproteobacteria* was found (Böckelmann et al. 2000; Simon et al. 2002). This is congruent with the finding of higher *Betaproteobacteria* abundances in lakes, compared to higher *Gammaproteobacteria* abundances in marine systems, in the free living fraction (Glöckner et al. 1999).

In marine systems, *Gammaproteobacteria* and *Bacteroidetes* are the dominating clades on aggregates (DeLong et al. 1993; Rath et al. 1998; Moeseneder et al. 2001). Both clades are highly diverse and many different species may colonize aggregates, even though in Western Mediterranean waters the diversity within the *Gammaproteobacteria* community on marine snow aggregates was low (Acinas et al. 1999). High *Gammaproteobacteria* abundances are in accordance with recent findings of *Gammaproteobacteria* involved in DOC degradation (Puddu et al. 2003). Metagenomic analyses showed increased transcription of genes encoding for enzymes which enable the degradation of DOM, such as TonB-associated transporters, nitrogen assimilation genes, and fatty acid catabolism genes (McCarren et al. 2010). It is assumed that *Bacteroidetes* are also capable for the degradation of various DOC and POC compounds. Recent studies found genes for hydrolytic enzymes, polysaccharide, N-acetylglucosamine and protein

Introduction

consumption, chitin and peptidoglycan degradation and cell attachment, indicating the utilization DOC and POC in *Bacteroidetes* (Cottrell and Kirchman 2000; Bauer et al. 2006; Gómez-Pereira et al. 2012). *Alphaproteobacteria* are not known to be major DOC or POC degraders, beside members of the *Roseobacter* clade which may live attached to phytoplankton cells and are capable of Dimethylsulfoniopropionate (DMSP) utilization (Kiene et al. 2000 and references therein). Consequently, *Alphaproteobacteria* from the *Roseobacter* clade were also found on aggregates (Zubkov et al. 2001; Gram et al. 2002; Rooney-Varga et al. 2005). *Planctomycetes* were attached to aggregates, though only in low abundance (DeLong et al. 1993; Rath et al. 1998; Crump et al. 1999; Pizzetti et al. 2011).

1.7.2. Eukaryotic communities on aggregates

Besides bacterial colonization, also small eukaryotes were abundant on marine snow and occurring in higher numbers than in the free living fraction (Simon et al. 2002 and references therein). The community of protist on aggregates is diverse and differs from the free living fraction. Heterotrophic flagellates, ciliates, sarcodines and amoebae live attached to aggregates, implying a strong grazing on the attached living bacterial community (e.g. Rogerson and Laybourn-Parry 1992; Artolozaga et al. 1997; Zimmermann-Timm et al. 1998). While protists graze upon the bacterial community, predators grazing on protist might also be found in the vicinity of marine snow aggregates. Metazoans, such as copepods, are abundant on marine snow aggregates (e.g. Bochdansky and Herndl 1992; Zimmermann-Timm et al. 1998; Kiorboe 2000) and may also play a role in aggregate degradation (Iversen and Poulsen 2007).

1.8. Aggregate degradation

As stated above, marine snow aggregates can be destroyed or degraded by higher organisms, such as copepods, by several mechanisms. Direct feeding on fecal pellets (coprophagy), fecal pellets disruption by sloppy feeding, disruption of refused fecal pellets in the feeding current (coprohaxy) or loosening of the fecal pellets (coprochaly) are major processes in zooplankton aided fecal pellets degradation (Iversen and Poulsen 2007). These processes were investigated for fecal pellets, but it can be assumed that similar mechanisms also apply for marine snow aggregates of similar size. For aggregates, zooplankton swimming is an important factor of

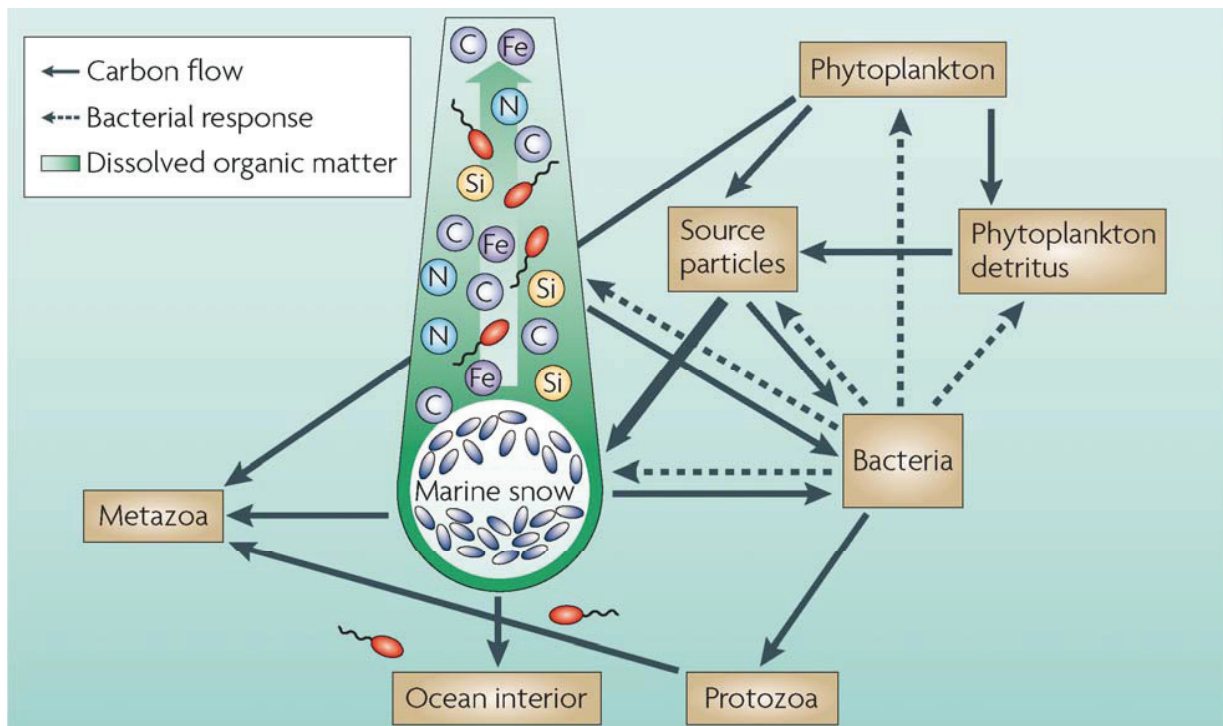


FIG 4: The microbial loop on sinking aggregates (adapted from Azam and Malfatti 2007).

fragmentation (Dilling and Alldredge 2000; Goldthwait et al. 2004). However, these processes affect the degradation rather indirectly, by disruption of the aggregate and release of the smaller aggregate fragments into the water. The reduced sinking velocity might then favour other degradation processes, such as bacterial aggregate degradation.

In fact, bacterial biomass production and respiration, bacterial substrate release, POC solubilisation, bacterial substrate hydrolysis and subsequent uptake or release into the environment, are the major microbial processes of aggregate modification and degradation. The production of biomass on aggregates is relatively low with <14% in oligotrophic and around 30% at eutrophic systems. The growth rates and thymidine and leucine incorporation rates were rarely found higher in attached living bacterial communities as compared to the free living fraction (Simon et al. 2002 and references therein). Nevertheless, respiration leads to the release of CO_2 from the aggregates, which enters the DIC pool. The detection of higher ectoenzymatic activities, of aminopeptidase, phosphatase, protease, lipase, nuclease, chitinase and glucosidase, compared to the surrounding water, indicate high POC degradation rates (Azam and Malfatti 2007 and references therein). The compounds resulting from ectoenzyme activity, e.g. amino acids, organic carbon compounds and inorganic nutrients, are not used to the full extent by the attached living

bacterial cells. A part is released into the environment leading to the formation of a plume and a release of DOC into the water column, where it is available for the free living bacterial community (Simon et al. 2002; Azam and Malfatti 2007). This may be the source of nutrition for large fractions of the free living bacterial community (FIG 4; Kiørboe and Jackson 2001).

In combination with the DOC release by the attached living bacterial community, these bacteria might function as food for the likewise attached living protist community (Kiørboe et al. 2003). This leads to a transfer of the bacterial biomass into higher trophic levels and carbon enters the microbial loop directly on the aggregate. Although the cycling inside the microbial loop would lead to retention of carbon at the aggregate, the overall respiration of bacteria and protozoa, in combination with the release of DOC into the water column, leads to the degradation of the aggregate.

1.9. Sinking velocities and the efficiency of the biological carbon pump

The sinking velocity of aggregates is a key factor for the efficiency of the biological carbon pump. Sinking velocity of the aggregates determine the sinking rates of the POC. Low sinking velocities imply higher residence times in the surface layer and consequently enhanced degradation. Processes within the microbial loop are a key factor in the efficiency of the carbon pump, since these processes lead to remineralisation of carbon and the transfer into the non-sinking, dissolved carbon pool. These velocities range from non-sinking in the dissolved state to velocities $> 700 \text{ m d}^{-1}$ (Ploug et al. 2008a; Fischer and Karakaş 2009; Fischer et al. 2009). A number of factors, such as aggregate size and density, interactions of the POC with ballast materials influence the sinking velocities (Ploug et al. 2008a; b; Iversen and Ploug 2010), and biological interaction with phytoplankton, zooplankton and bacteria (e.g. Simon et al. 2002; Iversen and Poulsen 2007) influence the sinking velocity. Large aggregate size, in combination with high porosity, usually leads to lower sinking velocities (Johnson et al. 1996; Kindler et al. 2010). The sinking velocity might increase when the pores are clogged with TEP structures, organic, or inorganic particles. Higher aggregate density increases sinking velocity, for example dense fecal pellets have high sinking velocities and are more likely to drive carbon export than slow sinking particles (Yoon et al. 2001). The density of the aggregates can be influenced by the incorporation of ballast materials, such as opal, calcium carbonate, aeolian dust particles and other inorganic materials with high density (Ploug et al. 2008a; b; Iversen and Ploug 2010). Besides the higher density,

which increases sinking velocity, these compounds may also lead to destabilisation of the aggregates and thus to decreased sinking velocities (Armstrong et al. 2001; Francois et al. 2002; Hamm 2002; Klaas and Archer 2002; Passow and De La Rocha 2006). Due to these processes, the aggregate can constantly shift between different conditions and different sinking velocities.

These processes are mediating the efficiency of the biological carbon pump. However, the efficiency of the biological carbon pump is highly variable at different regions and thus exact measurements remain challenging. While many of the interacting physical and chemical factors are known and can be quantified, the biological factors, such as bacterial interactions with POC and DOC still need further investigation. Areas of high POC and DOC production, such as phytoplankton blooms, provide optimal conditions to investigate the role of microbial communities within the biological carbon pump.

1.10. Phytoplankton blooms

Vast areas of the ocean provide favourable conditions to establish phytoplankton blooms. These blooms might be reoccurring seasonal blooms in areas with high nutrient fluctuations, such as coastal areas or seasonal upwelling systems (Gattuso et al. 1998). Large scale upwelling systems, in contrast, can provide sufficient nutrients year round and thus harbour permanent phytoplankton blooms (Aristegui et al. 2009) as further depicted in chapter 1.12.. In addition to natural occurring blooms, iron limited areas of the ocean can be fertilized and phytoplankton blooms can be artificially established (Martin et al. 1994) as further depicted in chapter 1.11..

1.10.1. Bloom forming organisms

Most phytoplankton blooms follow a succession pattern of organisms (reviewed in Cloern 1996). Due to the bottom up control of phytoplankton by nutrient availability, the initial step for the formation of a bloom is the increase of nutrients. The behaviour of rapid growth triggered by increasing nutrient concentrations is also known as “boom (or bloom) and bust” response. Diatoms are one of the major organisms that are promoted under such conditions, due to their fast growth rates, and display a “boom and bust” response (Furnas 1990). This response is often supported by increasing water temperatures, light intensities and other physicochemical factors that provide favourable conditions. In eutrophic oceanic regions the blooms are dominated by

organisms, such as diatoms, coccolithophorids, dinoflagellates, while in oligotrophic waters blooms are often dominated by eukaryotic nano- and picoplankton or *Cyanobacteria* (Olson et al. 1988, 1990; Campbell and Vaultot 1993). Major bloom forming diatoms are *Thalassiosira*, *Chaetoceros*, and *Pseudo-nitzschia* species (e.g. Rines and Theriot 2003; Armbrust et al. 2004; Trainer et al. 2012), while *Emiliania huxleyi* is the worldwide most dominant member of the coccolithophorids and forms extensive blooms ($> 100.000 \text{ km}^2$) in oligotrophic waters (e.g. Okada and Honjo 1973; Okada and McIntyre 1979; Flores et al. 2010). Many dinoflagellates species are known to form blooms (Taylor et al. 2008). Some dinoflagellates, but also diatom species are intensely studied due to their toxin production and the formation of harmful algae blooms (Hallegraeff 1993; Anderson et al. 2012). However, these organisms are not the scope of this study and will only be discussed briefly.

1.10.2. Nano- and picoplankton communities during phytoplankton blooms

Nano- and picoplankton species are so far not as deeply studied and thus their role in the formation of blooms is rather unknown, except of *Phaeocystis*, which are well studied and form blooms worldwide (Schoemann et al. 2005). The smallest bloom forming picoplankton species are *Micromonas* (Not et al. 2004) and *Ostreococcus* (O'Kelly et al. 2003). However, only few studies have been conducted aiming on the response of these organisms on phytoplankton blooms and possible succession patterns of these small eukaryotes (Coale et al. 2004; Peloquin et al. 2011a), possibly as a reason of the difficulties in identification of these organisms.

Due to the similar round or pear-shaped body morphology, microscopic identification of nano- and picoplankton cells is challenging and often organisms are only classified due to their cell size. Picoplankton is in the range of 0.2-2.0 μm and nanoplankton in the range of 2.0-20 μm . The phylogeny of these organisms is far more diverse and they appear in various groups of aquatic organisms. Major clades are e.g. *Prasinophyceae*, *Stramenopila*, *Alveolata*, and *Haptophyta* (FIG 5). Classical light microscopic determination of the different species provides only a very low resolution in diversity and community composition. Scanning electron microscopy (SEM) has great potential to provide more morphological information, but processing environmental samples is not trivial and most of the cells are identified on a low taxonomic level or remain unidentified (Vørs et al. 1995; Zingone et al. 1999). Another method frequently used to determine

nano- and picoplankton communities is the usage of pigments as markers for chemical taxonomy (Jeffrey and Wright 2006 and references therein).

Only recently molecular tools, based on the 18S rRNA gene sequence, were introduced into the field of nano- and picoplankton research. Finger printing techniques like denaturing gradient gel electrophoresis (DGGE), automated ribosomal intergenic spacer analyses (ARISA) or next generation sequencing were used to investigate the diversity. In addition, fluorescence *in situ* hybridization (FISH) techniques have been applied to quantify certain groups of nano- and picoplankton (Wolf et al. in press, in prep.; Not et al. 2004; Berglund et al. 2005; Massana et al. 2006; Stoeck et al. 2010; Cheung et al. 2010).

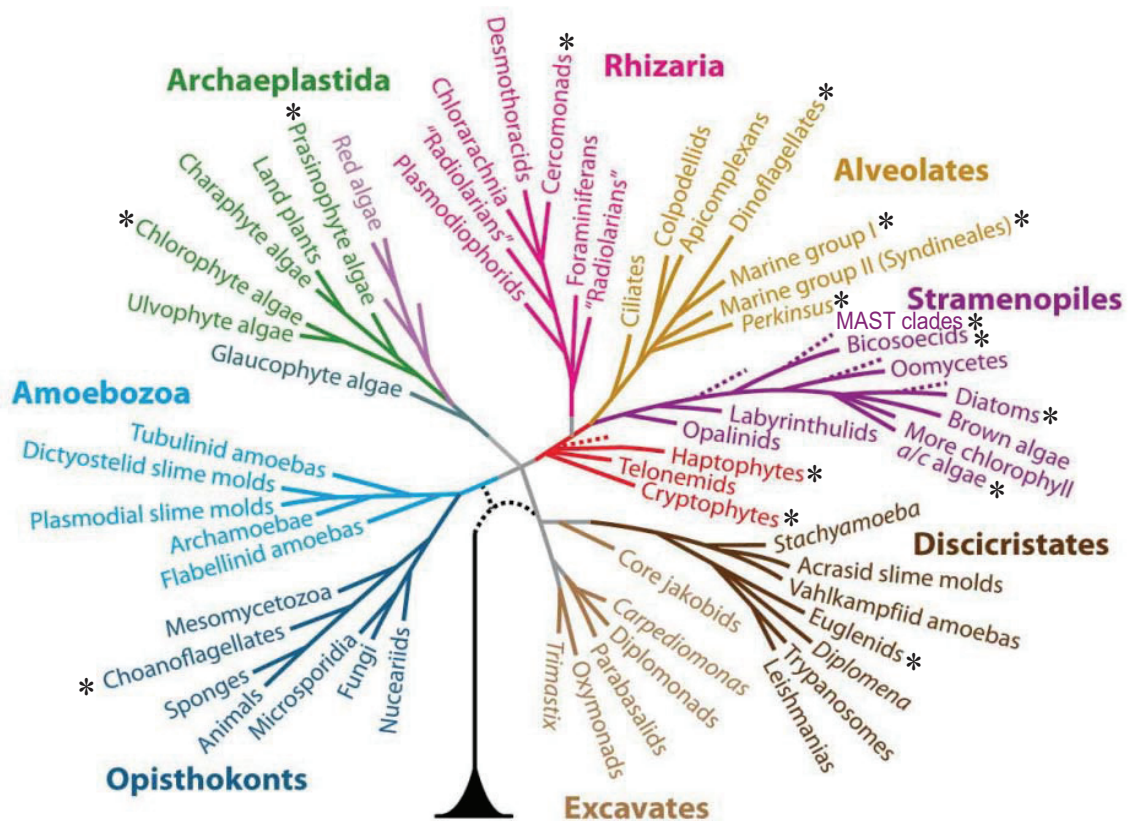


FIG 5: Phylogenetic consensus tree of the *Eukarya* (modified after Baldauf 2008). Groups with major clades of marine nano- or picoeukaryotes are indicated by asterisks. Small stages in life cycles are not considered. Dotted lines in the *Stramenopiles* indicate possible new clades according to Massana and co-workers (Massana et al. 2006) and the MAST clades were placed arbitrarily since a clear taxonomic positioning is not yet available. The two current proposed roots are also indicated as dotted lines.

1.10.3. The bacterial and archaeal community response during phytoplankton blooms

The most important bacterial phytoplankton group are *Cyanobacteria*. Unicellular *Synechococcus* and *Prochlorococcus* are the most important species and are well studied (e.g. Waterbury et al. 1979; Glover et al. 1988; Chisholm et al. 1988; Partensky et al. 1999). However, we focus on the response of heterotrophic bacteria to phytoplankton blooms. After the initial increase of phytoplankton biomass and the subsequent DOC and POC release, heterotrophic bacterial and archaeal clades respond to the nutrient input by an increase of growth rates. Bloom ecosystems are often dominated by fast growing bacterial clades such as *Gammaproteobacteria*, *Bacteroidetes* and *Roseobacter* (e.g. Fandino et al. 2001; Pinhassi et al. 2004; West et al. 2008), while non bloom situations are often dominated by persistent clades such as the SAR11 clade or the SAR86 clade (Pernthaler et al. 2002; Morris et al. 2002; Mary et al. 2006). These preferences reflect the different niches of the different groups. A strong bacterial clade succession occurs over the course and the decay of phytoplankton blooms, due to changes in substrate availability (Teeling et al. 2012).

Many studies used micro- and mesocosms to simulate blooms or addressed the bacterial with limited taxonomic or temporal resolution (Pinhassi et al. 1999, 2004; Riemann et al. 2000; Fandino et al. 2001; Lau et al. 2007). Only one study intensively investigated the succession patterns of the bacterial and archaeal community during a spring bloom in the North Sea. It was shown, that a series of ecological niches occurred most likely due to the successive availability of algal polysaccharides bacterial succession patterns were bottom up controlled by substrates (Teeling et al. 2012).

The study revealed a dominance of *Alphaproteobacteria*, mainly the SAR11 clade, in the pre-bloom phase, followed by a succession of defined *Bacteroidetes* clades from the *Flavobacteria* class. *Ulvibacter* was followed by *Formosa*-related and *Polaribacter* species. A later response to the bloom situation was found for *Gammaproteobacteria*, where *Reinekea* species and members of the SAR92 clade increased in abundance. Within the *Roseobacter*, a shift from the NAC11-7 clade towards the RCA clade (now DC5-80-3 clade) occurred from the early to the late bloom phase. The study was able to link the different stages of the succession to different expression levels of genes related to the uptake or utilization of different carbon compounds. *Bacteroidetes* are dependent on higher molecular weight compounds, while *Gammaproteobacteria* utilize lower molecular weight compounds. This implies that niche partitioning is realized by the availability

of different carbon compounds during the bloom phase. In the later bloom phase, *Polaribacter* and *Formosa* were found in higher abundances in the particle attached fraction, indicating that spatial niche partitioning may also play a role in the succession pattern (Teeling et al. 2012).

1.11. Iron fertilization experiments

1.11.1. Iron – limiting factor in the open ocean

About 25% of the world's oceans are low in chlorophyll a concentrations despite their high nutrient concentrations. These areas, so called High Nutrient – Low Chlorophyll (HNLC) areas, can be found in the Equatorial Pacific off the Galapagos Islands (Ecuador), in the subarctic North East Pacific off the coast of Alaska, and in the Southern Ocean (Chavez and Barber 1987; Martin et al. 1994; Chavez et al. 1996; Boyd et al. 1998, 2000). These areas are characterized by nutrient concentrations high enough to sustain extensive phytoplankton blooms, but are iron limited. This finding lead to the formulation of the “iron hypothesis”, which postulates that iron is the limiting nutrient for phytoplankton growth and consequently iron fertilization would lead to phytoplankton bloom formation (Martin 1990).

Four sources of iron are proposed to naturally fertilize the oceans. The major iron source is aeolian dust transported into the ocean by storms. Enhanced primary production has been found in the southern North Atlantic due to influx of Sahara dessert dust (Duce and Tindale 1991; Jickells et al. 2005). Upwelling of iron rich sediment particles can be a source for iron in coastal areas and upwelling systems (Bruland et al. 2001). Another source of iron are riverine iron compounds purged into the ocean (Figuères et al. 1978). In the Southern Ocean, ice bergs have been proposed to be a source of bioavailable iron (Smith et al. 2007; Raiswell et al. 2008). From the melting ice bergs, bioavailable iron could be release into the ocean directly, as dissolved iron, as iron containing sediment or dust trapped in the ice berg, and as nanoparticulate iron (Raiswell et al. 2008). These iron influxes support the formation of blooms in areas with sufficient nutrients.

1.11.2. Iron fertilization experiments

After the verification of the iron hypothesis in Equatorial Pacific waters (Martin et al. 1994), twelve iron fertilization experiments have been conducted in different HNLC areas (FIG 6). All

experiments successfully established a phytoplankton bloom, as shown by increased chlorophyll *a* values (deBaar et al. 2005; Peloquin et al. 2011a; Smetacek et al. 2012). These blooms consisted of different phytoplankton communities, depending on the nutrient composition of the fertilized waters and the predominant organisms in the area. Most of the induced blooms were dominated by diatoms, often *Pseudo-nitzschia* species and *Fragilariopsis kerguelensis*, and those blooms were also found highest in chlorophyll *a* values (deBaar et al. 2005). Due to the increased photosynthesis rates, the DIC in the surface layer was transferred into biomass, measurable by a decrease of DIC in most experiments (deBaar et al. 2005). Convergence of atmospheric CO₂ into the surface water was measured in most experiments and is as small as ~ 8% of the DIC removal rate, but further convergence can be expected after the experiments (deBaar et al. 2005). However, POC formation was found during the first 8 experiments and is about 25% of the primary production, while the remaining 75% are assumed to be cycled in the surface layer (deBaar et al. 2005). POC export rates have been achieved for some of the experiments, using sulfur hexafluoride (SF₆) tracer (SEEDS, EisenEx, and LOHAFEX), sediment traps (SOIREE, SERIES and LOHAFEX), or ²³⁴Thorium export rates (SOFeX South and LOHAFEX). However, the export rates were rather low for SEEDS, SOIREE, SOFeX South, and SERIES (Nodder and Waite 2001; Tsuda et al. 2003; Boyd et al. 2004; Buesseler et al. 2004). Elevated export rates of POC into deeper water layers, of 50% of the bloom biomass were found only during EisenEx (Smetacek et al. 2012).

1.11.3. The role of silicate

Like iron also silicate is of importance for the formation of phytoplankton blooms. Depending on silica concentrations in the fertilized waters, the induced blooms can consist of diatoms (Gall et al. 2001; Tsuda et al. 2005; Marchetti et al. 2006; Assmy et al. 2007; Suzuki et al. 2009) or are formed by autotrophic and mixotrophic nano- and picoplankton (Peloquin et al. 2011a). Most iron fertilization experiments were conducted in silicate-rich HNLC areas (HNLC-HSi) and the iron-induced blooms were dominated by diatoms. Although, SOFeX-North was conducted in low silicate waters (3 μM) still 50% of bloom biomass was contributed by diatoms (Coale et al. 2004). The only iron fertilization experiment performed in silicate limited (<2 μM) areas (HNLC-LSi), the SAGE experiment, showed a muted increase in bloom biomass and the bloom was dominated by pico- and nanoflagellates (Peloquin et al. 2011b). Blooms formed by nano- and

picoplankton lead to an accelerated cycling of carbon in the surface layer, due to the short cut in the microbial loop. This process played a major role during the SAGE experiment and led to carbon retention in the surface layer (Harvey et al. 2011). It shows the importance of the microbial loop in iron induced blooms and the effect on the biological carbon pump. However, not much is known about the response of bacterial and nano- and picoplankton community onto iron fertilization.

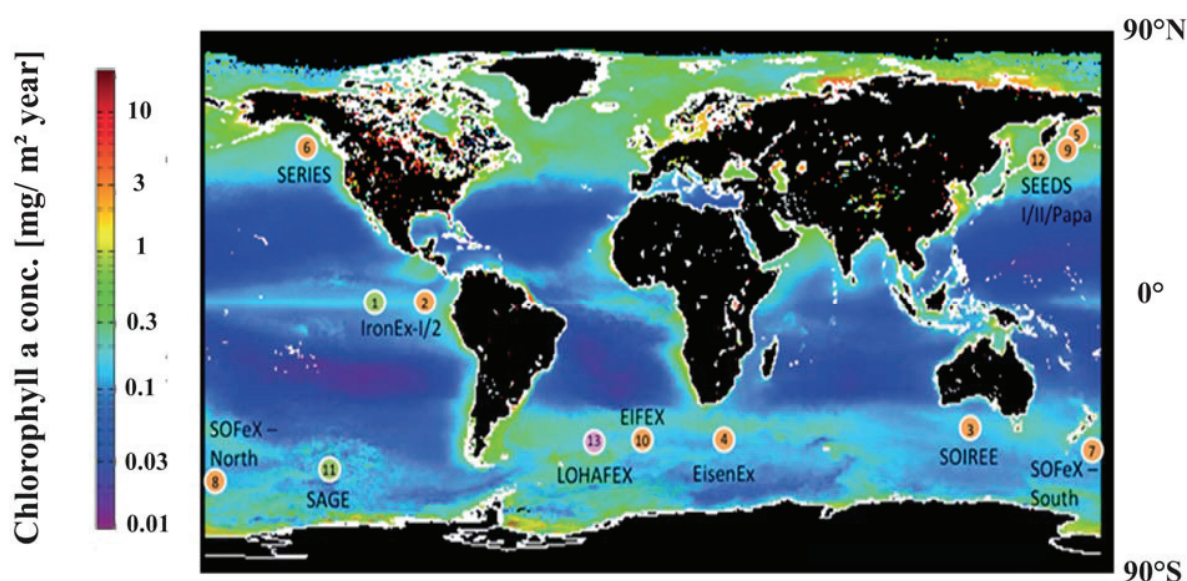


FIG 6: Map of the worldwide distribution of Chlorophyll a in marine and limnic systems. The spheres indicate locations of iron fertilization experiments. Numbers in the spheres mark the chronological order of the experiments, while sphere colour indicates the predominant plankton group (orange = diatoms, green = nano- and picophytoplankton, pink = zooplankton and nano- and picophytoplankton). 1 – IronEx-I, 1993; 2 – IronEx-II, 1995; 3 – SOIREE, 1999; 4 – EisenEx, 2000; 5 – SEEDS-I, 2001; 6 – SERIES, 2002; 7 – SOFeX North, 2002; 8 – SOFeX South, 2002; 9 – SEEDS-II, 2004; 10 – EIFEX, 2004; 11 – SAGE, 2004; 12 – PAPA-SEEDS, 2006; 13 – LOHAFEX, 2009 (Adapted from Morrissey and Bowler 2012).

1.11.4. Bacterial and archaeal response to iron fertilization

Besides the finding of increased bacterial activity in several former iron fertilization experiments (Hall and Safi 2001; Cochlan 2001; Oliver et al. 2004; Suzuki et al. 2005), the bacterial and archaeal community composition and succession was only accessed during EisenEx and during the KEOPS experiment, an investigation of a natural fertilized bloom off Kerguelen Island in the

Introduction

Southern Ocean (Arrieta et al. 2004; West et al. 2008). During the EisenEx experiment no significant change within the heterotrophic bacterial community, using terminal restriction fragment length polymorphisms (T-RFLP), were detected (Arrieta et al. 2004). In contrast, West and co-workers found significant differences in the bacterial community inside the naturally fertilized area as compared to outside, using clone libraries. *Roseobacter* species of the NAC11-7 clade, members of the gammaproteobacterial SAR92 clade, and *Bacteroidetes* of the AGG58 Branch1 clade were found abundant inside the bloom. The bacterial community outside of the bloom was dominated by members of the SAR11 clade, belonging to the surface group I (including *Cand. Pelagibacter ubique*), and *Bacteroidetes* from the genus *Polaribacter* (West et al. 2008).

1.11.5. Thesis project I – Investigation of the bacterial and archaeal community response to iron fertilization during LOHAFEX

We investigated the response of the bacterial and archaeal community towards iron fertilization during the LOHAFEX experiment, using molecular techniques like catalyzed reporter deposition FISH (CARD FISH) and 454 tag pyrosequencing. Next generation sequencing provides high sequence read numbers and a higher resolution of the community diversity than sequencing from clone libraries, and provides taxonomic information in contrast to T-RFLP community fingerprinting. FISH techniques enable quantitative analyses and are thus favorable compared to fingerprinting techniques. Furthermore, FISH offers the opportunity of spatial resolution and thus enables fine scale investigations without possible amplification biases during PCR reactions (Farris and Olson 2007).

Manuscript I reports the result of the investigations of the community composition and diversity over the course of the induced bloom. This study showed that the bacterial and archaeal community change only minute during the experiment and showed no significant succession pattern in the expected bacterial clades. Members of the SAR11 and SAR86 clades were high in numbers, probably due to the small cell size. This small cell size might enable these cells to escape grazing pressure of bacterivorous grazers (Pernthaler 2005), which might have kept the system in top-down control and hindered a bacterial succession pattern.

1.11.6. Thesis project II – Investigation of the nano- and picoplankton community response to iron fertilization during LOHAFEX

Similar to the bacterial and archaeal community, the response of the nano- and picoplankton community onto iron fertilization was not sufficiently addressed so far. Using flow cytometry increasing total cell numbers of nano- and picoplankton were found over the course of the SOIREE experiment (Hall and Safi 2001). During the SAGE experiment the picoplankton community increased, as investigated by flow cytometry. An increase in nanoflagellate biomass was determined by microscopic counting after primulin staining. Identification of the organisms was done during the SAGE experiment using pigments as chemotaxonomic markers. This suggested the dominance of prasinophytes, pelagophytes and haptophytes type 8 within the bloom (Peloquin et al. 2011b). However, molecular techniques have rarely been applied to the nano- and picoplankton community, and also not to investigate succession patterns during bloom situations.

Chapter 1.10.2. discusses the difficulties of nano- and picoplankton investigations by classical methods, such as light microscopy, SEM and chemotaxonomy. We used CARD FISH and 454 tag sequencing to investigate the nano- and picoplankton community during the LOHAFEX experiment. We successfully applied these methods to monitor the nano- and picoplankton diversity and community composition, and were able to design two new probes targeting groups of the *Syndiniales* clade. The results are presented in Manuscript II and show a similar stable community structure and diversity pattern than it was found for the bacterial and archaeal community. Only *Micromonas* and *Pelagophyceae* increased shortly after the second iron fertilization, but decreased immediately again. As stated for the bacterial and archaeal community, this implies strong top down control by dinoflagellates and ciliates, and a tight coupling of the microbial loop inside the induced bloom.

1.12. The bacterial community of sinking aggregates

Besides iron fertilized phytoplankton blooms, upwelling systems provide favourable conditions to investigate microbial mediated processes in the biological carbon pump. In some upwelling systems nutrients are year round transported to the surface layer and result in perennial, highly productive phytoplankton blooms. The most productive upwelling systems are the eastern

boundary upwelling systems (EBUS) found at the eastern margins of South America, North America and Africa (Carr and Kearns 2003).

1.12.1. The Eastern Boundary Upwelling Systems (EBUS)

The four major EBUS are the Humboldt Current Upwelling off the coast of Peru, the Canary Current Upwelling off Morocco and Mauretania, The Benguela Upwelling off Namibia and the Californian Upwelling off the coast of California (USA). In these systems, winds along the Pacific or Atlantic coasts, oriented towards the equator, create offshore Ekman transport systems. This transport creates an upwelling of nutrient rich waters into the surface layer and thereby favours sustainable phytoplankton blooms in these areas (Carr and Kearns 2003). These systems are highly productive and show not only vertical carbon export, but also horizontal carbon transport towards the open ocean (Aristegui et al. 2004).

Although, the Humboldt Current Upwelling system was thought to be the most productive in the world (Behrenfeld and Falkowski 1997; Chavez and Messié 2009), the African EBUSs display higher net primary production (Lachkar and Gruber 2011). The Canary Current Upwelling is the second most productive upwelling system of the EBUS with an estimated annually production of 0.33 Gt carbon (Carr 2001; Lachkar and Gruber 2011). This system can be divided into a northern and a southern part, due to the presence of the Canary Islands. The more productive southern part, off the area of Cape Blanc (Mauretania), sustains phytoplankton blooms year round (Aristegui et al. 2009). This results in high POC production and consequently increased efficiency of the biological carbon pump. This highly productive system provides optimal conditions for the investigation of aggregates and the attached living bacterial and archaeal communities.

1.12.2. Changes of the aggregate attached bacterial community with increasing depth

As stated in chapter 1.7.2., the bacterial community on aggregates is often dominated by *Gammaproteobacteria* and *Bacteroidetes*. However, not much is known about the response of the microbial community to the sinking of the aggregate. During the sinking process, pressure increases constantly, while temperature decreases at the thermocline until a stable temperature of about 4°C is reached. In laboratory studies, changes in the bacterial community with increasing

depth were found. It was indicated that on fecal pellets and in artificially bacterial communities *Gammaproteobacteria* are favoured against other bacteria at increasing depth (Tamburini et al. 2009; Grossart and Gust 2009). This is congruent with changing bacterial and archaeal communities on aggregates (>3 µm filter fraction) with increasing depth in the Aegean Sea (Moeseneder et al. 2001). However, the bacterial activity did not change with increasing pressure (Tamburini et al. 2002). This stands in contrast to a 3.5 fold higher carbon specific respiration rate found at 15°C compared to 4°C, found in a laboratory experiment (Iversen and Ploug 2013).

1.12.3. Thesis project III – Investigation of the bacterial community on marine snow aggregates and TEP structures at two different depths from the Canary Current Upwelling

We used a drifting sediment trap to collect marine snow aggregates *in situ* at 100 m and 400 m depth and collected TEP structures formed in roller tanks from 65 m and 400 m depth. These aggregates were analyzed using a novel three dimensional FISH approach to investigate the bacterial community structure and the possible changes with depth (Manuscript III).

Marine snow aggregates were dominated by *Synechococcus*, *Bacteroidetes* and *Alteromonas*, while the TEP structures were highly dominated by *Alteromonas*. All groups were enriched compared to the free living community. The community on the aggregates differed significantly at both depths, due to a decrease of *Bacteroidetes* and *Alteromonas* towards greater depth. This does not hold true for the TEP structures, where no significant difference of both communities were found. From these results we hypothesize a change in the bacterial community during sinking due to a combined effect of changes in nutrient quality due to degradation processes, grazing, decreasing temperature and increasing pressure.

2. Methods

The full-cycle rRNA approach was developed as a phylogeny-based toolbox for cultivation-independent studies of microbial diversity and ecology (Amann et al. 1995). Due to the importance of this approach, a review was written focussing on FISH techniques (Appendix I). A brief overview of methods used in this study will be given here, while detailed information are provided in the manuscripts.

Manuscript I

- CARD FISH according to the review by Thiele (Appendix I)
- Manual and semi-automated cell enumeration using counting machine in the semi-automatic mode (Pernthaler et al. 2003).
- Next generation sequencing using Roche/454 GS FLX Titanium technology (Ronaghi et al. 1996)

Manuscript II

- CARD FISH according to the review by Thiele (Appendix I) modified to suit nano- and picoplankton.
- Manual and automated cell enumeration using an automated counting machine using the macro MPISYS (Zeder unpublished) and the analyzes program ACMEtool 0.76 (Zeder unpublished)

Manuscript III

- Formation of aggregates using roller tanks (Shanks and Edmondson 1989) and *in situ* sampling of aggregates using a drifting sediment trap.
- Standard FISH and CARD FISH according to the review by Thiele (Appendix I)
- Manual and automated cell enumeration using an automated counting machine using the macro MPISYS (Zeder unpublished) and the analyzes program ACMEtool 0.76 (Zeder unpublished)
- Confocal laser scanning microscopy and three dimensional biovolume calculations using the program PHLIP (Mueller et al. 2006)

Methods

Some additional methods were used by co-authors of the three manuscripts. A brief overview will also be given here, while for details I refer to the manuscripts.

Manuscript I

- N. Ramaiah used thymidine (Fuhrman and Azam 1980) and leucine (Kirchman et al. 1985) uptake rates to determine bacterial activity

Manuscript II

- C. Wolf used Roche/454 GS FLX Titanium technology (Ronaghi et al. 1996)
- B. Fuchs used a FACScalibur flow cytometer to determine total cell numbers

3. Aims

3.1. General objective

The aim of this PhD thesis was to identify and investigate specific microbial communities, which are of importance for processes within the biological carbon pump.

3.2. Specific objectives

- I) During the iron fertilization experiment LOHAFEX, a response of the bacterial and archaeal community was predicted, following certain succession patterns based on differential niche preference and availability during the course of the bloom. The aim was to detect major bacterial and archaeal clades within the bloom and follow the succession during the 38 days from the bloom initiation to its decay, using molecular tools.

Manuscript I

- II) During the investigation of the bacterial and archaeal community during the LOHAFEX experiment, the hypothesis of a top-down control of nano- and picoplankton grazers on the bacterial and archaeal community was formulated. Consequently, the nano- and picoplankton community was investigated in order to identify the major groups in of these small eukaryotes and follow their succession over the course of the experiment.

Manuscript II

- III) Traditional methods for phytoplankton investigations, such as light microscopy, scanning electron microscopy, or marker pigment analyses, cannot provide sufficient taxonomical information to identify most nano- and picoplankton groups. Therefore, molecular methods were used for the investigation of these groups and the procedures had to be optimized for the samples prepared for classical analyses.

Manuscript II

- IV) Aggregate degradation is a major process within the biological carbon pump and bacteria were identified to be the major POC degrader. Still, not much is known about the identity

of these bacteria and the change of the aggregate attached community at different depths. The aim of the study was to identify the dominant bacterial groups on marine snow aggregates and TEP structures at different depths.

Manuscript III

- V) In order to investigate the bacterial community on sinking aggregates and TEP structures, a drifting sediment trap for *in situ* sampling and a novel three dimensional FISH approach had to be developed.

Manuscript III

4. Manuscripts

I. Microbial Community Response during the Iron Fertilization Experiment LOHAFEX

Stefan Thiele, Bernhard M. Fuchs, Nagappa Ramaiah, Rudolf Amann

Published 2012 in *Applied and Environmental Microbiology* 78(24): 8803-8812

Idea: S.T., B.M.F. and R.A.; Research designed by S.T. and B.M.F.; Sampling was done by B.M.F.; Experimental work was done by S.T.; Experimental data contribution by N.R.; The manuscript was written by S.T. with editorial assistance from B.M.F. and R.A.

II. Investigation of the nano- and picoplankton community during the iron fertilization experiment LOHAFEX

Stefan Thiele, Christian Wolf, Isabelle Schulz, Philipp Assmy, Katja Metfies, Bernhard M. Fuchs, Rudolf Amann

Submitted 2013 to *Applied and Environmental Microbiology*

Idea: S.T., B.M.F., P.A. and K.M.; Research designed by S.T., C.W., K.M. and B.M.F.; Sampling was done by B.M.F. and P.A.; Experimental work was done by S.T. and C.W.; The manuscript was written by S.T. with editorial assistance from B.M.F. and R.A.

III. Investigation of bacterial communities within *in situ* collected settling marine snow at different depths

Stefan Thiele, Bernhard M. Fuchs, Rudolf Amann, Morten H. Iversen

In preparation 2013

Idea: S.T., B.M.F. and M.H.I.; Research designed by S.T., M.H.I. and B.M.F.; Sampling was done by S.T. and M.H.I.; Experimental work was done by S.T.; Additional data contribution by M.H.I.; The manuscript was written by S.T. with editorial assistance from B.M.F., R.A. and M.H.I.

Manuscript I

Microbial Community Response during the Iron Fertilization Experiment LOHAFEX

Stefan Thiele, Bernhard M. Fuchs, Nagappa Ramaiah, Rudolf Amann

Published 2012 in *Applied and Environmental Microbiology* 78(24): 8803-8812

The pdf-document of this publication is not displayed due to copyright reasons. The publication can be accessed at: <http://aem.asm.org/content/78/24/8803.long>; DOI: 10.1128/AEM.01814-12.

Manuscript II

Investigation of the nano- and picoplankton community during the iron fertilization experiment LOHAFEX

Stefan Thiele, Christian Wolf, Isabelle Schulz, Philipp Assmy, Katja Metfies, Bernhard M. Fuchs,
Rudolf Amann

Submitted to *Applied and Environmental Microbiology*

1 **Investigation of the nano- and picoplankton community during the iron**
2 **fertilization experiment LOHAFEX**

3

4

5 Stefan Thiele^{1*}, Christian Wolf^{2*}, Isabelle Schulz^{2,3}, Philipp Assmy⁴, Katja Metfies²,
6 Bernhard M. Fuchs^{1#}, Rudolf Amann¹

7

8 ¹Max Planck Institute for Marine Microbiology, Celsiusstr. 1, 28359 Bremen, Germany

9 ²Alfred Wegener Institute for Polar and Marine Research, Am Handelshafen 12, 27570
10 Bremerhaven, Germany

11 ³MARUM – Center for Marine Environmental Sciences, University of Bremen, Leobener
12 Str., 28359 Bremen

13 ⁴Norwegian Polar Institute, Fram Centre, Hjalmar Johansens gt. 14, 9296 Tromsø,
14 Norway

15

16 # corresponding author

17 * these authors contributed equally

18 contact: Max Planck Institute for Marine Microbiology, Celsiusstr. 1, D-28359 Bremen,
19 Germany

20

21 email: bfuchs@mpi-bremen.de

22 phone: +49 421 2028-935

23 fax: +49 421 2028-790

24

25 **Acknowledgements**

26 We would like to thank the captain and crew of the RV Polarstern, the chief scientists of
27 the LOHAFEX project, V. Smetacek and W. Naqui, and all collaborators within
28 LOHAFEX. Furthermore we thank J. Köhler and E. Ruff for their help. This work was
29 funded by the Max Planck Society and funds dedicated to the Young Investigator Group
30 PLANKTOSENS (VH-NG-500) by the Initiative and Networking Fund of the Helmholtz
31 Association.

32

33

34

35

36

37

38

39

40

41

42

43

44

45

46

47 **Abstract**

48 Iron fertilization experiments are known to induce phytoplankton blooms in ocean areas
49 with low chlorophyll concentrations despite high nutrient concentrations. In silicate
50 limited waters iron fertilization experiments often induce phytoplankton blooms, which
51 consist mainly of nano- and picoplankton. We used flow cytometry, tag pyrosequencing
52 and catalyzed reported deposition fluorescence in situ hybridization (CARD-FISH) to
53 investigate the diversity and community structure of the nano- and picoplankton during
54 the iron fertilization experiment LOHAFEX. As previously shown for the bacterial
55 community, the diversity and community structure of the nano- and picoplankton
56 remained remarkably stable during the course of the experiment. Besides *Phaeocystis*, the
57 main bloom forming organism, *Syndiniales* and *Micromonas* phylotypes made up the
58 main part of the tag sequences within the fertilized patch. By CARD-FISH only
59 *Micromonas* and *Pelagophyceae* showed a peak in numbers at day 22 of the experiment,
60 while numbers of *Phaeocystis* and clades I and II of *Syndiniales* were almost constant
61 throughout the experiment inside the fertilized patch. The stable numbers within all
62 investigated groups are most likely indicative for a strong top down control by larger
63 grazers. With the combination of tag pyrosequencing and fluorescence in situ
64 hybridization with automated cell counting we were able to shed light into the “black
65 box” of the nano- and picoplankton during the LOHAFEX experiment.

66 **Introduction**

67 Phytoplankton blooms thrive seasonally or continuously in large parts of the oceans,
68 where nutrients are found in plenty. However, large areas of the oceans exhibit low
69 chlorophyll a concentrations despite high nutrient levels, a paradox known as the high
70 nutrient-low chlorophyll areas (HNLCs). For example, large parts of the Southern Ocean
71 are iron limited and thus do not support extensive phytoplankton blooms (1). In several
72 experiments it could be shown, that an artificial fertilization with iron induced
73 phytoplankton blooms. Although, these blooms were often dominated by diatoms (2–4),
74 nano- and picoplankton can make up a substantial fraction of the induced phytoplankton
75 blooms (5, 6). In areas with both iron and silicate limitations, nano- and picoplankton can
76 even dominate the blooms as found for example during the SAGE iron fertilization
77 experiment (7).

78 The iron fertilization experiment LOHAFEX ('loha' is Hindi for 'iron'; FEX for
79 Fertilization EXperiment) was conducted in a cold core eddy in the Southern Atlantic to
80 induce a phytoplankton bloom and investigate the effects on the biological carbon pump.
81 A phytoplankton bloom, dominated by nano- and picoplankton, was induced and
82 monitored over the course of the experiment (8). However, these small *Eukarya*, ranging
83 from 2 – 20 μm (nanoplankton) and 0.2 – 2 μm (picoplankton), are rarely explored in
84 detail and remain a "black box" in most studies.

85 In previous studies the identification of eukaryotic nano- and picoplankton was done by
86 direct microscopic counting of Lugol-fixed samples by the Utermöhl method (9),
87 scanning electron microscopy (SEM) (e.g. 61), and marker pigment analyzes (reviewed
88 in 23). More recently molecular biological tools, like catalyzed reporter deposition

89 fluorescence in situ hybridization (CARD FISH) and 454 tag pyrosequencing were
90 established for the identification and quantification of nano- and picoplankton (12–16).
91 Using the molecular techniques it was found that *Haptophyta* is one of the most abundant
92 marine groups which includes a high diversity of picoeukaryotes (17, 18) The most
93 prominent members of this group comprise the genus *Phaeocystis*, which forms large
94 blooms worldwide (19), and members of the class *Coccolithophyceae*. Recently a high
95 diversity especially for *Phaeocystis* was found using a set of molecular biological tools
96 (20). Within the *Chlorophyta*, the *Prasinophyceae* are highly diverse (18, 21, 22) and
97 paraphyletic and thus need to be newly classified based on molecular data (23, 24).
98 Investigations of this group were so far focused mainly on few subgroups. For example,
99 *Micromonas*, a genus within the *Mamiellophyceae* including the single species *M. pusilla*,
100 was found in high numbers in the British Channel (15), in clone libraries of pacific
101 coastal waters, in the Sargasso Sea (22), and in Arctic waters (25). Ribosomal RNA
102 studies showed, that members of the class *Pelagophyceae* (*Heterokonta*) are major
103 contributors to marine nano- and picoplankton communities (25, 26). Different clades of
104 the Marine Stramenopiles (MAST) were abundant worldwide (14).
105 In our earlier study, we could observe only little changes in the community composition
106 and abundance of *Bacteria* and *Archaea* in response to the iron fertilization experiment
107 LOHAFEX. We postulated a high grazing pressure onto this community exerted by nano-
108 and picoplankton grazers (27). In this study we used cutting edge molecular methods,
109 including flow cytometry, tag pyrosequencing (28) and CARD FISH (29) to investigate
110 the diversity and community structure of the nano- and picoplankton community during
111 LOHAFEX.

112 **Material & Methods**

113 Sampling

114 The iron fertilization experiment LOHAFEX was conducted during the RV “Polarstern”
115 cruise ANT XXV/3 (12th January till 6th March, 2009) as described previously (27).
116 Briefly, a cold core eddy in the South Atlantic was fertilized twice with 10 t Fe(II)SO₄
117 (on days 0 and 18) and monitored for 38 days. Samples for CARD-FISH analyses were
118 taken on day -1, prior to the start of the experiment, on days 5, 9, 14, 18, 22, 24, 33, 36
119 inside the fertilized patch (“IN” stations) and days 4, 16, 29, 35 (only 20 m), and 38
120 outside the fertilized patch (“OUT” stations, FIG. 1). Both IN and OUT stations were
121 situated within the eddy. On each day, 190 ml of water from 20 m and 40 m depth were
122 fixed with 10 ml acidic Lugol solution (5% final conc. v/v) and stored in brown glass
123 bottles at 4°C in the dark for 3 years until CARD FISH analysis. For DNA extraction for
124 tag pyrosequencing 90 l (day -1) , 85 l (day 9) , 75 l (day 16/ OUT), 67 l (day 18) were
125 sampled from 20 m depth on 0.2 µm pore size cellulose acetate filters (Sartorius,
126 Göttingen, Germany) after a prefiltration step over 5 µm. These samples were stored at -
127 80°C.

128

129 Flow cytometric cell counting

130 Total nano- and picoplankton was counted after fixation of fresh samples with particle-
131 free formaldehyde solution (final conc. 1% v/v) and staining with SYBR Green I
132 (1:10,000 dilution of stock) using a FACScalibur flow cytometer (BD Biosciences,
133 Heidelberg, Germany) as described previously (30, 31).

134

135 Tag-pyrosequencing

136 DNA extraction was done using the E.Z.N.A.TM SP Plant DNA Kit (Omega Bio-Tek,
137 Norcross, USA). Initially, the filters were incubated in lysis buffer at 65°C for 10 min
138 before performing all further steps as described in the manufacturer's instructions. The
139 eluted DNA was stored at -20°C until further analysis.

140 We amplified ~670 bp fragments of the 18S rRNA gene, containing the highly variable
141 V4-region, using the primer-set 528F (5'-GCGGTAATTCCAGCTCCAA-3') and 1055R
142 (5'-ACGGCCATGCACCACCACCCAT-3') modified after H.J. Elwood (32) as
143 described by Wolf (33). Pyrosequencing was performed on a Genome Sequencer FLX
144 system (Roche, Penzberg, Germany) by GATC Biotech AG (Konstanz, Germany).

145 Raw sequence reads were processed to obtain high quality reads. Reads with a length
146 below 300 bp, reads longer than >670 bp and reads with more than one uncertain base (N)
147 were excluded from further analysis. Chimera sequences were excluded using the
148 software UCHIME 4.2 (Edgar et al. 2011). The high quality reads of all samples were
149 clustered into operational taxonomic units (OTUs) at the 97% similarity level using the
150 software Lasergene 10 (DNASTAR, Madison, USA). Subsequently, reads not starting
151 with the forward primer were manually removed. Consensus sequences of each OTU
152 were generated and used for further analyses. The 97% similarity level was found
153 suitable to reproduce original eukaryotic diversity (34) and brace the sequencing errors
154 (35). Furthermore, it excludes intragenomic SSU polymorphisms, that can be as high as
155 2.9% of the sequence in dinoflagellate species (36). OTUs comprised of only one
156 sequence (singletons) were removed. The consensus sequences were aligned using the
157 software HMMER 2.3.2 (37) and implemented into a reference tree, containing about

158 1,200 high quality sequences of *Eukarya* from the SILVA reference database (SSU Ref
159 108), using the software pplacer 1.0 (Matsen et al. 2010). OTUs assigned to fungi and
160 metazoans were excluded from further analysis. Rarefaction curves were computed using
161 the freeware program Analytic Rarefaction 1.3. The data set generated in this study has
162 been deposited at GenBank's Short Read Archive (SRA) under Accession No
163 SRA064723.

164

165 CARD FISH

166 Nano- and picoplankton abundances were quantified for all stations in samples from 20 m
167 and 40 m depth by CARD FISH. In preliminary tests, the Lugol-fixed samples could not
168 be used directly for CARD FISH. Bright signals and stable cell counts could be achieved
169 only after an additional fixation step with formaldehyde. Hundred milliliter of the Lugol-
170 fixed sample was fixed for 1 h with formaldehyde (1% final concentration), destained
171 with 1 M sodium thiosulfate and filtered onto polycarbonate filters with 0.8 μm pore size
172 (Millipore, Tullagreen, Ireland). Due to limited sample amount, only 25 ml and 70 ml
173 were filtered for samples of day -1 and day 38 (both 20 m depth). CARD FISH was done
174 as described previously (29) modified after Thiele (38). Briefly, a permeabilization step
175 was done with Proteinase K (5 $\mu\text{g}/\text{ml}$) for 15 minutes for *Phaeocystis* samples, due to the
176 enhanced length (34 bp) of probe PHAEO03. Hybridization and amplification was done
177 on glass slides using 50 ml tubes or in Petri dishes using 700 ml glass chambers as
178 moisture chambers at 46°C. We used 14 horseradish peroxidase (HRP) labeled
179 oligonucleotide probes (TAB. 1) including the probe NON338 (39) as a control. All other
180 probes were chosen according to 454 tag sequencing results. For signal amplification,

Alexa488 labeled tyramides (40) were used for all probes and samples were stained with DAPI after the CARD procedure.

Fluorescence signals were counted manually on an Eclipse 50i microscope (Nikon, Amstelveen, Netherland), at 1000x magnification in 50 fields of view (FOV) per sample of duplicates. Since the wind mixed layer (WML) was 60 – 80 m deep during the experiment, results from 20 m and 40 m depth were treated as replicates. Quantification of cell numbers after CARD FISH was done with a Zeiss Axio Imager.Z2 microscope (Zeiss, Jena, Germany) with an automated stage. Image acquisition was done using the software package AxioVision Release 7.6 (Zeiss, Jena, Germany) and the macro MPISYS (Zeder unpublished) based on an automated focusing routine, sample area definition and image quality assessment (41–43). Only samples with a minimum of 15 picture pairs were taken into account and evaluated using the software ACMEtool 0.76 (Zeder unpublished) with an algorithm for nanoflagellate quantification. We used a combination of natural fluorescence of the cells, autofluorescence of cell pigments and probe signals which appeared to be clearly visible on pictures. DAPI signals were sometimes covered by strong autofluorescence, making a counting of the signals difficult. In addition, not all cells are autofluorescent or stained by the probe EUK516, thus making both signals insufficient for total cell counting. Therefore, we used the combination of all three signals to determine cells for total cell counts. Results from both depths were pooled and total cell numbers were calculated as a mean value of a minimum of 13 samples.

Probe design and re-evaluation

We designed two new probes for the subclades I and II of the *Syndiniales* clade (TAB. 1) using the ARB SILVA ref 108 database (44). We used 20% formamide for hybridization with both

probes. SYNI 1161 targets 71% of the *Syndiniales* group I sequences, with 151 outgroup hits within the dinoflagellates and 220 outgroup hits in other *Eukarya*. SYNII 675 targets 58% of the *Syndiniales* group II with 28 outgroup hits within the dinoflagellates and 347 in other *Eukarya* (SUP. 2)

The probe PRAS04 (15) was designed for *Prasinophyceae*. Since the clade was recently found to be paraphyletic and thus phylogenetically reviewed, we evaluated the probe PRAS04 and found a coverage of 95% for the class *Mamiellophyceae* (45) with only one outgroup hit in the *Dinophyceae* and one in the *Chrysophyceae*. Thus, we propose to use the probe only for *Mamiellophyceae*.

Statistics

The total cell numbers achieved by flow cytometry and automated counting of CARD FISH cells were compared using linear regressions. CARD FISH data were tested on normal distribution of the data using the Kolmogorov-Smirnov test and analyses of variance (ANOVA) were done accordingly. Normal distributed data were tested using one way ANOVAs including Holm-Sidak comparison and not-normal distributed data were tested using ANOVA on ranks. Differences between the IN and OUT stations were verified using t-tests. All analyses were done using SigmaStat 3.5 (Statcon, Witzenhausen, Germany).

225 **Results**

226

227 Nano- and picoplankton cell numbers

228 During LOHAFEX, the nano- and picoplankton cells were enumerated on freshly fixed
229 samples inside and outside the fertilized patch by flow cytometry on board. Inside the
230 patch nano- and picoplankton abundances increased significantly ($p < 0.001$) from $7.5 \times$
231 10^3 cells ml^{-1} on day 5 to 1.9×10^4 cells ml^{-1} on day 22 (FIG. 2 A). Outside the fertilized
232 patch cell numbers were rather stable ($1.0 \times 10^4 \pm 1.2 \times 10^3$ cells ml^{-1}) but showed two
233 maxima on day 29 (1.8×10^4 cells ml^{-1}) and day 38 (1.7×10^4 cells ml^{-1}) (FIG. 2 A).

234 Cell counts obtained with automated cell counting after CARD FISH of Lugol- and
235 formaldehyde fixed samples were by a factor of ~ 2 (1.2- 3.1) lower compared to the flow
236 cytometric direct counts. Similar to the flow cytometric counts, abundances peaked on
237 day 22 with 9.3×10^3 cells ml^{-1} ($p < 0.001$), but otherwise cell numbers remained rather
238 constant at $6.1 \pm 1.3 \times 10^3$ cells ml^{-1} (FIG. 2 B).

239 Community composition

240 The eukaryotic diversity in the 0.2 to 5 μm fraction was assessed in the eddy one day
241 before the start of the experiment, during the experiment on days 9 and 18 inside the
242 fertilized patch, and at day 16 outside the fertilized patch using tag pyrosequencing (FIG
243 3). The Shannon diversity index increased from 3.49 at day -1 to 3.93 at day 18 inside the
244 patch and to 3.86 outside the patch (TAB 2). The chao1 index showed an increase from
245 633 (day -1) to 879 (day 9) and 803 (day 18), but showed numbers as high as 899 at the
246 OUT station on day 16 (TAB 2).

247 Although, the diversity increased over the course of the experiment, all four samples were
248 similar in the major group composition (FIG 3). The most frequent tags in all samples
249 originated from *Syndiniales* (~26-33%), followed by *Chlorophyta* (24-29%) and
250 *Haptophyceae* (~21-28%). Some of the 21 abundant phylotypes (>1% of all sequences)
251 showed some fluctuations in sequence abundance over the course of the experiment (FIG
252 3). The most abundant genus was *Phaeocystis* (*Haptophyta*) accounting for ~14% (day 18)
253 to ~23% (day -1) of all sequences (FIG 3). This phylotype showed a slight decrease
254 inside the fertilized patch. Among the *Mamiellophyceae*, a class within the *Chlorophyta*,
255 two different phylotypes affiliated to the genus *Micromonas* were most dominant (17.3-
256 18.5%) inside the patch. Within this genus we observed a shift from *Micromonas*
257 phylotype A to *Micromonas* phylotype B inside the patch, while both phylotypes
258 decreased in the OUT station (FIG 3). A phylotype of the *Monomastix* genus (8.5%) was
259 dominating the *Mamiellophyceae* outside the fertilized patch. Only the *Pelagophyceae*
260 showed a distinct decrease in sequence abundance from 5.8% at day -1 to 2.0% at day 18
261 inside the patch. The two abundant phylotypes within the *Pelagophyceae* were found in
262 highest abundance at the OUT station on day 16, with ~5% (*Pelagomonas* sp.) and ~3%
263 (uncultured *Pelagophyceae*) of total sequences (FIG 3). Inside the fertilized patch both
264 were found only in low sequence abundances (~1-2% of total sequences). Only two
265 abundant phylotypes belonging to MAST (*Stramenopila*) were found, each with the
266 highest sequence abundance of ~1.2% at day 18 (FIG 3). *Syndiniales* were present with
267 seven different abundant unclassified phylotypes which were labeled arbitrarily with
268 letters from A to G (SUP 2). The phylotype *Syndiniales* A (Dino-group II) was by far the
269 most abundant one in all samples with a sequence abundance of ~11-15%, while other

270 *Syndiniales* phylotypes showed sequence abundances of ~1-3.5% or were absent in some
271 samples (FIG 3).

272

273 Quantification of specific nano- and picoplankton clades

274 For eight of the dominant clades in tag pyrosequencing, specific probes were used to
275 quantify their *in situ* abundance by CARD FISH. The EUK516 probe, specific for most
276 *Eukarya* (39), showed abundances which were about 1.8-fold lower than the total cell
277 numbers (FIG. 4). The numbers of EUK516 stained cells were highest at day -1 with 5.8
278 $\times 10^3$ cells ml^{-1} , decreasing to 1.9×10^3 cells ml^{-1} on day 9, before a second peak of $4.7 \times$
279 10^3 cells ml^{-1} and 4.8×10^3 cells ml^{-1} on days 22 and 24 inside the fertilized patch (FIG. 4
280 A). EUK-positive cell numbers were relatively constant outside the patch, but were as
281 high as 7.0×10^3 cells ml^{-1} on day 38, which was significantly different from the
282 comparable IN station on day 36 ($p=0.045$) (FIG. 4 B).

283 In order to investigate the nano- and picoplankton community, we used CARD FISH
284 probes with a nested specificity with different taxonomic depths. The sum of the counts
285 with these nested probes covered the counts of the EUK516 probe in most of the samples
286 analyzed (FIG. 4A, 4B). Within the nano- and picoplankton community inside the
287 fertilized patch, *Haptophyta*, mainly from the genus *Phaeocystis* were contributors to the
288 nano- and picoplankton community. However, abundances of both clades did not change
289 significantly within the fertilized patch over the course of the experiment (FIG. 5 A + B).
290 Values were constant at about 1.0×10^3 cells ml^{-1} for *Haptophyta* and 5.0×10^2 cells ml^{-1}
291 for *Phaeocystis*, thus *Phaeocystis* accounted for about 50% of the *Haptophyta*. At the
292 OUT station on day 16, higher numbers of *Phaeocystis* were found with 1.1×10^3 cells

293 ml⁻¹, resulting also in significantly higher numbers of *Haptophyta* (1.5×10^3 cells ml⁻¹)
294 ($p=0.01$). *Mamiellophyceae*, a second dominant clade in the tag sequences, showed a
295 higher variation in cell numbers inside the fertilized patch, while cell numbers in the
296 OUT stations remained rather constant. After a rather dramatic initial decrease from $3.2 \times$
297 10^3 cells ml⁻¹ to 5.9×10^2 cells ml⁻¹ on day 9 inside the patch, cells increased again to 1.8
298 $\times 10^3$ cells ml⁻¹ on day 22. This abundance of *Mamiellophyceae* was significantly ($p=0.03$)
299 higher compared to the OUT station on day 29 (FIG. 5 C). The dominant subgroup of
300 *Mamiellophyceae*, namely *Micromonas*, mimicked these patterns, showing a decrease in
301 cell numbers from 1.3×10^3 cells ml⁻¹ on day -1 to numbers around 4.4×10^2 cells ml⁻¹ on
302 day 9. Again elevated numbers were found on day 22, which were as high as 1.2×10^3
303 cells ml⁻¹ and thus significantly ($p=0.028$) higher than the following OUT station at day
304 29. On average *Micromonas* accounted for ~72% of the *Mamiellophyceae* (FIG. 5 D).
305 *Pelagophyceae* were also found rather stable in- and outside of the patch with a pattern
306 similar to the *Mamiellophyceae* (FIG 5 E). Elevated numbers as high as 7.2×10^2 cells
307 ml⁻¹ and 7.6×10^2 cells ml⁻¹ were found on days -1 and 22, respectively. No significant
308 differences to the OUT stations were found for this clade. Abundances of Marine
309 Stramenopiles (MAST) were low and never exceeded 1.7×10^2 cells ml⁻¹ during the
310 course of the experiment (FIG 5 F). Also the numbers of both *Syndiniales* clades were
311 low and oscillated around 7.7×10^1 cells ml⁻¹ (*Syndiniales* clade I) and around 1.8×10^2
312 cells ml⁻¹ (*Syndiniales* clade II) within and outside of the fertilized patch (FIG. 5 G + H).
313 For both *Syndiniales* clades no cells could be detected on day 29.

314 **Discussion**

315

316 During the 38 days of the LOHAFEX experiment a phytoplankton bloom was induced
317 and the chlorophyll a concentration inside the fertilized patch more than doubled (27). On
318 board analyses already indicated that diatoms were limited by silicate ($<2 \mu\text{M}$) and thus
319 showed only a moderate response to iron addition. The major biomass of the bloom was
320 constituted by the pico- and nanoflagellate community (8). The high abundance of nano-
321 and picoplankton was postulated to exert grazing pressure on the bacterial and archaeal
322 community (27). Consequently, we investigated the nano- and picoplankton community
323 using a combination of flow cytometry, tag pyrosequencing, CARD FISH and automated
324 cell counting. It turned out that the methods used had some technical challenges.

325 Shipboard flow cytometry revealed consistently higher cell numbers compared to
326 automated microscopic cell counting. An overestimation of cell counts by flow cytometry
327 was previously reported (46) and might originate from autofluorescent detritus as well as
328 from the detection of large bacterial cells such as *Roseobacter* or *Gammaproteobacteria*.
329 Both bacterial groups were abundant during the LOHAFEX experiment (27). In turn,
330 fixation could lead to an underestimation of total cell counts due to cell shrinkage and cell
331 disruption caused by the fixative (47). Formaldehyde fixation was used for flow
332 cytometric analyses, while for automated cell counting and CARD FISH cell were first
333 fixed with Lugol solution and subsequently with formaldehyde. Possibly the long-term
334 storage the samples of >3 years might have caused cell loss which led to approximately
335 50% lower microscopic cell counts compared to flow cytometric counts. Another source
336 of cell loss might be the filtration and washing steps necessary for CARD FISH. Small

337 picoplankton cells might have passed the polycarbonate filter pores (48, 49) or might
338 have been lost in washing steps during CARD FISH. However, we were able to
339 successfully apply CARD FISH and automated cell counting on Lugol fixed samples
340 even after the prolonged storage time.

341 With the probe EUK516, targeting *Eukarya*, about 50-70% of all nano- and pico
342 eukaryotic cells showed a signal in our samples after CARD FISH. The sum of cells
343 detected by all clade-specific probes was almost as high as the counts of the EUK516
344 probe (~90%) and resembled largely the representation of dominant clades found with tag
345 pyrosequencing.

346 The high representation of *Phaeocystis* sequences in the tag libraries somehow conflicted
347 with low CARD FISH numbers. This is surprising, because observations by microscopy
348 identified *Phaeocystis* responsible for the main increase in chlorophyll a values (8). Most
349 likely fluorescence *in situ* hybridization signals have been quenched by the strong
350 autofluorescence of the *Phaeocystis* chloroplasts resulting in false-negative cells (50).

351 Alternatively organic scales, found in Scanning Electron Microscopy (SEM) pictures of
352 solitary *Phaeocystis* cells from the LOHAFEX experiment (8), might have hindered the
353 penetration of the probe into the cell. Thus, cell counts might be underestimated for
354 *Phaeocystis*. Also for *Syndiniales* the fraction of tag sequences largely deviate from the
355 relative abundance of cells detected as *Syndiniales* by CARD FISH. A possible
356 explanation might be that members of the *Syndiniales* group have been described as
357 parasites (51, 52). Cells residing inside dinoflagellates might be inaccessible for large
358 HRP-labeled oligonucleotide probes. Furthermore, the detection of the newly designed
359 probes SYNI 1161 and SYNII 675 might remain insufficient for the detection of all cells

360 of this group, since no *Syndiniales* culture was available and probe testing had to be done
361 directly on the samples. Besides technical challenges, *Syndiniales* might have multiple
362 chromosome copies, as it is known for the neighboring group of *Dinoflagellata* (53).
363 Thus, the number of 18S rRNA gene copies might be elevated, resulting in high
364 abundances in the tag sequences.

365 For the different MAST clades we used specific oligonucleotide probes and found a
366 rather stable community structure. However, all clades were found in rather low numbers
367 compared to the reported $>1.0 \times 10^2$ MAST 1 cells ml⁻¹ in the Southern Ocean (14).

368 In several clades an initial decrease in abundance was followed by a peak on day 22
369 inside the fertilized patch. This pattern was especially pronounced for the
370 *Mamiellophyceae* in general and for the clades *Micromonas* and *Pelagophyceae* in
371 particular. A possible explanation for the initial massive decrease in cell numbers might
372 be an active grazer community, which developed during a bloom prior to the experiment
373 and which immediately counteracted the response of the nano- and picoplankton
374 community to the iron fertilization. The subsequent increase of these clades towards day
375 22 might be caused by the second iron fertilization on day 18. Ultimately nano- and
376 picoplankton could benefit from elevated iron concentrations and started to out-compete
377 their grazers and to increase in cell numbers (54). Another reason might be a release of
378 grazing pressure on the nano- and picoplankton community by increased copepod
379 numbers, which kept the dinoflagellate and ciliate grazer community under control.
380 Interestingly, highest numbers in the bacterial and archaeal community were found on
381 day 18 and thus could support growth of the hetero- and mixotroph nano- and
382 picoplankton (27). heterotrophic pico-eukaryotes like MAST (14) or mixotrophic

383 *Micromonas* are known to feed on bacteria (55) and might profit from higher prey
384 numbers. The second cell decline after the maximum on day 22 could be the result of a
385 reinforced grazing pressure on nano- and picoplankton by predators, which grew on the
386 increased nano- and picoplankton numbers.

387 Our results show that tag pyrosequencing and CARD FISH are suitable tools to open the
388 “black box” of the small marine *Eukarya*. While tag pyrosequencing provides valuable
389 information about the diversity and community structure, it also provides guidance for the
390 selection of oligonucleotide probes for CARD FISH quantifications. These enumerations
391 have a profound taxonomic resolution compared to light microscopy and pigment
392 analyses, and allow for faster sample analyses than electron microscopy. In addition, we
393 were able to show that samples fixed with Lugol solution for light microscopy can be
394 used for CARD FISH analyses even after long storage times. Still not all nano- and
395 picoplankton clades can be covered, showing the urgent need of further sequencing and
396 probe design, in order to fully investigate these important mediators between the world of
397 *Bacteria* and *Archaea* and the world of the microzooplankton.

398 **References**

- 399 1. **Martin JH**. 1990. Glacial-interglacial CO₂ change: The iron hypothesis.
400 *Paleoceanography* **5**:PP. 1–13.
- 401 2. **Martin JH, Coale KH, Johnson KS, Fitzwater SE, Gordon RM, Tanner SJ,**
402 **Hunter CN, Elrod VA, Nowicki JL, Coley TL, Barber RT, Lindley S, Watson**
403 **AJ, Van Scoy K, Law CS, Liddicoat MI, Ling R, Stanton T, Stockel J, Collins**
404 **C, Anderson A, Bidigare R, Ondrusek M, Latasa M, Millero FJ, Lee K, Yao W,**
405 **Zhang JZ, Friederich G, Sakamoto C, Chavez F, Buck K, Kolber Z, Greene R,**
406 **Falkowski P, Chisholm SW, Hoge F, Swift R, Yungel J, Turner S, Nightingale**
407 **P, Hatton A, Liss P, Tindale NW**. 1994. Testing the iron hypothesis in ecosystems
408 of the equatorial Pacific Ocean. *Nature* **371**:123–129.
- 409 3. **deBaar HJW, Boyd PW, Coale KH, Landry MR, Tsuda A, Assmy P, Bakker**
410 **DCE, Bozec Y, Barber RT, Brzezinski MA, Buesseler KO, Boyé M, Croot PL,**
411 **Gervais F, Gorbunov MY, Harrison PJ, Hiscock WT, Laan P, Lancelot C, Law**
412 **CS, Levasseur M, Marchetti A, Millero FJ, Nishioka J, Nojiri Y, Oijen T van,**
413 **Riebesell U, Rijkenberg MJA, Saito H, Takeda S, Timmermans KR, Veldhuis**
414 **MJW, Waite AM, Wong C-S**. 2005. Synthesis of iron fertilization experiments:
415 From the iron age in the age of enlightenment. *J. Geophys. Res.* **110**:24 PP.
- 416 4. **Smetacek V, Klaas C, Strass VH, Assmy P, Montresor M, Cisewski B, Savoye**
417 **N, Webb A, D' Ovidio F, Arrieta JM, Bathmann U, Bellerby R, Berg GM,**
418 **Croot P, Gonzalez S, Henjes J, Herndl GJ, Hoffmann LJ, Leach H, Losch M,**
419 **Mills MM, Neill C, Peeken I, Röttgers R, Sachs O, Sauter E, Schmidt MM,**
420 **Schwarz J, Terbrüggen A, Wolf-Gladrow D**. 2012. Deep carbon export from a
421 Southern Ocean iron-fertilized diatom bloom. *Nature* **487**:313–319.
- 422 5. **Hall JA, Safi K**. 2001. The impact of in situ Fe fertilisation on the microbial food
423 web in the Southern Ocean. *Deep Sea Res. Part II: Topical Studies in Oceanography*
424 **48**:2591–2613.
- 425 6. **Coale KH, Johnson KS, Chavez FP, Buesseler KO, Barber RT, Brzezinski MA,**
426 **Cochlan WP, Millero FJ, Falkowski PG, Bauer JE, Wanninkhof RH, Kudela**
427 **RM, Altabet MA, Hales BE, Takahashi T, Landry MR, Bidigare RR, Wang X,**
428 **Chase Z, Strutton PG, Friederich GE, Gorbunov MY, Lance VP, Hiltling AK,**
429 **Hiscock MR, Demarest M, Hiscock WT, Sullivan KF, Tanner SJ, Gordon RM,**
430 **Hunter CN, Elrod VA, Fitzwater SE, Jones JL, Tozzi S, Koblizek M, Roberts**
431 **AE, Herndon J, Brewster J, Ladizinsky N, Smith G, Cooper D, Timothy D,**
432 **Brown SL, Selph KE, Sheridan CC, Twining BS, Johnson ZI**. 2004. Southern
433 Ocean iron enrichment experiment: Carbon cycling in high- and low-Si waters.
434 *Science* **304**:408–414.
- 435 7. **Peloquin J, Hall J, Safi K, Ellwood M, Law CS, Thompson K, Kuparinen J,**
436 **Harvey M, Pickmere S**. 2011. Control of the phytoplankton response during the
437 SAGE experiment: A synthesis. *Deep Sea Res. Part II: Topical Studies in*
438 *Oceanography* **58**:824–838.
- 439 8. **Schulz I, Assmy P, Rajdeep R, Gauns M, Thiele S, Wolf C, Klaas C, Smetacek**
440 **V**. 2013. Mechanisms determining species succession and dominance during an
441 iron-induced phytoplankton bloom in the Southern Ocean (LOHAFEX). In
442 preparation.

- 443 9. **Utermöhl H.** 1958. Zur Vervollkommnung der quantitativen Phytoplankton-
 444 Methodik. Mitt. int. Ver. theor. angew. Limnol. **9**:1–38.
- 445 10. **Zingone A, Chretiennot-Dinet M-J, Lange M, Medlin L.** 1999. Morphological
 446 and genetic charecterization of *Phaeocystis cordata* and *P. jahnii*
 447 (*Prymnesiophyceae*), two new species from the mediterranean sea. J. Phycol. 1322–
 448 1337.
- 449 11. **Jeffrey S, Wright S.** 2006. Photosynthetic pigments in marine microalgae: insights
 450 from cultures and the sea. Algal cultures, Analogues of blooms and applications,
 451 volume 1.
- 452 12. **Cheung MK, Au CH, Chu KH, Kwan HS, Wong CK.** 2010. Composition and
 453 genetic diversity of picoeukaryotes in subtropical coastal waters as revealed by 454
 454 pyrosequencing. ISME J. **4**:1053–1059.
- 455 13. **Massana R, Guillou L, Díez B, Pedrós-Alió C.** 2002. Unveiling the Organisms
 456 behind Novel Eukaryotic Ribosomal DNA Sequences from the Ocean. Appl.
 457 Environ. Microbiol. **68**:4554–4558.
- 458 14. **Massana R, Terrado R, Forn I, Lovejoy C, Pedrós-Alió C.** 2006. Distribution
 459 and abundance of uncultured heterotrophic flagellates in the world oceans. Environ.
 460 Microbiol. **8**:1515–1522.
- 461 15. **Not F, Latasa M, Marie D, Cariou T, Vaultot D, Simon N.** 2004. A Single Species,
 462 *Micromonas pusilla* (*Prasinophyceae*), Dominates the Eukaryotic Picoplankton in
 463 the Western English Channel. Appl. Environ. Microbiol. **70**:4064–4072.
- 464 16. **Stoeck T, Bass D, Nebel M, Christen R, Jones MDM, Breiner H-W, Richards
 465 TA.** 2010. Multiple marker parallel tag environmental DNA sequencing reveals a
 466 highly complex eukaryotic community in marine anoxic water. Mol. Ecol. **19**:21–31.
- 467 17. **Moon-van der Staay SY, Van der Staay GWM, Guillou L, Vaultot D, Claustre
 468 H, Medlin LK.** 2000. Abundance and Diversity of *Prymnesiophytes* in the
 469 Picoplankton Community from the Equatorial Pacific Ocean Inferred from 18S
 470 rDNA Sequences. Limnol. Oceanogr. **45**:98–109.
- 471 18. **Cuvelier ML, Allen AE, Monier A, McCrow JP, Messié M, Tringe SG, Woyke
 472 T, Welsh RM, Ishoey T, Lee J-H, Binder BJ, DuPont CL, Latasa M, Guigand C,
 473 Buck KR, Hilton J, Thiagarajan M, Caler E, Read B, Lasken RS, Chavez FP,
 474 Worden AZ.** 2010. Targeted Metagenomics and Ecology of Globally Important
 475 Uncultured Eukaryotic Phytoplankton. PNAS **107**:14679–14684.
- 476 19. **Schoemann V, Becquevort S, Stefels J, Rousseau V, Lancelot C.** 2005.
 477 *Phaeocystis* blooms in the global ocean and their controlling mechanisms: a review.
 478 J. Sea Res. **53**:43–66.
- 479 20. **Medlin L, Zingone A.** 2007. A Taxonomic Review of the Genus *Phaeocystis*.
 480 Biogeochemistry **83**:3–18.
- 481 21. **Guillou L, Eikrem W, Chrétiennot-Dinet M-J, Le Gall F, Massana R, Romari
 482 K, Pedrós-Alió C, Vaultot D.** 2004. Diversity of Picoplanktonic *Prasinophytes*
 483 Assessed by Direct Nuclear SSU rDNA Sequencing of Environmental Samples and
 484 Novel Isolates Retrieved from Oceanic and Coastal Marine Ecosystems. Protist
 485 **155**:193–214.
- 486 22. **Worden AZ.** 2006. Picoeukaryote diversity in coastal waters of the Pacific Ocean.
 487 Aquat Microb Ecol **43**:165–175.

- 488 23. **Lewis LA, McCourt RM.** 2004. Green Algae and the Origin of Land Plants. *Am. J.*
489 *Bot.* **91**:1535–1556.
- 490 24. **Adl SM, Simpson AGB, Farmer MA, Andersen RA, Anderson OR, Barta JR,**
491 **Bowser SS, Brugerolle G, Fensome RA, Fredericq S, James TY, Karpov S,**
492 **Kugrens P, Krug J, Lane CE, Lewis LA, Lodge J, Lynn DH, Mann DG,**
493 **Mccourt RM, Mendoza L, Moestrup Ø, Mozley-Standridge SE, Nerad TA,**
494 **Shearer CA, Smirnov AV, Spiegel FW, Taylor MFJR.** 2005. The New Higher
495 Level Classification of Eukaryotes with Emphasis on the Taxonomy of Protists. *J.*
496 *Euk. Microbiol.* **52**:399–451.
- 497 25. **Balzano S, Marie D, Gourvil P, Vaultot D.** 2012. Composition of the summer
498 photosynthetic pico and nanoplankton communities in the Beaufort Sea assessed by
499 T-RFLP and sequences of the 18S rRNA gene from flow cytometry sorted samples.
500 *ISME J.* **6**:1480–1498.
- 501 26. **Andersen RA, Sounders GW, Paskind MP, Sexton JP.** 1993. Ultrastructure and
502 18S rRNA gene sequence for *Pelagomonas Calceolata* Gen. et Sp. Nov. and the
503 Description of a new algal class, the Pelagophyceae Classis Nov. *J. Phycol.* **29**:701–
504 715.
- 505 27. **Thiele S, Fuchs BM, Ramaiah N, Amann R.** 2012. Microbial Community
506 Response During the Iron Fertilization Experiment LOHAFEX. *Appl. Environ.*
507 *Microbiol.* **78**:8803–8812.
- 508 28. **Ronaghi M, Karamohamed S, Pettersson B, Uhlén M, Nyrén P.** 1996. Real-
509 Time DNA Sequencing Using Detection of Pyrophosphate Release. *Analyt.*
510 *Biochem.* **242**:84–89.
- 511 29. **Pernthaler A, Pernthaler J, Amann R.** 2002. Fluorescence in situ hybridization
512 and catalyzed reporter deposition for the identification of marine bacteria. *Appl.*
513 *Environ. Microbiol.* **68**:3094–3101.
- 514 30. **Marie D, Partensky F, Jacquet S, Vaultot D.** 1997. Enumeration and Cell Cycle
515 Analysis of Natural Populations of Marine Picoplankton by Flow Cytometry Using
516 the Nucleic Acid Stain SYBR Green I. *Appl. Environ. Microbiol.* **63**:186–193.
- 517 31. **Tarran GA, Heywood JL, Zubkov MV.** 2006. Latitudinal changes in the standing
518 stocks of nano- and picoeukaryotic phytoplankton in the Atlantic Ocean. *Deep Sea*
519 *Res. Part II: Topical Studies in Oceanography* **53**:1516–1529.
- 520 32. **Elwood HJ, Olsen GJ, Sogin ML.** 1985. The small-subunit ribosomal RNA gene
521 sequences from the hypotrichous ciliates *Oxytricha nova* and *Stylonychia pustulata*.
522 *Mol. Biol. Evol.* **2**:399–410.
- 523 33. **Wolf C, Frickenhaus S, Kiliyas ES, Peeken I, Metfies K.** In Press. Regional
524 variability in eukaryotic protist communities in the Amundsen Sea. *Antarctic*
525 *Science*.
- 526 34. **Behnke A, Engel M, Christen R, Nebel M, Klein RR, Stoeck T.** 2011. Depicting
527 more accurate pictures of protistan community complexity using pyrosequencing of
528 hypervariable SSU rRNA gene regions. *Environment. Microbiol.* **13**:340–349.
- 529 35. **Kunin V, Engelbrekton A, Ochman H, Hugenholtz P.** 2009. Wrinkles in the rare
530 biosphere: pyrosequencing errors can lead to artificial inflation of diversity
531 estimates. *Environ. Microbiol.* **12**:118–123.

- 532 36. **Miranda LN, Zhuang Y, Zhang H, Lin S.** 2012. Phylogenetic analysis guided by
533 intragenomic SSU rDNA polymorphism refines classification of “*Alexandrium*
534 *tamarense*” species complex. *Harmful Algae* **16**:35–48.
- 535 37. **Eddy SR.** 2011. Accelerated Profile HMM Searches. *PLoS Comput Biol*
536 **7**:e1002195.
- 537 38. **Thiele S, Fuchs B, Amann R.** 2011. Identification of microorganisms using the
538 ribosomal RNA approach and fluorescence in situ hybridization, p. 171–189. *In*
539 *Treatise on Water Science* Wilderer, P. Elsevier, Oxford: Academic Press.
- 540 39. **Amann RI, Binder BJ, Olson RJ, Chisholm SW, Devereux R, Stahl DA.** 1990.
541 Combination of 16S rRNA-targeted oligonucleotide probes with flow cytometry for
542 analyzing mixed microbial populations. *Appl. Environ. Microbiol.* **56**:1919–1925.
- 543 40. **Pernthaler J, Amann R.** 2004. Sensitive multi-color fluorescence in situ
544 hybridization for the identification of environmental microorganisms. *Molecular*
545 *Microbial Ecology Manual* **3**:711–726.
- 546 41. **Zeder M, Kohler E, Pernthaler J.** 2009. Automated quality assessment of
547 autonomously acquired microscopic images of fluorescently stained bacteria.
548 *Cytometry* **9999A**:NA–NA.
- 549 42. **Zeder M, Ellrott A, Amann R.** 2011. Automated sample area definition for high-
550 throughput microscopy. *Cytometry* **79A**:306–310.
- 551 43. **Zeder M, Pernthaler J.** 2009. Multispot live-image autofocusing for high-
552 throughput microscopy of fluorescently stained bacteria. *Cytometry* **75A**:781–788.
- 553 44. **Pruesse E, Quast C, Knittel K, Fuchs BM, Ludwig W, Peplies J, Glöckner FG.**
554 2007. SILVA: a comprehensive online resource for quality checked and aligned
555 ribosomal RNA sequence data compatible with ARB. *Nucl. Acids Res.* **35**:7188–
556 7196.
- 557 45. **Marin B, Melkonian M.** 2010. Molecular Phylogeny and Classification of the
558 Mamiellophyceae class. nov. (Chlorophyta) based on Sequence Comparisons of the
559 Nuclear- and Plastid-encoded rRNA Operons. *Protist* **161**:304–336.
- 560 46. **Li WKW, Wood AM.** 1988. Vertical distribution of North Atlantic
561 ultraphytoplankton: analysis by flow cytometry and epifluorescence microscopy.
562 *Deep Sea Res. Part I: Oceanograph. Res. Papers* **35**:1615–1638.
- 563 47. **Choi JW, Stoecker DK.** 1989. Effects of Fixation on Cell Volume of Marine
564 Planktonic Protozoa. *Appl. Environ. Microbiol.* **55**:1761–1765.
- 565 48. **Cynar FJ, Estep KW, Sieburth JM.** 1985. The Detection and Characterization of
566 Bacteria-Sized Protists in “Protist-Free” Filtrates and Their Potential Impact on
567 Experimental Marine Ecology. *Microb. Ecol.* **11**:281–288.
- 568 49. **Gasol JM, Morn XAG.** 1999. Effects of filtration on bacterial activity and
569 picoplankton community structure as assessed by flow cytometry. *Aquat Microb*
570 *Ecol* **16**:251–264.
- 571 50. **Lange M, Guillou L, Vaultot D, Simon N, Amann RI, Ludwig W, Medlin LK.**
572 1996. Identification of the class Prymnesiophyceae and the genus *Phaeocystis* with
573 ribosomal RNA-targeted nucleic acid probes detected by flow cytometry. *J. Phycol.*
574 **32**:858–868.
- 575 51. **Coats DW, Bockstahler KR.** 1994. Occurrence of the Parasitic Dinoflagellate
576 *Amoebophrya ceratii* in Chesapeake Bay Populations of *Gymnodinium sanguineum*.
577 *J. Euk. Microbiol.* **41**:586–593.

- 578 52. **Coats DW, Adam EJ, Gallegos CL, Hedrick S.** 1996. Parasitism of
579 Photosynthetic Dinoflagellates in a Shallow Subestuary of Chesapeake Bay, USA.
580 53. **Spector DL.** 1984. Dinoflagellate nuclei, p. 107–147. *In* Dinoflagellates, D. L.
581 Spector [ed.]. Academic Press, Inc., Orlando, Florida, USA.
582 54. **Rokkan Iversen K, Seuthe L.** 2010. Seasonal microbial processes in a high-
583 latitude fjord (Kongsfjorden, Svalbard): I. Heterotrophic bacteria, picoplankton and
584 nanoflagellates. *Polar Biol.* **34**:731–749.
585 55. **Gonzalez JM, Sherr BF, Sherr E.** 1993. Digestive enzyme activity as a
586 quantitative measure of protistan grazing: the acid lysozyme assay for bacterivory.
587 *Mar. Ecol. Prog. Ser.* **100**:197–206.
588 56. **Quast C, Pruesse E, Yilmaz P, Gerken J, Schweer T, Yarza P, Peplies J,**
589 **Glockner FO.** 2012. The SILVA ribosomal RNA gene database project: improved
590 data processing and web-based tools. *Nucl. Acids. Res.* **41**:D590–D596.
591 57. **Wallner G, Amann R, Beisker W.** 1993. Optimizing fluorescent in situ
592 hybridization with rRNA-targeted oligonucleotide probes for flow cytometric
593 identification of microorganisms. *Cytometry* **14**:136–143.
594 58. **Simon N, Campbell L, Ornlófsdóttir E, Groben R, Guillou L, Lange M, Medlin**
595 **LK.** 2000. Oligonucleotide probes for the identification of three algal groups by dot
596 blot and fluorescent whole-cell hybridization. *J. Eukaryot. Microbiol.* **47**:76–84.

597 **Tables**

598 TAB 1: List of oligonucleotides used in this study. ^a Formamide concentration in the
599 CARD FISH hybridization buffer.

600

601 TAB 2: List of diversity indices calculated from the tag sequences.

602

603 **Figures**

604 FIG 1: Map of the fertilized area. The chlorophyll *a* picture shows the LOHAFEX bloom
605 (encircled). Stations and experiment days of both the IN (black) and OUT stations (white)
606 are shown in the small map. The X marks day -1 before the experiment. The globe and
607 the inset map were generated with the M_Map package for Matlab (version 7.12.0.635;
608 MathWorks, Natick, MA). The chlorophyll *a* data were downloaded from the NASA
609 website <http://oceancolor.gsfc.nasa.gov/>.

610

611 FIG 2: Total cell counts of all stations inside the fertilized patch achieved by using flow
612 cytometric (FCM) counting and automated microscopic counting after CARD FISH
613 staining. Black spheres with straight lines represent stations inside while white spheres
614 with dashed lines represent stations outside the fertilized patch.

615

616 FIG 3: Relative 18S rRNA gene amplicon frequency revealed by tag pyrosequencing at
617 20 m depth.

618

619 FIG 4: Total cell numbers of cells stained with the EUK516 probe of the IN (black, A)
620 and OUT (white, B) stations. Bar charts represent the coverage of the EUK516 probe by
621 all other probes used in this study.

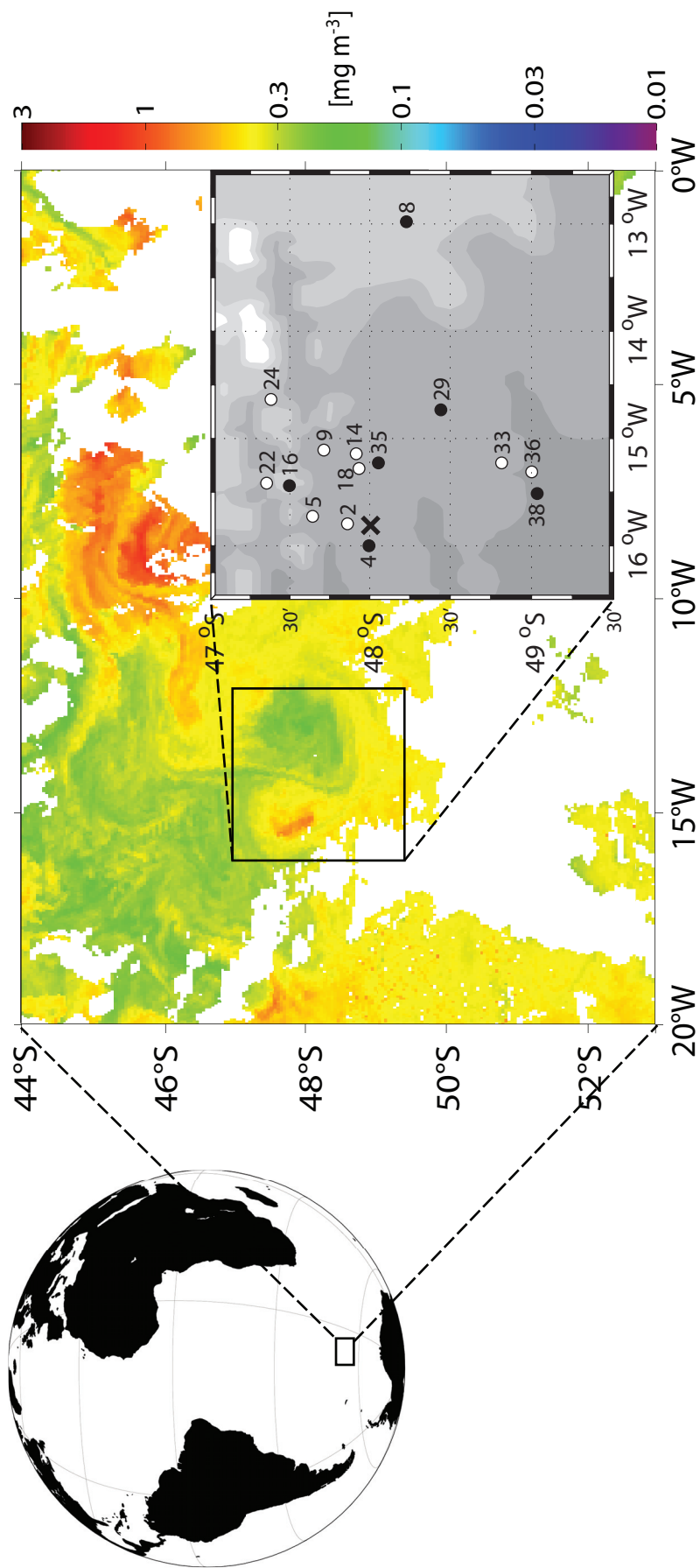
622

623 FIG 5: Total cell numbers of different groups counted using CARD FISH for the IN
624 (black spheres, straight lines) and OUT (white spheres, dashed lines) stations. Please note
625 different scales.

Probe	Target organism	Sequence (5' → 3')	FA (%) ^a	Reference
EUK516	<i>Eukarya</i>	ACCAGACTTGCCCTCC	0	(39)
NON338	Control	ACTCTACGGGAGGCAGC	35	(57)
PRAS04	<i>Mamiellophyceae</i>	CGTAAAGCCCGCTTTGAAC	40	(15)
PRYM02	<i>Haptophyta</i>	GGAATACGAGTGCCCTGAC	40	(58)
MICRO01	<i>Micromonas pusilla</i>	AATGGAACACCCCGGGCG	40	(15)
PHAE003	<i>Phaeocystis</i>	GAGTAGCCCGGGTCTCCGGAAAGAAGGCCCGCGCC	20	(10)
PELA01	<i>Pelagophyceae</i>	GCAACAATCAATCCCAATC	20	(58)
MAST1A	MAST 1 clade	ATTACCTCGATCCGCAAA	30	(14)
MAST1B	MAST 1 clade	AACGCAAGTCTCCCGCG	30	(14)
MAST1C	MAST 1 clade	GTGTTCCCTAACCCCGAC	30	(14)
MAST3	MAST 3	ATTACCTTGGCCCTCCAAC	30	(13)
MAST4	MAST 4	TACTTCGGTCTGCAAAACC	30	(13)
SYNI 1161	<i>Syndiniales</i> group I	TCCTCGCGTTAGACACGC	20	This study
SYNII 675	<i>Syndiniales</i> group II	CACCTCTGACCGGTTAAT	20	This study

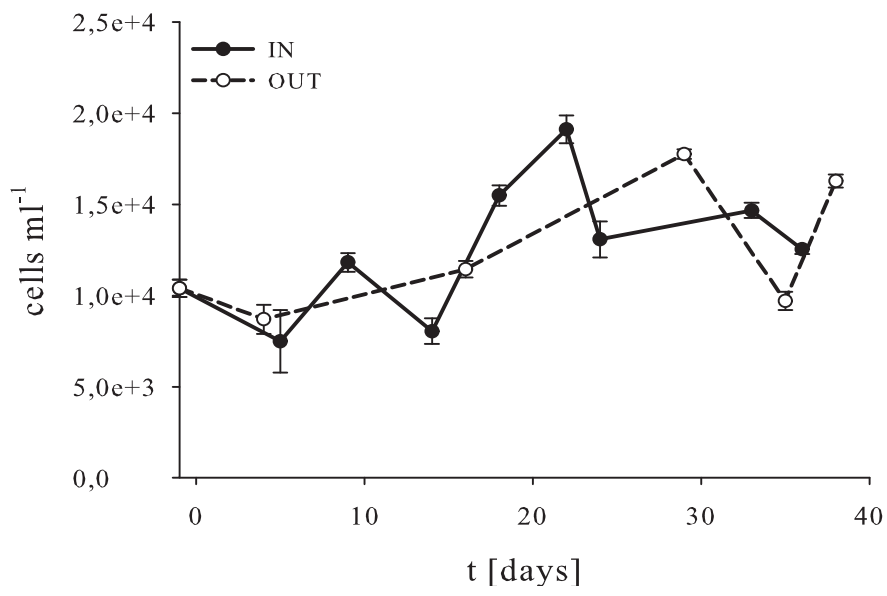
	day -1	day 9	day 18	day 16 (OUT)
No. of OTUs	459	714	599	702
Chao1 index	633	879	803	899
Shannon index	3.49	3.72	3.93	3.86

627



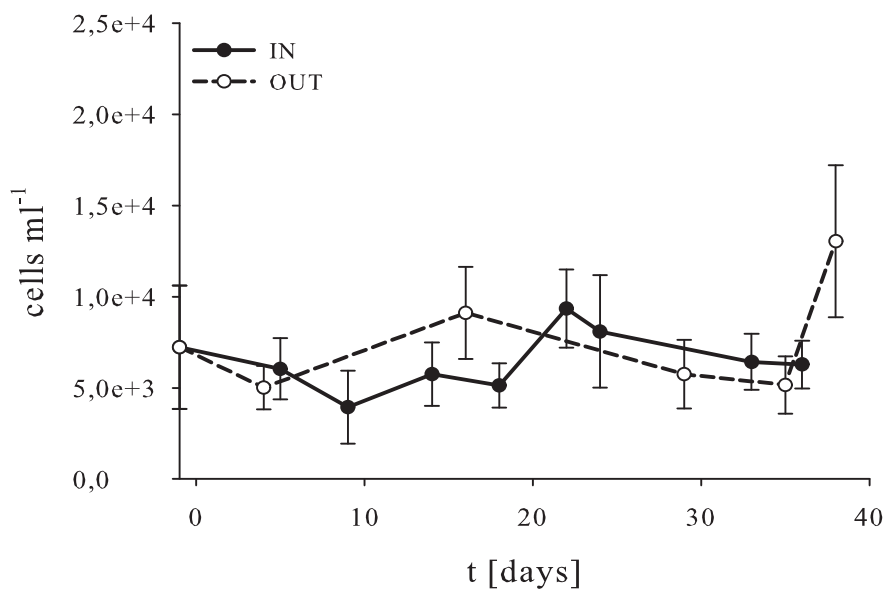
A

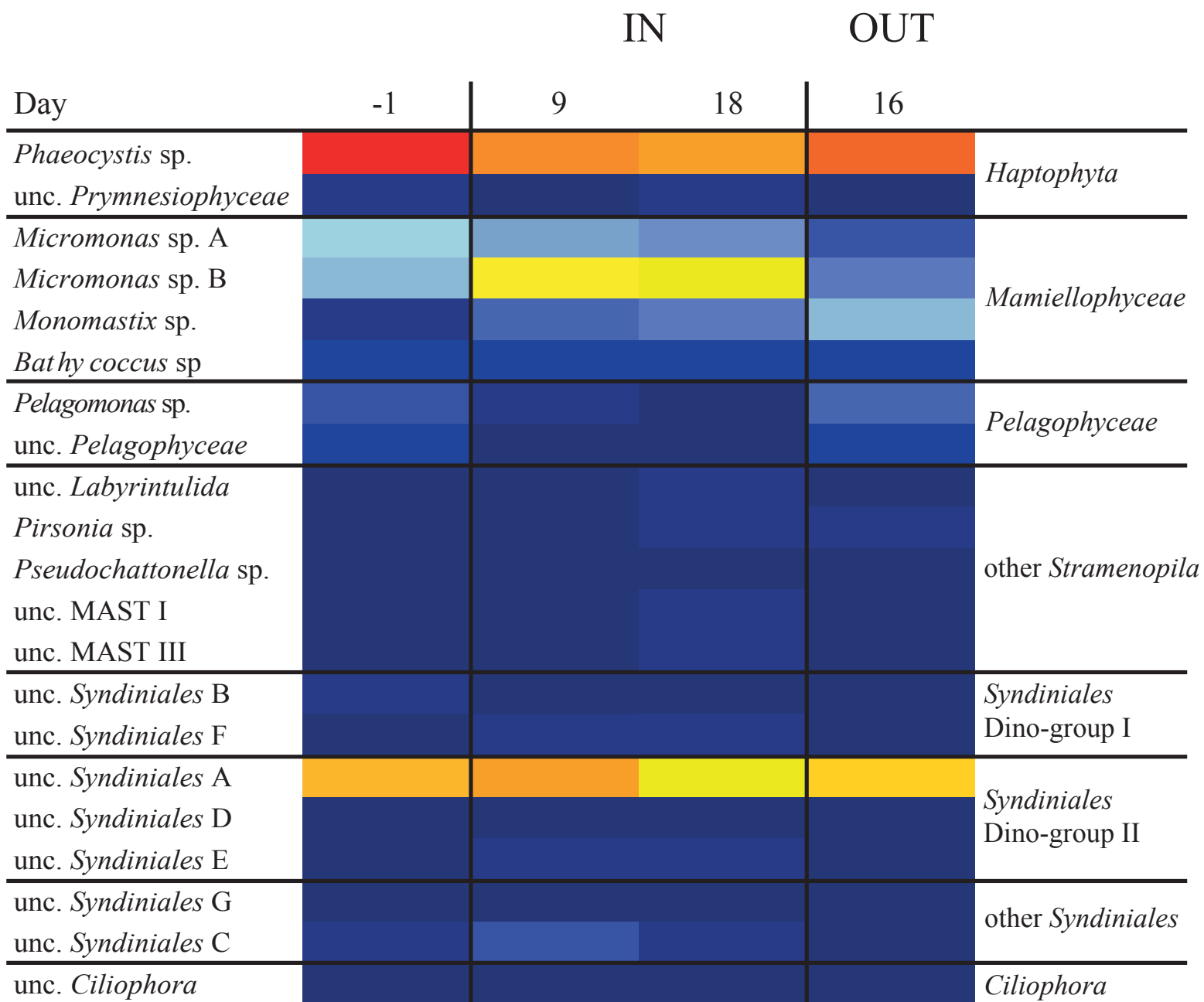
FCM counting

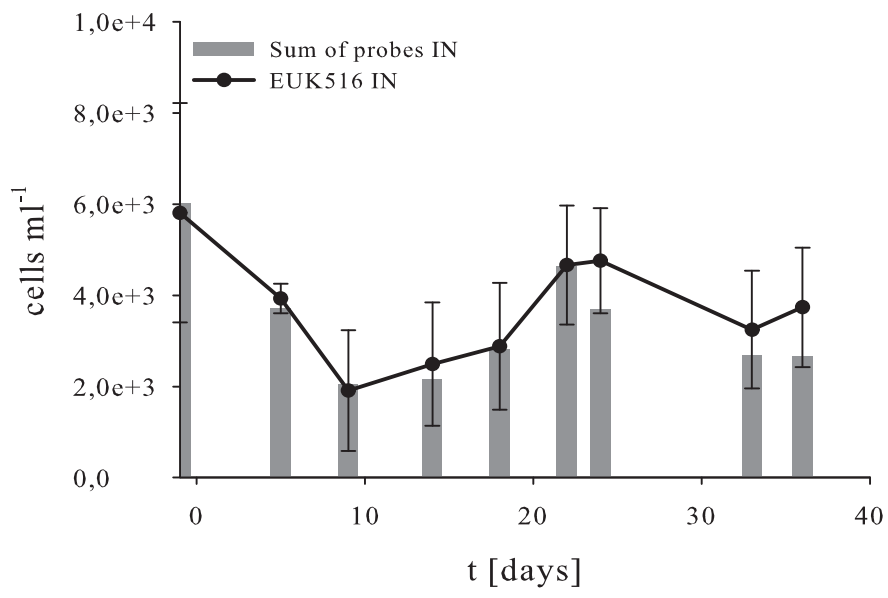
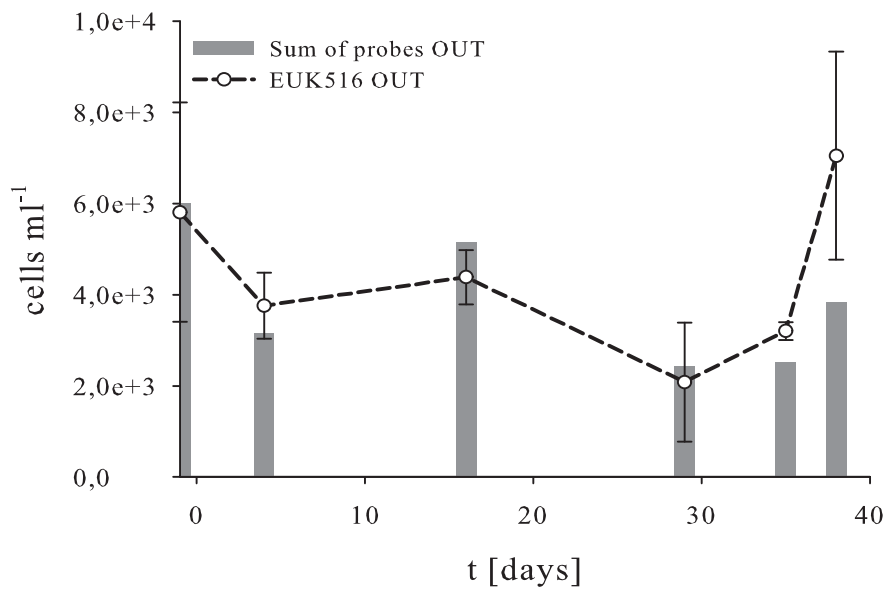


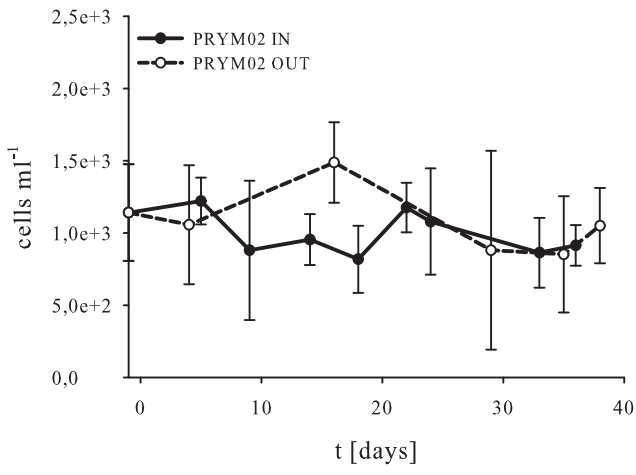
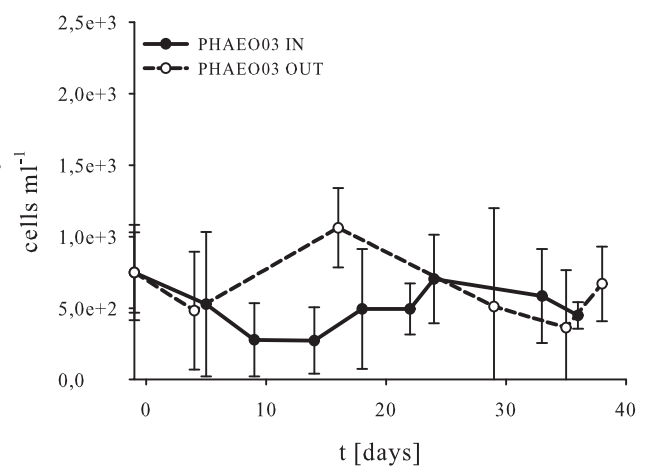
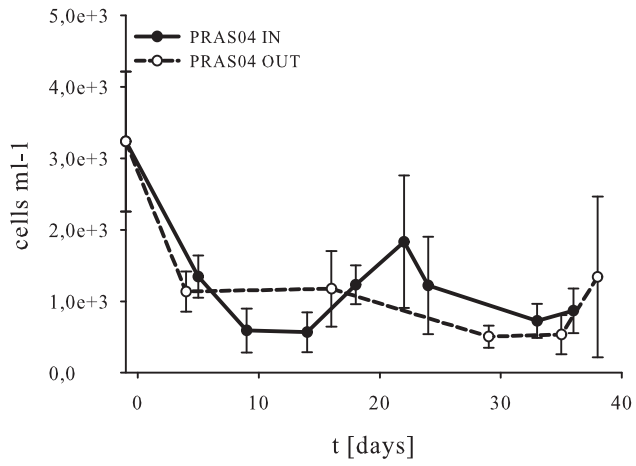
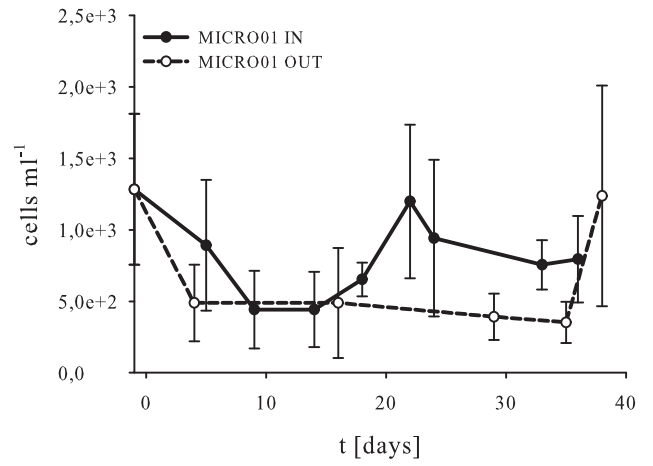
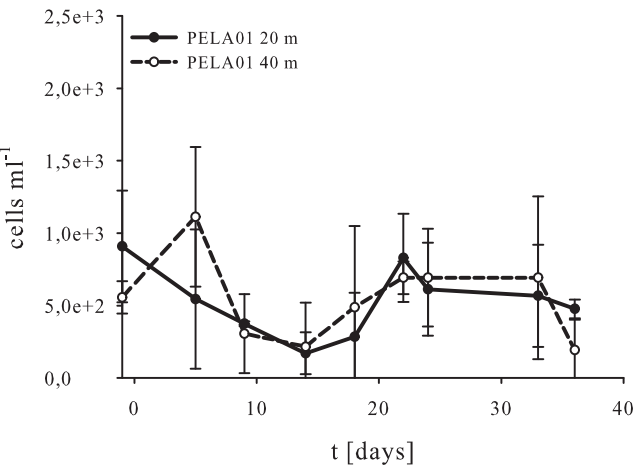
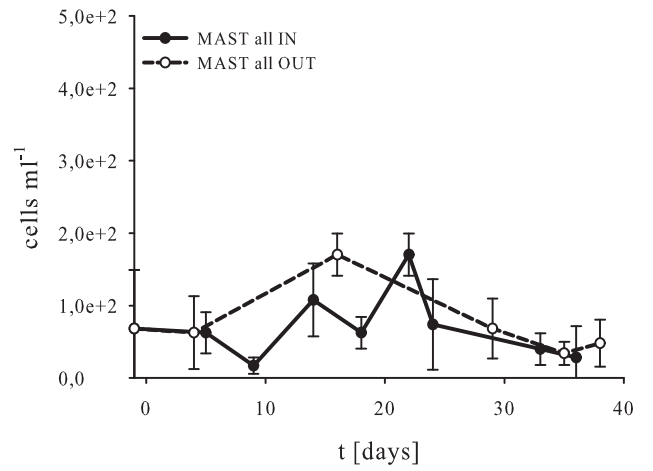
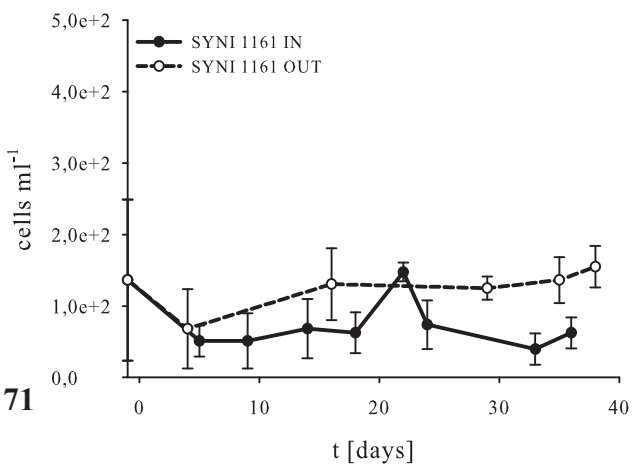
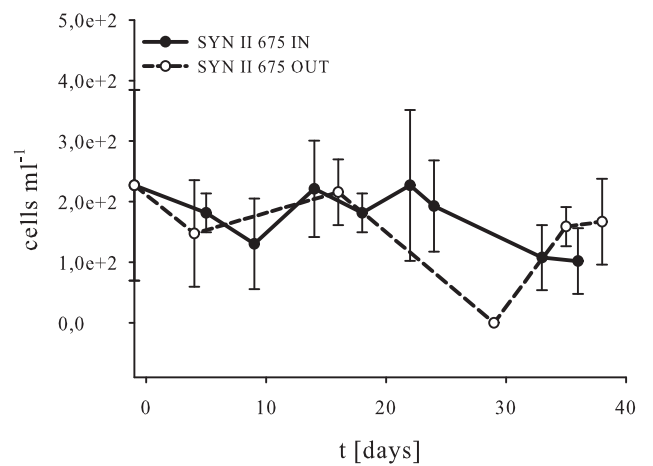
B

Autom. counting





A**EUK516 IN****B****EUK516 OUT**

A*Haptophyta***B***Phaeocystis***C**
Mamiellophyceae**D***Micromonas***E**
Pelagophyceae**F**
MAST clades**G**
Syndiniales clade I**H**
Syndiniales clade II

Manuscript III

Investigation of the bacterial community on *in situ* sampled marine snow aggregates from the epipelagic and mesopelagic zone

Stefan Thiele, Bernhard M. Fuchs, Rudolf Amann, Morten H. Iversen

Manuscript in preparation. Intended as article in *The ISME Journal*.

1 **Investigation of the bacterial community on *in situ* sampled**
2 **marine snow aggregates from the epipelagic and mesopelagic**
3 **zone**
4

5 Stefan Thiele¹, Bernhard M. Fuchs¹, Rudolf Amann¹, Morten H. Iversen^{2#}

6

7 ¹ Max Planck Institute for Marine Microbiology, Celsiusstr. 1, D-28359 Bremen,
8 Germany

9 ² Faculty of Geosciences and MARUM, University of Bremen, Klagenfurter and
10 Leobener Strasse, 28359 Bremen, Germany

11

12

13 # corresponding author

14 contact: Faculty of Geosciences and MARUM, University of Bremen, Klagenfurter and
15 Leobener Strasse, 28359 Bremen, Germany

16

17 email: miversen@marum.de

18 phone: + 49 421 218 65065

19

20

21

22

23 **Abstract**

24 Within marine carbon cycling, the biological carbon pump plays a pivotal role in the
25 sequestration of carbon into the deep sea. The vehicle of carbon transport are aggregates,
26 which are colonized and degraded by bacteria, thus counteracting carbon sequestration.
27 Here we report data obtained with novel techniques for the investigation of the bacterial
28 community on marine snow aggregates and transparent exopolymeric particle (TEP)
29 structures. Free drifting sediment traps were used for the *in situ* sampling of aggregates
30 and roller tank incubations for the sampling of TEP structures in the Canary Current
31 Upwelling System off Cape Blanc (Mauretania). Three dimensional fluorescence *in situ*
32 hybridization was used to compare the different bacterial communities associated with
33 the *in situ* collected marine snow and roller tank derived TEP structures. The microbial
34 communities within these aggregates were dominated by cyanobacteria of the genus
35 *Synechococcus* at both depths. A significant decrease in abundance with increasing depth
36 was found for likewise dominating *Bacteroidetes* and *Alteromonas* spp.. Roller tank
37 derived TEP structures were dominated by *Alteromonas*, both from incubation with
38 water collected at 65 and 400 m. Our study suggests that the bacterial communities within
39 aggregates are determined during their formation in the surface ocean. Therefore, we
40 hypothesize, that changes in the bacterial community associated with marine snow as
41 they sink are due to changes mainly in the nutrient composition of the aggregate and the
42 resulting succession of ecological niches, but also grazing pressure on the bacterial
43 community, in combination with sinking temperature and increasing pressure.

44 Key words : *Alteromonas*/ *Bacteroidetes*/ 3D FISH/ TEP/ microbial loop

45 **Introduction**

46 The Eastern Boundary Upwelling Systems (EBUS) account for ~10% of the global
47 primary production and are characterized by high organic carbon export (Chavez &
48 Messié 2009). The Canary Current System and the area off Cape Blanc (NW Africa) is
49 the second most productive of the EBUS (Behrenfeld & Falkowski 1997; Chavez &
50 Messié 2009). Here the upwelling of North and South Atlantic Central Water transports
51 nutrients to the surface layer and thus supports the formation of large phytoplankton
52 blooms throughout the year (Aristegui et al. 2009). During these blooms, carbon dioxide
53 is fixed by phytoplankton via photosynthesis. Part of the resulting biomass from the
54 bloom may eventually form sinking organic aggregates and be transported from the
55 surface ocean to the deep ocean and the sea floor where it is sequestered, a process called
56 the biological carbon pump (Volk & Hoffert 1985; Ducklow et al. 2001). The majority of
57 the material exported out of the photic zone is in the form of macro-aggregates > 500 µm
58 in size, called marine snow, and zooplankton fecal pellets (e.g. Simon et al. 2002).
59 Settling marine aggregates harbor diverse microbial communities which play an
60 important role in the degradation of the organic compounds and release of dissolved
61 nutrients into the water column (Urban-Rich 1999; Simon et al. 2002). This microbial
62 aggregate degradation counteracts the biological carbon pump. Insights into the diversity
63 and functioning of the bacterial and archaeal community within marine aggregates are
64 therefore pivotal to our understanding of the carbon cycling in the ocean. Previous studies
65 found a dominance of bacteria within aggregates of limnic, riverine and marine origin.
66 Their abundance generally ranges from 1×10^2 to >math>1 \times 10^9</math> cells per aggregate (Simon et
67 al. 2002; Alldredge & Gotschalk 1990), often dominated by *Gammaproteobacteria* and

68 members of the *Bacteroidetes* phylum (DeLong et al. 1993; Moeseneder et al. 2001; Rath
69 et al. 1998; Acinas et al. 1999).

70 Still, little is known about bacterial community composition and distribution within
71 marine snow and how these communities might change as the aggregates descent through
72 the water column. Previous investigations observed different clustering of free-living
73 bacteria compared to those associated with sinking aggregates through the water column
74 (Moeseneder et al. 2001), suggesting that attached bacteria create their own
75 microenvironments independent from the trophic situation in the surrounding water.
76 Further, the authors observed a decline in the diversity of the attached bacterial
77 community within aggregates at depth, indicating that the metabolic activity of attached
78 bacteria lead to more refractory particles. Using increasing pressure to simulate particle
79 sinking to the deep ocean, Tamburini et al. (Tamburini et al. 2009) and Grossart and
80 Gust (Grossart & Gust 2009) observed different bacterial communities within aggregates
81 exposed to high pressure, compared to incubation at atmospheric pressure. Further, the
82 microbial activity of aggregate-associated bacteria has been shown to decrease when
83 using either only pressure (Tamburini et al. 2006, 2009) or only temperature (Iversen &
84 Ploug 2013) to simulate aggregate sinking to the deep ocean. However, due to difficulties
85 of sampling of intact marine snow at depths below the reach of scuba divers, no studies
86 have directly investigated the composition of bacterial communities within these
87 aggregates. Without such investigations, it is not possible to conclude whether the
88 decreasing decomposition of sinking aggregates with increasing depth is due to changes
89 in the attached microbial community or lower metabolic activity of a non-changing
90 community.

91 Investigations of microbial communities on aggregates are challenging, due to the three
92 dimensional structure of the aggregate. Overlapping signals, especially after CARD FISH
93 staining, in a 3D object and interference of autofluorescent organic material may lead to
94 underestimation of abundances when using manual cell counting. Therefore, we used
95 catalyzed reporter deposition fluorescence *in situ* hybridization (CARD FISH) in a three
96 dimensional approach and confocal laser scanning microscopy (CLSM) in combination
97 with biovolume calculations, as frequently used for eukaryotic cell structures or
98 symbiotic bacteria in host tissue (e.g. Solovei et al. 2002; Halary et al. 2008). Here we
99 report the investigation of the bacterial community within *in situ* sampled marine snow
100 aggregates and re-assembled TEP structures from two different depths.

101 **Materials & Methods**

102 *Sampling*

103 Samples were taken during two cruises in the area off Cape Blanc (Mauretania).
104 Sampling for *in situ* investigation of bacterial communities within aggregates and free
105 living were performed during the RV Maria S. Merian cruise 18-1 (MSM18-1). The free-
106 living communities were investigated in water samples collected at 150 m and 400 m
107 depth on 1st of May 2011 at station GeoB15704 (20° 35 N; 18° 03 W) using a Rosette
108 water sampler equipped with a Seabird CTD (FIG 1). At each depth, samples were fixed
109 with formaldehyde (1% final concentration) for 1 to 3 h at room temperature. Thereafter,
110 the samples were fractionated into three size classes; larger than 10 µm, between 10 and 3
111 µm, and between 3 and 0.22 µm by filtering onto polycarbonate filters (Millipore,
112 Billerica, USA) at low vacuum. This was done in triplicates for each size fraction at each
113 depth and subsequently the samples were frozen at -20 °C until further analysis.

114 The collection of *in situ* formed marine snow were performed with a single free-drifting
115 sediment trap equipped with two trap cylinder containing a trap insert filled with ~200
116 mL viscous gel (Tissue-Tek O.C.T. Compound Cryogel, Sakura Finetek, Alphen aan den
117 Rijn, The Netherlands) (SUP 1). The viscous gel enabled preservation of the fragile
118 aggregate structures after their collection in the trap cylinders, which were deployed in
119 pairs at each collection depth; 100 and 400 m. The sediment trap was deployed on the
120 30th of April 2011 at position (20°45 N; 18°44 W) and drifted southeast to position
121 (20°38 N; 18°43 W), where it was recovered after 3 days (FIG 1). Before deployment, we
122 filled the two trap cylinders at each depth with GF/F filtered sea water in a three layer
123 density gradient created by addition of sea salt; a top layer with an ambient salinity of 34,

124 a middle layer with a salinity of 38, and a bottom layer with a salinity of 42. By adding
125 formaldehyde to a 1% final concentration to the middle layer we were able to fix the
126 bacterial communities within the aggregates while they settled through the trap cylinder
127 and to wash the fixed aggregates in the bottom layer, before they were collected in the
128 viscous gel in the trap insert (SUP 1). Upon trap recovery, the overlying water was
129 siphoned out and the gel containing trap inserts carefully removed and frozen at -20 °C
130 until further processing.

131 During the RV Poseidon cruise 396 (POS396) samples were collected from 65 m and 400
132 m to investigate bacterial communities within aggregates formed from roller tank
133 incubations and to investigate the free-living bacterial communities. These samples were
134 collected with a Rosette sampler equipped with a Seabird CTD on the 2nd of March, 2010,
135 at station GeoB14204 (20° 60 N; 19° 10W) (FIG 1). The samples for investigations of the
136 free-living bacterial and archaeal communities were processed as described above. To
137 form aggregates, we incubated water from each depth in five 1.2 l roller tanks rotated at 2
138 rpm for 18-24 hours. After incubation, we collected the formed aggregates from each
139 roller tank. These aggregates mainly consisted of mucous structures with detritus and
140 phytoplankton cells attached in rather low concentrations (not quantified, FIG 6). Since
141 the aggregates were neither appendicularian houses nor typical phytoplankton-derived
142 aggregates, we will refer to these aggregates as TEP structure, though we did not have
143 Alcian Blue onboard to do staining for TEP. After collection, the TEP structures were
144 fixed in formaldehyde (1% final concentration) for 2 h at room temperature. Before
145 filtering the TEP structures onto 0.22 µm pore size polycarbonate filters (Millipore,

146 Billerica, USA), they were broken apart by vortexing. Each filter was washed with
147 distilled water before the filters were stored at -20°C until further analysis.

148

149 *Aggregate isolation, filtration, and volume determination*

150 Preparation of the *in situ* aggregates for the investigation for CARD FISH analyses
151 included the determination of the aggregate size. Thus, blocks of ~1.5 cm² size were cut
152 from the frozen gel and thawed in small petri dishes. Pictures of aggregates were taken
153 using a Canon EOS 550D digital camera equipped with a Sigma 105mm macro zoom
154 objective. The pixel area of each aggregate was determined using the software ImageJ
155 and converted to mm² using a stage micrometer to determine the length of 1 pixel. The
156 equivalent circular diameter of each aggregate was calculated from the area. Calculations
157 of the total aggregate volumes were done using the equivalent circular diameter
158 determined from the pictures assuming a spherical shape of the aggregate. Aggregates
159 were subsequently isolated washed in PBS overnight and filtered on 0.22 µm pore size
160 polycarbonate filters (Millipore, Billerica, USA) and used for CARD FISH analyses.
161 TCCs per aggregate were calculated using the TCC of EUB I-III and total aggregate
162 volume.

163

164 *Fluorescence in situ hybridization (FISH) and catalyzed reporter deposition (CARD)*

165 *FISH*

166 Quantification of the initial free living bacterial and archaeal community and the changes
167 in the bacterial and archaeal community during the roller tank incubations was done using
168 CARD FISH specific for various clades on samples from all depths using specific

169 oligonucleotide probes according to Pernthaler et al. (Pernthaler et al. 2002), modified
170 after Thiele et al. (Thiele et al. 2011) (TAB.1). The hybridization was done using a probe
171 to hybridization buffer mix of 1:100 on glass slides for 2 h. Amplification was done,
172 using a 5-(and 6-)-carboxyfluorescein or Alexa488 labelled tyramide to amplification
173 buffer mix of 1:100, on glass slides for 45 minutes. All filters were DAPI stained and
174 counted manually (POS396 cruise) with min. 1000 DAPI signals, using an
175 epifluorescence microscope (Zeiss Axioplan II, Carl Zeiss AG, Jena, Germany). CARD
176 FISH on samples from the MSM18-1 cruise were done as described above, but
177 quantification of cell numbers after CARD FISH was done with a Zeiss Axio Imager.Z2
178 microscope (Carl Zeiss AG, Jena, Germany) with an automated stage. Image acquisition
179 was done using the software package AxioVision Release 7.6 (Carl Zeiss AG, Jena,
180 Germany) and the macro MPISYS (Zeder unpublished). Only samples with a minimum
181 of 15 picture pairs were taken into account and evaluated using the software ACMETool
182 0.76 (Zeder unpublished).

183 Analyses of the bacterial communities within marine snow collected during the trap
184 deployment were done using CARD FISH as described for the free-living bacteria. Filters
185 containing individual aggregates were cut in half or quarters and used for CARD FISH.
186 Half of each filter was used for hybridized with different specific probes, while one
187 quarter of the remaining filter was hybridized with the EUB I-III probe mix (TAB. 1).
188 Three different aggregates were used for every probe and compared to the corresponding
189 EUB I-III count from a filter-quarter.

190 Analyses of the bacterial community in association with the TEP structures were done on
191 3 TEP structures from each depth. Duplicates from each filter were analyzed with FISH

192 (Amann et al. 1995) using mono labelled oligonucleotide probes (TAB 1). EUB I-III was
193 combined with one specific probe for double hybridization. We used 4-times click
194 labelled EUB I-III probes in a later phase of the experiment (TAB 1).

195

196 *Confocal Laser Scanning Microscopy (CLSM)*

197 Individual *in situ* collected marine snow was analysed using a confocal laser scanning
198 microscope (Zeiss LSM 780, Carl Zeiss AG, Jena, Germany) including the software
199 ZEN2011 (Carl Zeiss AG, Jena, Germany). Two aggregate pieces per triplicate of the
200 probe and analysed filter piece were scanned using single scans of ~30-40 sec. per focal
201 plane. This resulted in a total of 6 z-stacks which were used to determined biovolume of
202 the specific bacterial clade hybridized with CARD FISH. In addition to the probe channel,
203 one channel with a broad detection range was scanned for volume calculations of the
204 aggregate fragment.

205 Z-stacks of the TEP structures were made using a confocal laser scanning microscope
206 (Zeiss LSM 510, Carl Zeiss AG, Jena, Germany) including the software Zeiss LSM 510
207 version 3.2 SP2 (Carl Zeiss AG, Jena, Germany). We used summed analyzes of 4 scans
208 and scanning times of ~10 sec. per focal plane. A minimum of two TEP structures were
209 analyzed per filter. TEP structures including high concentrations of phytoplankton had to
210 be avoided due to high autofluorescence signal which resulted in overestimations of the
211 total bacterial biovolume calculations.

212

213 *Specific biovolume calculation*

214 To achieve biovolumes from the z-stacks, we used ImageJ (Image processing and
215 analysis in Java; National Institute of Health, Bethesda, USA) and PHLIP (Phobia laser
216 scanning microscopy image processor v4.0.; (Mueller et al. 2006) in Matlab R2010b (The
217 Mathworks Inc, Natick, USA). In ImageJ we used a mean filter with a radius of 2 pixels
218 for the TEP structure images. For the *in situ* collected marine snow, no post processing of
219 the confocal laser scanning microscope images were needed. These were analyzed in
220 PHLIP using manual threshold settings according to sample we obtained bacterial
221 biovolumes for each channel of the z-stacks.

222

223 *Biovolume measurements and total bacterial cell count calculation*

224 To calculate the total cell counts per sample for each probe of the marine snow, we
225 measured the average biovolume of single CARD FISH stained bacteria cells using the
226 YABBA software (Zeder et al. 2011). TCC were calculated by dividing the average
227 bacterial biovolume with the total bacterial biovolume and normalized to analyzed
228 aggregate volume for each sample. The TCC of EUB I-III was compared to the TCC of
229 specific probes to estimate the relative abundance of each specific probe in relation to
230 total EUB I-III counts. The normalization of cell numbers to relative abundance was
231 necessary due to the high fluctuations in the total cell counts between the different
232 aggregates. Comparisons between different depths were done using t-tests in SigmaStat
233 3.5 (Statcon, Witzenhausen, Germany).

234 In order to achieve the cell volume of single cells from the TEP structures, we measured
235 the length and width of 10 randomly chosen cell per probe with the program Axiovision
236 4.8.2. (Carl Zeiss AG, Jena, Germany) and calculated their volume using as $V = 4\pi r^2/3 +$

237 $\pi r^2 (1-2r)$ for cylinders with hemispheric ends (Blackburn et al. 1998). The resulting
238 average cell volume was used to calculate the number of bacterial cells per probe from
239 the total bacterial volume of the probe. This was done, since the cells densities were too
240 high for reliable determinations of single bacterial cells using the YABBA software
241 (Zeder et al. 2011).

242

243 *Statistics*

244 Data were tested for normal distribution with the Kolmogorov-Smirnov test. Normal
245 distributed CARD FISH data for the free-living community was tested for significant
246 differences using one-way ANOVA and non-normal distributed data were tested for
247 significant differences using ANOVA on ranks. Significant differences in abundances at
248 different depths were tested with Students t-tests. Student's t-test was also used to test for
249 significant differences between TCC at different depth. Significant differences in total
250 bacterial cell numbers for different probes were tested with Students t-tests and in case of
251 non-normal distribution with Spearman rank correlations. All statistical analyses were
252 performed with SigmaStat 3.5 (Statcon, Witzenhausen, Germany).

253 **Results**254 *Bacterial abundances on aggregates*

255 We observed a tendency for higher total bacterial abundance (median EUB I-III counts)
256 within *in situ* collected marine snow at 400 m compared to those at 100 m, though not at
257 significant levels; $7.5 \times 10^7 \pm 3.6 \times 10^8$ cells mm^{-3} (n=39) at 400 m depth and $5.0 \times 10^7 \pm$
258 1.5×10^8 cells mm^{-3} at 100 m (n=38) (Fig. 2A). The bacterial concentrations within
259 marine snow were about five orders of magnitudes higher compared to those in the
260 surrounding water at both depths (FIG 2 B). No differences were observed in the median
261 bacterial abundance per aggregate: $8.1 \times 10^6 \pm 2.9 \times 10^7$ cells agg^{-1} (n=38) at 100 m and
262 $9.9 \times 10^6 \pm 8.5 \times 10^7$ cells agg^{-1} (n=39) at 400 m (FIG 2C).

263 *Synechococcus* was dominant within *in situ* collected marine snow at both depths and
264 showed no significant differences in relative abundance at the two depths; $40\% \pm 12\%$ at
265 100 m and $49\% \pm 37\%$ at 400 m (FIG 3 A; FIG 4 A+B). There were significantly lower
266 relative abundances of *Synechococcus* in surrounding waters, where only $2\% \pm 1.3\%$ and
267 $5\% \pm 1.3\%$ were found at 100 m and 400 m, respectively (FIG 3 B). *Bacteroidetes*
268 abundances were relatively constant with $3\% \pm 0.6\%$ at 150 m and $4\% \pm 0.2\%$ at 400 m
269 in the free living fraction (FIG 3 B). In contrast, *Bacteroidetes* abundances on aggregates
270 were significantly higher on the marine snow aggregates than in the free living fraction,
271 still the relative abundance was lower at 400 m compared to 100 m, with $7\% \pm 3.3\%$ at
272 400 m and $42\% \pm 28\%$ at 100 m. *Bacteroidetes* were by far the most abundant
273 heterotrophic bacteria at 100 m (FIG 3 A; FIG 4 C+D). Within marine snow,
274 *Gammaproteobacteria* showed slightly lower abundances at 400 m compared to 100 m
275 (from $11\% \pm 4\%$ and $14\% \pm 10\%$, respectively). These values were still significantly

276 higher than in the free living fraction with ~3% at both 100 m and 400 m, respectively
277 (FIG 3 B). Within the *Gammaproteobacteria*, *Alteromonas* were found in relative
278 abundances of ~2% in the free living fraction at both 100 m and 400 m (FIG 3 B), but
279 were strongly enriched on aggregates. With a relative abundance of $18\% \pm 10\%$ at 100 m
280 depth they accounted for all *Gammaproteobacteria*, whereas at 400 m depth they
281 accounted only for <1% of the aggregate attached bacteria, a significant decrease
282 ($p=0.022$) (FIG 3 A+B; FIG 4 E+F). *Pseudoalteromonas* showed stable relative
283 abundance at ~2% in the free living fraction and ~4% within marine snow at both depths
284 (FIG 3 A). *Roseobacter* had relative abundances of ~1% both at 150 m and 400 m depth.
285 Within marine snow they had relative abundances of $10\% \pm 12\%$ at 100 m and $8\% \pm 10\%$
286 at 400 m (FIG 3 A+B). Although, *Planctomycetes* were low in abundance, a significant
287 ($p=0.02$) decrease from 2.5% to <1% was found with depth on the marine snow
288 aggregates (FIG 3 A), while the free living fraction was relatively stable at ~1.5% (FIG 3
289 B). *Thaumarchaeota*, *Euryarchaea* Marine Group II, *Prochlorococcus* and the SAR324
290 clade did not account for significant fractions on the aggregates and were no investigated
291 in the free living fraction (TAB 1).

292

293 *Bacterial abundances on TEP structures*

294 TEP structures formed in roller tanks from water sampled at 65 m and 400 m depth had
295 total cell numbers that were not significantly different between both depths and ranged
296 from $6.3 \pm 3.5 \times 10^7$ cells ml⁻¹ (n=10) at 65 m to $5.2 \pm 6.2 \times 10^7$ cells ml⁻¹ (n=20) at 400
297 m depth (FIG 2 D). However, cell numbers were higher on TEP structures than in the

298 surrounding water, where $4.2 \pm 3.2 \times 10^5$ cells ml⁻¹ EUB I-III stained cells were found at
299 65 m and $3.2 \pm 1.7 \times 10^5$ cells ml⁻¹ at 400 m depth (FIG 2 E).

300 We chose 3 bacterial groups for investigations, *Alteromonas*, *Bacteroidetes* and
301 *Pseudoalteromonas*, based on preceding tests on previously sampled TEP structures.
302 These tests showed no occurrence of SAR11 and *Archaea* on the aggregates and only
303 very low amounts of *Roseobacter* and *Planctomycetes*. The relative abundance of
304 *Alteromonas* was $74\% \pm$ at 65 m depth and increased significantly ($p=0.007$) to $90\% \pm$
305 9% on TEP structures formed in roller tanks from water sampled at 400 m depth (FIG 5
306 A). This was significantly ($p<0.001$) higher than in the free living fraction ($<2\%$; FIG 5
307 B). The relative abundance of *Pseudoalteromonas* decreased with depth, though not
308 significantly, from $9\% \pm 11\%$ to $4\% \pm 6\%$ (FIG 5 A), and was higher than in the
309 surrounding water ($<1\%$) (FIG 5 B). *Bacteroidetes* were found in relative abundances of
310 about $8\% \pm 6\%$ at both depths (FIG 5 A). In free living fraction $22\% \pm 12\%$ were found
311 at 65 m and $6\% \pm 3\%$ at 400 m (FIG 5 B). The coverage of the bacterial community on
312 roller tank formed TEP structures by these three clades was $>90\%$.

313

314 **Discussion**

315 To our knowledge, no previous studies have investigated bacterial communities within
316 individual phytoplankton-based macroaggregates collected *in situ* from depths between
317 100 and 500 m. Therefore, the usage of drifting sediment traps with viscous gel filled
318 collector tubes is a promising new approach to investigate the bacterial communities at
319 different depths. The only previous assessments of bacterial abundances on marine
320 aggregates from those depths have been done on mucous aggregates produced by the
321 larvacean *Bathochordaeus* collected using a remotely operated vehicle (Silver et al. 1998),
322 while other previous studies investigated bacterial densities within *in situ* collected
323 marine snow from depths between 7 and 15 m (Alldredge et al. 1986; Herndl 1988) and
324 observed that the particle-associated bacterial numbers were up to several hundred-folds
325 higher than those in the surrounding sea water. We observed bacterial abundances within
326 *in situ* collected marine snow, from a single deployment of a drifting sediment trap, that
327 were five orders of magnitude higher compared to the surrounding sea water, at both 100
328 and 400 m depths, supporting the suggestions that aggregates harbor more favourable
329 nutritive conditions than those in the surrounding water (reviewed in Simon et al. 2002).

330 The aggregate-associated bacterial community at 100 m was dominated by
331 *Synechococcus*, *Bacteroidetes*, and *Alteromonas*. The community was different at 100 m
332 and 400 m depth, due to a decrease in *Bacteroidetes* and *Alteromonas*, whereby
333 *Synechococcus* was the solely dominating organism at 400 m. *Synechococcus* displays
334 positive chemotaxis behavior toward nitrogenous compounds (Willey & Waterbury 1989).
335 Both ammonia and nitrate are highly enriched within aggregates compared to the
336 surrounding water (Shanks & Trent 1979), suggesting that the general high relative

337 abundances of *Synechococcus* on aggregates (Vanucci et al. 2001) is a result of active
338 chemotactic behavior. Despite evidence of mixotrophic growth of *Synechococcus*
339 (Zubkov et al. 2003; Zubkov & Tarran 2005) and suggestions that they can survive in
340 darkness (Cottrell & Kirchman 2009), we cannot provide evidence to whether
341 *Synechococcus* is adapted to colonization or simply trapped within sinking aggregates.
342 However, the dominance of photoautotrophy in *Synechococcus* indicates that they are
343 trapped within the rapidly sinking marine snow.

344 *Bacteroidetes* and *Gammaproteobacteria* are known to colonize marine snow (DeLong et
345 al. 1993; Rath et al. 1998; Moeseneder et al. 2001) and potentially utilize various DOM
346 and POM compounds within the aggregate (Cottrell & Kirchman 2000; Puddu et al. 2003;
347 Bauer et al. 2006; McCarren et al. 2010; Gómez-Pereira et al. 2012). *Bacteroidetes* have
348 been suggested to colonize marine snow by first attaching to small particles (Kirchman
349 2002; Alonso et al. 2007) which eventually form marine snow (Azam & Malfatti 2007).
350 We observed high abundances of *Bacteroidetes* at marine snow collected at 100 m. Their
351 non-motile behavior suggests that they remain permanently attached to aggregates,
352 possibly due to embedding in the matrix within aggregates (Kjørboe et al. 2002). This
353 and previous studies observed low, if any, bacterial exchange between settling aggregates
354 and the surrounding water at depth (Moeseneder et al. 2001; Eloë et al. 2011), suggesting
355 that bacteria colonized the aggregates during aggregate-formation in the surface ocean
356 and remained attached while the aggregates settled to depths.

357 We observed a significant decrease in the relative abundance of *Bacteroidetes*,
358 *Alteromonas*, and *Planctomycetes* at 400 m compared to 100 m. However, the total
359 bacterial cell numbers within the aggregates at the two depths were still similar. This

360 shows that the microbial community within marine snow changes during aging and
361 sinking, as observed previously within lake snow (Grossart & Simon 1998). The species
362 composition of the microbial community within aggregates is dependent on the initially
363 colonizing group and the trapped organisms during sinking, but certain groups may
364 decrease with depth and the aggregates might be re-colonized by groups abundant in the
365 deeper water layers. However, no evidence for re-colonization was found on the marine
366 snow aggregates at 400 m depth. This might be due to the colonization of a group which
367 was not covered by the applied oligonucleotide probes.

368 As aggregates settle through the water column, their attached microbial communities
369 becomes exposed to increasing pressure, decreasing temperature, changing organic matter
370 and nutrient conditions, and potentially interactions with other colonizers (grazers and
371 competitors). No studies have investigated these combined effects on the activity and
372 development of microbial communities within aggregates. Investigating pressure effects
373 on bacterial species composition showed increasing abundances for *Roseobacter*,
374 *Gammaproteobacteria*, and *Bacteroidetes* at 500 m compared to 250 m (Grossart & Gust
375 2009). We observed no changes in the abundances of *Roseobacter* and a significant
376 decrease for *Bacteroidetes* and *Alteromonas* at 400 m compared to 100 m, while
377 Tamburini and co-worker (Tamburini et al. 2006) found that pressure had no influence on
378 the attached microbial community, but that additions of fresh diatom detritus induced
379 higher total bacterial cell counts and high abundances of *Bacteroidetes*. Both increasing
380 hydrostatic pressure (Tamburini et al. 2006) and decreased temperature (Iversen & Ploug
381 2013) have resulted in decreased microbial degradation activity within organic aggregates,
382 suggesting that bacteria adapted to the surface ocean have lower metabolic activity when

383 settling to depths with higher pressure and lower temperature. For lower temperature, this
384 is congruent with the assumption of a 2-4 fold decrease of enzymatic activity in relation
385 with a temperature decrease of 10°C, following the Arrhenius equation. Thus, changes in
386 the degradation rates over depth do not necessarily correlate with changes in the
387 microbial community.

388 A model study showed that aggregate-attached bacterial communities are controlled by
389 flagellate grazing, and that flagellate and ciliate populations were determined by
390 colonization and detachment (Kjørboe et al. 2002). *Alteromonas*, but also members of the
391 *Bacteroidetes*, are prone to grazing due to their large cell size (Beardsley et al. 2003;
392 Pernthaler 2005; Weinbauer et al. 2007) and thus the decrease of these groups with depth
393 imply, that grazing might be the most pronounced factor determining the change of the
394 bacterial community during sinking. However, *Synechococcus* are also prone to grazing
395 but do not show decreased abundances with depth (Dolan & Simek 1999; Christaki et al.
396 1999; Guillou et al. 2001). Although, grazing preferences or grazer deterrence cannot be
397 excluded, the results imply a rather low effect of grazing on the community structure on
398 the aggregates.

399 Previous studies found that both initial composition of organic matter and its lability
400 varies with aggregate sinking speed and that fast-sinking aggregates were dominated by
401 phytoplankton biomarkers and slow-sinking aggregates by bacterial biomarkers (Goutx et
402 al. 2007). This suggests that aging during sinking of aggregates might influence the
403 bacterial community. Labile carbon compounds are degraded first (Goutx et al. 2007) and
404 the refractory carbon compounds remain on the aggregate and sink towards deeper layers.
405 Thus, the quality of the nutrient sources changes and therefore the ecological niche

406 provided by the aggregate changes. One of the few studies investigating the influence
407 from rapidly changing environments on bacterial communities found that multiple
408 ecological niches were provided for a diverse range of bacterial populations in the
409 shallow southeastern North Sea during periods with abundant organic matter (Teeling et
410 al. 2012).

411 Therefore, we hypothesize that *Alteromonas* and *Bacteroidetes* actively or passively
412 detach from the aggregates due to a change in the ecological niches provided by the
413 aggregate. In the vicinity of aggregates, a huge number of ectoenzymes for carbon
414 degradation were found (Arnosti 2011; Azam & Malfatti 2007; Simon et al. 2002).
415 Members of the *Bacteroidetes* may produce these carbon active enzymes, which may be
416 functionally related to the attachment of cells to organic materials (Bauer et al. 2006;
417 Kataeva et al. 2002). Thus, *Bacteroidetes* might use polysaccharide residues as
418 attachment “anchors” and degrade these residues. Therefore, Sus-like proteins might be
419 used in combination with TonB-like membrane transporters, which are found in several
420 members of the *Bacteroidetes* (Martens et al. 2009). After degradation, the cells might
421 glide onwards to the next chemical anchor, ensuring attachment or may passively detach
422 from the aggregate. This is supported by the findings of genes for polymere degradation
423 in *Bacteroidetes* and the resulting substrate preferences (Cottrell & Kirchman 2000;
424 Bauer et al. 2006; Gómez-Pereira et al. 2012). However, we were not able to investigate
425 mechanisms of attachment and detachment and thus further verification of this hypothesis
426 is necessary.

427 The TEP structures were dominated by *Alteromonas* at both depths. Opposite to the *in*
428 *situ* collected marine snow, the TEP structures were not exposed to decreasing

429 temperature or increasing pressure during the roller tank incubations. The incubations
430 were done with relatively small amounts of natural sea water (1.2 l) from either 65 m or
431 400 m which most likely excluded grazers from higher trophic levels. We therefore
432 assume that the roller tank incubations excluded influence from changing temperature
433 and pressure and only allowed limited grazing pressure on the bacterial communities
434 attached to the TEP structures. Generally, incubation experiments show a “bottle effect”
435 with increasing abundances of *Alteromonas*. Grazing sensitive *Gammaproteobacteria*
436 may benefit most from the truncated food webs in laboratory incubations (Eilers et al.
437 2000; Schäfer et al. 2000; Fuchs et al. 2000). To test this, we investigated the free-living
438 bacterial community within a roller tank after 19 h of incubation and found 46% of total
439 bacteria to be *Alteromonas* within the roller tank compared to <1% of the free-living
440 bacterial community in the sampled sea water (data not shown).

441 Similarly, other studies have found strong indications of bottle effects on the free living
442 bacterial community during incubation experiments (Fuchs et al. 2000; Schäfer et al.
443 2000; Heike et al. 2000). Therefore, the use of drifting sediment traps equipped with
444 viscous gel provides a unique method to investigate attach bacterial communities within
445 *in situ* collected marine snow from depth below the reach of scuba diving, eliminating the
446 need for laboratory incubations. Although aggregates presented in this study were
447 strongly compressed by the filtration process necessary for the FISH investigations, the
448 method provides the opportunity to achieve the full three dimensional structure of the
449 aggregates and future work might include a 3D reconstruction of the bacterial community
450 on marine snow aggregates.

451 In summary, we showed that *Synechococcus*, *Bacteroidetes* and *Alteromonas* are the
452 dominant groups on marine snow aggregates off Cape Blanc. The abundances of
453 *Bacteroidetes* and *Alteromonas* decreased at depth, indicating that changes in temperature,
454 pressure, grazing pressure, and detachment possibly triggered by the decreasing
455 nutritional value of the aggregates, may lead to changes in the bacterial communities
456 within marine snow. Considering these effects through the whole water column, the
457 composition of sinking aggregates will change due to degradation processes and might
458 show a more pronounced effect on the community composition (Azam & Malfatti 2007).
459 Since aggregate-associated microorganisms are the main degraders of marine snow at
460 depths (Stemmann et al. 2004; Iversen et al. 2010) and their abundances determines the
461 rate of degradation (Ploug & Grossart 2000; Grossart & Ploug 2001), understanding the
462 processes determining the species composition and abundances on aggregates at depth is
463 pivotal for predictions of marine biogeochemical cycles.

464 **Acknowledgements**

465 We acknowledge the captains and crews of the RV Poseidon and the RV Maria S. Merian.
466 Furthermore we would like to thank Gerhard Fischer, Götz Ruhland, Marko Klann,
467 Andreas Basse and Nicolas Nowald for their help during the sampling procedures and
468 Dennis Fink for the help with image processing. This study was supported by the Max
469 Planck Society and the DFG-Research Center/Cluster of Excellence “The Ocean in the
470 Earth System”.

471

472

473

474

475

476

477

478

479

480

481

482

483

484

485

486

487

488 **References**

- 489 Acinas S, Antón J, Rodríguez-Valera F. (1999). Diversity of free-living and attached
490 bacteria in offshore Western Mediterranean waters as depicted by analysis of genes
491 encoding 16S rRNA. *Appl. Environ. Microbiol.* 65:514–522.
- 492 Alldredge AL, Cole JJ, Caron DA. (1986). Production of heterotrophic bacteria
493 inhabiting macroscopic organic aggregates (marine snow) from surface waters. *Limnol.*
494 *Oceanogr.* 31:68–78.
- 495 Alldredge AL, Gotschalk CC. (1990). The relative contribution of marine snow of
496 different origins to biological processes in coastal waters. *Cont. Shelf Res.* 10:41–58.
- 497 Alonso C, Warnecke F, Amann R, Pernthaler J. (2007). High local and global diversity of
498 Flavobacteria in marine plankton. *Environ. Microbiol.* 9:1253–1266.
- 499 Amann R I, Ludwig W, Schleifer KH. (1995). Phylogenetic identification and in situ
500 detection of individual microbial cells without cultivation. *Microbiol. Rev.* 59:143–169.
- 501 Amann RI, Krumholz L, Stahl D. (1990). Fluorescent-oligonucleotide probing of whole
502 cells for determinative, phylogenetic, and environmental studies in microbiology. *J.*
503 *Bacteriol.* 172:762–770.
- 504 Aristegui J, Barton ED, Álvarez-Salgado XA, Santos AMP, Figueiras FG, Kifani S, et al.
505 (2009). Sub-regional ecosystem variability in the Canary Current upwelling. *Prog.*
506 *Oceanogr.* 83:33–48.
- 507 Arnosti C. (2011). Microbial extracellular enzymes and the marine carbon cycle. *Ann.*
508 *Rev. Mar. Sci.* 3:401–425.
- 509 Azam F, Malfatti F. (2007). Microbial structuring of marine ecosystems. *Nat. Rev.*
510 *Microbiol.* 5:782–791.
- 511 Bauer M, Kube M, Teeling H, Richter M, Lombardot T, Allers E, et al. (2006). Whole
512 genome analysis of the marine Bacteroidetes ‘Gramella forsetii’ reveals adaptations to
513 degradation of polymeric organic matter. *Environ. Microbiol.* 8:2201–2213.
- 514 Beardsley C, Pernthaler J, Wosniok W, Amann R. (2003). Are Readily Culturable
515 Bacteria in Coastal North Sea Waters Suppressed by Selective Grazing Mortality? *Appl.*
516 *Environ. Microbiol.* 69:2624–2630.
- 517 Behrenfeld M, Falkowski P. (1997). Photosynthetic rates derived from satellite-based
518 chlorophyll concentration. *Limnol. Oceanogr.* 42:1–20.

- 519 Blackburn N, Hagström Å, Wikner J, Cuadros-Hansson R, Bjørnsen PK. (1998). Rapid
520 determination of bacterial abundance, biovolume, morphology, and growth by neural
521 network-based image analysis. *Appl. Environ. Microbiol.* 64:3246–3255.
- 522 Chavez FP, Messié M. (2009). A comparison of Eastern Boundary Upwelling
523 Ecosystems. *Prog. Oceanogr.* 83:80–96.
- 524 Christaki U, Jacquet S, Dolan JR, Vaultot D, Rassoulzadegan F. (1999). Growth and
525 grazing on *Prochlorococcus* and *Synechococcus* by two marine ciliates. *Limnol.*
526 *Oceanogr.* 44:52–61.
- 527 Cottrell MT, Kirchman D. L. (2000). Natural assemblages of marine proteobacteria and
528 members of the Cytophaga-Flavobacter cluster consuming low- and high-molecular-
529 weight dissolved organic matter. *Appl. Environ. Microbiol.* 66:1692–1697.
- 530 Cottrell MT, Kirchman David L. (2009). Photoheterotrophic microbes in the Arctic
531 Ocean in summer and winter. *Appl. Environ. Microbiol.* 75:4958–4966.
- 532 Daims H, Bruhl A, Amann R., Schleifer KH, Wagner M. (1999). The domain-specific
533 probe EUB338 is insufficient for the detection of all Bacteria: Development and
534 evaluation of a more comprehensive probe set. *Syst. Appl. Microbiol.* 22:434–444.
- 535 DeLong E F, Franks DG, Alldredge AL. (1993). Phylogenetic diversity of aggregate-
536 attached vs. free-living marine bacterial assemblages. *Limnol. Oceanogr.* 38:924–934.
- 537 Dolan J, Simek K. (1999). Diel periodicity in *Synechococcus* populations and grazing by
538 heterotrophic nanoflagellates: analysis of food vacuole contents. *Limnol Oceanogr*
539 44:1565–1570.
- 540 Ducklow HW, Steinberg DK, Buessler KO. (2001). Upper ocean carbon export and the
541 biological pump. *Oceanography* 14:50–58.
- 542 Eilers H, Pernthaler J, Amann R. (2000). Succession of pelagic marine bacteria during
543 enrichment: a close look at cultivation-induced shifts. *Appl. Environ. Microbiol.*
544 66:4634–4640.
- 545 Eilers H, Pernthaler J, Peplies J, Glöckner FO, Gerdt G, Amann R. (2001). Isolation of
546 novel pelagic bacteria from the German Bight and their seasonal contributions to surface
547 picoplankton. *Appl. Environ. Microbiol.* 67:5134–5142.
- 548 Eilers H, Pernthaler K, Glöckner FO, Amann R. (2000). Culturability and in situ
549 abundance of pelagic bacteria from the North Sea. *Appl. Environ. Microbiol.* 66:3044–
550 3051.
- 551 Eloë EA, Shulse CN, Fadrosch DW, Williamson SJ, Allen EE, Bartlett DH. (2011).
552 Compositional differences in particle-associated and free-living microbial assemblages
553 from an extreme deep-ocean environment. *Environ. Microbiol. Rep.* 3:449–458.

- 554 Fuchs BM, Zubkov Mikhail V., Sahm K, Burkill PH, Amann R. (2000). Changes in
555 community composition during dilution cultures of marine bacterioplankton as assessed
556 by flow cytometric and molecular biological techniques. *Environ. Microbiol.* 2:191–201.
- 557 Gómez-Pereira PR, Schüler M, Fuchs BM, Bennke C, Teeling H, Waldmann J, et al.
558 (2012). Genomic content of uncultured Bacteroidetes from contrasting oceanic provinces
559 in the North Atlantic Ocean. *Environ. Microbiol.* 14:52–66.
- 560 Goutx M, Wakeham SG, Lee C, Duflos M, Guigue C, Liu Z, et al. (2007). Composition
561 and degradation of marine particles with different settling velocities in the northwestern
562 Mediterranean Sea. *Limnol. Oceanogr.* 52:1645.
- 563 Grossart HP, Gust G. (2009). Hydrostatic pressure affects physiology and community
564 structure of marine bacteria during settling to 4000 m: an experimental approach. *Mar.
565 Ecol. Prog. Ser.* 390:97–104.
- 566 Grossart HP, Ploug Helle. (2001). Microbial degradation of organic carbon and nitrogen
567 on diatom aggregates. *Limnol. Oceanogr.* 45:1467–1475.
- 568 Grossart HP, Simon M. (1998). Bacterial colonization and microbial decomposition of
569 limnetic organic aggregates (lake snow). *Aquat. Microb. Ecol.* 15:127–140.
- 570 Guillou L, Jacquet Stéphan, Chrétiennot-Dinet M-J, Vaulot D. (2001). Grazing impact of
571 two small heterotrophic flagellates on *Prochlorococcus* and *Synechococcus*. *Aquat
572 Microb Ecol* 26:201–207.
- 573 Halary S, Riou V, Gaill F, Boudier T, Duperron S. (2008). 3D FISH for the quantification
574 of methane- and sulphur-oxidizing endosymbionts in bacteriocytes of the hydrothermal
575 vent mussel *Bathymodiolus azoricus*. *ISME J.* 2:284–292.
- 576 Herndl GJ. (1988). Ecology of amorphous aggregations(marine snow) in the northern
577 Adriatic Sea. 2. Microbial density and activity in marine snow and its implication to
578 overall pelagic processes. *Mar. Ecol. Prog. Ser.* 48:265–275.
- 579 Iversen MH, Nowald N, Ploug H, Jackson GA, Fischer G. (2010). High resolution
580 profiles of vertical particulate organic matter export off Cape Blanc, Mauritania:
581 Degradation processes and ballasting effects. *Deep-Sea Res. Pt. I* 57:771–784.
- 582 Iversen MH, Ploug H. (2013). Temperature effects on carbon-specific respiration rate and
583 sinking velocity of diatom aggregates – potential implications for deep ocean export
584 processes. *Biogeosciences Discuss.* 10:371–399.
- 585 Kataeva IA, Seidel III RD, Shah A, West LT, Li X-L, Ljungdahl LG. (2002). The
586 Fibronectin Type 3-Like Repeat from the *Clostridium thermocellum* Cellobiohydrolase
587 CbhA Promotes Hydrolysis of Cellulose by Modifying Its Surface. *Appl Environ
588 Microbiol* 68:4292–4300.

- 589 Kiørboe T, Grossart HP, Ploug H, Tang K. (2002). Mechanisms and rates of bacterial
590 colonization of sinking aggregates. *Appl. Environ. Microbiol.* 68:3996–4006.
- 591 Kirchman David L. (2002). The ecology of Cytophaga–Flavobacteria in aquatic
592 environments. *FEMS Microbiol. Ecol.* 39:91–100.
- 593 Manz W, Amann R, Ludwig W, Vancanneyt M, Schleifer K-H. (1996). Application of a
594 suite of 16S rRNA-specific oligonucleotide probes designed to investigate bacteria of the
595 phylum cytophaga-flavobacter-bacteroides in the natural environment. *Microbiology*
596 142:1097–1106.
- 597 Manz W, Amann R, Ludwig W, Wagner M, Schleifer K. (1992). Phylogenetic
598 Oligodeoxynucleotide Probes for the Major Subclasses of Proteobacteria: Problems and
599 Solutions. *Syst. Appl. Microbiol.* 15:593–600.
- 600 Martens EC, Koropatkin NM, Smith TJ, Gordon JI. (2009). Complex glycan catabolism
601 by the human gut microbiota: The Bacteroidetes Sus-like paradigm. *J Biol Chem*
602 284:24673–24677.
- 603 Massana R, Murray AE, Preston CM, DeLong EF. (1997). Vertical distribution and
604 phylogenetic characterization of marine planktonic Archaea in the Santa Barbara Channel.
605 *Appl. Environ. Microbiol.* 63:50–56.
- 606 McCarren J, Becker JW, Repeta DJ, Shi Y, Young CR, Malmstrom RR, et al. (2010).
607 Microbial community transcriptomes reveal microbes and metabolic pathways associated
608 with dissolved organic matter turnover in the sea. *Proc. Natl. Acad. Sci. USA* 107:16420–
609 16427.
- 610 Moeseneder MM, Winter C, Herndl GJ. (2001). Horizontal and vertical complexity of
611 attached and free-living bacteria of the eastern Mediterranean Sea, determined by 16S
612 rDNA and 16S rRNA fingerprints. *Limnol. Oceanogr.* 46:95–107.
- 613 Mueller LN, De Brouwer JF, Almeida JS, Stal LJ, Xaver JB. (2006). Analysis of a marine
614 phototrophic biofilm by confocal laser scanning microscopy using the new image
615 quantification software PHLIP. *BMC Ecology* 6.
- 616 Neef A, Amann R, Schlesner H, Schleifer KH. (1998). Monitoring a widespread bacterial
617 group: in situ detection of planctomycetes with 16S rRNA-targeted probes. *Microbiology*
618 (Reading, Engl.) 144 (Pt 12):3257–3266.
- 619 Pernthaler A, Pernthaler J, Amann R. (2002). Fluorescence in situ hybridization and
620 catalyzed reporter deposition for the identification of marine bacteria. *Appl. Environ.*
621 *Microbiol.* 68:3094–3101.
- 622 Pernthaler J. (2005). Predation on prokaryotes in the water column and its ecological
623 implications. *Nat. Rev. Micro.* 3:537–546.

- 624 Ploug Helle, Grossart H-P. (2000). Bacterial growth and grazing on diatom aggregates:
625 Respiratory carbon turnover as a function of aggregate size and sinking velocity. *Limnol.*
626 *Oceanogr.* 45:1467–1475.
- 627 Puddu A, Zoppini A, Fazi S, Rosati M, Amalfitano S, Magaletti E. (2003). Bacterial
628 uptake of DOM released from P-limited phytoplankton. *FEMS Microbiol. Ecol.* 46:257–
629 268.
- 630 Rappe MS, Connon SA, Vergin KL, Giovannoni SJ. (2002). Cultivation of the ubiquitous
631 SAR11 marine bacterioplankton clade. *Nature* 418:630–633.
- 632 Rath J, Ying Wu K, Herndl GJ, DeLong E F. (1998). High phylogenetic diversity in a
633 marine-snow-associated bacterial assemblage. *Aquat. Microb. Ecol.* 14:261–269.
- 634 Schäfer H, Servais P, Muyzer G. (2000). Successional changes in the genetic diversity of
635 a marine bacterial assemblage during confinement. *Arch. Microbiol.* 173:138–145.
- 636 Schattenhofer M, Fuchs BM, Amann R, Zubkov M V, Tarran GA, Pernthaler J. (2009).
637 Latitudinal distribution of prokaryotic picoplankton populations in the Atlantic Ocean.
638 *Environ. Microbiol.* 11:2078–2093.
- 639 Shanks AL, Trent JD. (1979). Marine snow: Microscale nutrient patched. *Limnol.*
640 *Oceanogr.* 24:850–854.
- 641 Silver MW, Coale SL, Pilskaln CH, Steinberg DR. (1998). Giant aggregates: Importance
642 as microbial centers and agents of material flux in the mesopelagic zone. *Limnol.*
643 *Oceanogr.* 43:498–507.
- 644 Simon M, Grossart H-P, Schweitzer B, Ploug H. (2002). Microbial ecology of organic
645 aggregates in aquatic ecosystems. *Aquat. Microb. Ecol.* 28:175–211.
- 646 Solovei I, Cavallo A, Schermelleh L, Jaunin F, Scasselati C, Cmarko D, et al. (2002).
647 Spatial preservation of nuclear chromatin architecture during three-dimensional
648 fluorescence in situ hybridization (3D-FISH). *Exp. Cell Res.* 276:10–23.
- 649 Stahl DA, Amann RI. (1991). Development and application of nucleic acid probes.
650 In: *Nucleic acid techniques in bacterial systematics*, Stackebrandt, E & Goodfellow, M,
651 eds (ed)., Chichester: John Wiley & Sons Ltd., pp. 205–248.
- 652 Stemmann L, Jackson GA, Gorsky G. (2004). A vertical model of particle size
653 distributions and fluxes in the midwater column that includes biological and physical
654 processes—Part II: application to a three year survey in the NW Mediterranean Sea.
655 *Deep-Sea Res. Pt. I* 51:885–908.
- 656 Tamburini C, Garcin J, Grgori G, Leblanc K, Rimmelin P, Kirchman David L. (2006).
657 Pressure effects on surface Mediterranean prokaryotes and biogenic silica dissolution
658 during a diatom sinking experiment. *Aquat. Microb. Ecol.* 43:267–276.

- 659 Tamburini C, Goutx M, Guigue C, Garel M, Lefèvre D, Charrière B, et al. (2009). Effects
660 of hydrostatic pressure on microbial alteration of sinking fecal pellets. *Deep-Sea Res. Pt.*
661 *II* 56:1533–1546.
- 662 Teeling H, Fuchs BM, Becher D, Klockow C, Gardebrecht A, Bennke CM, et al. (2012).
663 Substrate-controlled succession of marine bacterioplankton populations induced by a
664 phytoplankton bloom. *Science* 336:608–611.
- 665 Teira E, Reinthaler T, Pernthaler A, Pernthaler J, Herndl GJ. (2004). Combining
666 catalyzed reporter deposition-fluorescence in situ hybridization and
667 microautoradiography to detect substrate utilization by Bacteria and Archaea in the deep
668 ocean. *Appl. Environ. Microbiol.* 70:4411–4414.
- 669 Thiele S, Fuchs B, Amann R. (2011). Identification of microorganisms using the
670 ribosomal RNA approach and fluorescence in situ hybridization. In: *Treatise on Water*
671 *Science*, Wilderer, P, ed (ed). Vol. 3, Academic Press: Oxford, pp. 171–189.
- 672 Urban-Rich J. (1999). Release of dissolved organic carbon from copepod fecal pellets in
673 the Greenland Sea. *J. Exp. Mar. Biol. Ecol.* 232:107–124.
- 674 Vanucci S, Dell’Anno A, Pusceddu A, Fabiano M, Lampitt RS, Danovaro R. (2001).
675 Microbial assemblages associated with sinking particles in the Porcupine Abyssal Plain
676 (NE Atlantic Ocean). *Prog. Oceanogr.* 50:105–121.
- 677 Volk T, Hoffert MI. (1985). Ocean carbon pumps: Analysis of relative strengths and
678 efficiencies in ocean-driven atmospheric CO₂ changes. In: *Geophysical Monograph*
679 *Series*, Sundquist, ET & Broecker, WS, eds (ed). Vol. 32, American Geophysical Union,
680 Washington, DC (USA), pp. 99–110.
- 681 Wallner G, Amann R., Beisker W. (1993). Optimizing fluorescent in situ hybridization
682 with rRNA-targeted oligonucleotide probes for flow cytometric identification of
683 microorganisms. *Cytometry* 14:136–143.
- 684 Weinbauer MG, Hornák K, Jezbera J, Nedoma J, Dolan JR, Šimek K. (2007). Synergistic
685 and antagonistic effects of viral lysis and protistan grazing on bacterial biomass,
686 production and diversity. *Environ. Microbiol.* 9:777–788.
- 687 West NJ, Schönhuber WA, Fuller NJ, Amann RI, Rippka R, Post AF, et al. (2001).
688 Closely related *Prochlorococcus* genotypes show remarkably different depth distributions
689 in two oceanic regions as revealed by in situ hybridization using 16S rRNA-targeted
690 oligonucleotides. *Microbiology* 147:1731–1744.
- 691 Willey JM, Waterbury JB. (1989). Chemotaxis toward Nitrogenous Compounds by
692 Swimming Strains of Marine *Synechococcus* spp. *Appl. Environ. Microbiol.* 55:1888–
693 1894.

Manuscripts

- 694 Zeder M, Kohler E, Zeder L, Pernthaler J. (2011). A Novel Algorithm for the
695 Determination of Bacterial Cell Volumes That is Unbiased by Cell Morphology.
696 *Microscop. Microanal.* 17:799–809.
- 697 Zubkov M V., Fuchs BM, Tarran GA, Burkill PH, Amann R. (2003). High Rate of
698 Uptake of Organic Nitrogen Compounds by *Prochlorococcus* Cyanobacteria as a Key to
699 Their Dominance in Oligotrophic Oceanic Waters. *Appl. Environ. Microbiol.* 69:1299–
700 1304.
- 701 Zubkov M. V., Tarran GA. (2005). Amino acid uptake of *Prochlorococcus* spp. in surface
702 waters across the South Atlantic Subtropical Front. *Aquat. Microb. Ecol.* 40:241–249.
- 703

704 Tables

705

706 TAB 1: List of oligonucleotides used in this study. ^a Formamide concentration of the
707 hybridization buffer, ^b used in mix with BET42a (Manz et al. 1992) unlabeled as
708 competitor, ^c used in a mix and partly used as 4-times click labelled probes purchased
709 from Biomers (Biomers, Ulm, Germany).

710

711 Figures

712

713 FIG 1: Map of the sample area off Cape Blanc (Mauretania) showing all stations of the 2
714 cruises used for sampling. During POS396 a depth profile was done until 1000 m depth
715 and TEP structures were formed in roller tanks at station GeoB14204. During MSM 18-1
716 a depth profile was done at station GeoB15704 and a drifting trap to collect aggregates
717 was deployed at station GeoB15703-5 and recovered after 65 h at station 15707-1.

718

719 FIG 2: Box plots showing the total numbers of EUB I-III stained cells on (A) marine
720 snow aggregates sampled at 100 m (n=38) and 400 m depth (n=39), (B) the
721 corresponding free living bacteria at 150 m (n=3) and 400 m (n=3), (C) the total cell
722 number normalized to aggregate size at 100 m (n=38) and 400 m (n=39) depth, (D) on
723 TEP structures re-assembled from waters from 65 m (n=10) and 400 m (n=20) depth, and
724 (E) the corresponding free living community (n=3).

725

726 FIG 3: Comparison of relative abundances of the attached living bacterial community on
727 marine snow aggregates at 100 m (black) and 400 m (white) depth from the drifting
728 sediment trap (A) and relative abundances in the free living bacterial community at 150
729 m and 400 m depth at station GeoB15704 (B). Abundances of *Synechococcus* (SYN405),
730 *Bacteroidetes* (CF319a), *Roseobacter* (ROS537), *Gammaproteobacteria* (GAM42a),
731 *Alteromonas* (ALT1413), *Pseudoalteromonas* (PSA184), and *Planctomycetes* (PLA46)
732 cells are shown.

733

734 FIG 4 Pictures of aggregates from 100 m (A,C,E) and 400 m (B,D,F) depth of
735 *Synechococcus* (A+B), *Bacteroidetes* (C+D) and *Alteromonas* (E+F). DAPI stained cells
736 are shown in blue, while cells stained by specific probes are green. The autofluorescence
737 with DAPI exaltation shows the total aggregate (red).

738

739 FIG 5: Comparison of the of the attached living bacterial community on TEP structures
740 (A) and relative abundances of the corresponding free living bacteria (B) at 65 m (black)
741 and 400 m (white) depth at station GeoB14204. Abundances of *Alteromonas* (ALT1413),
742 *Pseudoalteromonas* (PSA184) and *Bacteroidetes* (CF319a) cells are shown.

743

744

745 **Supplementary information**

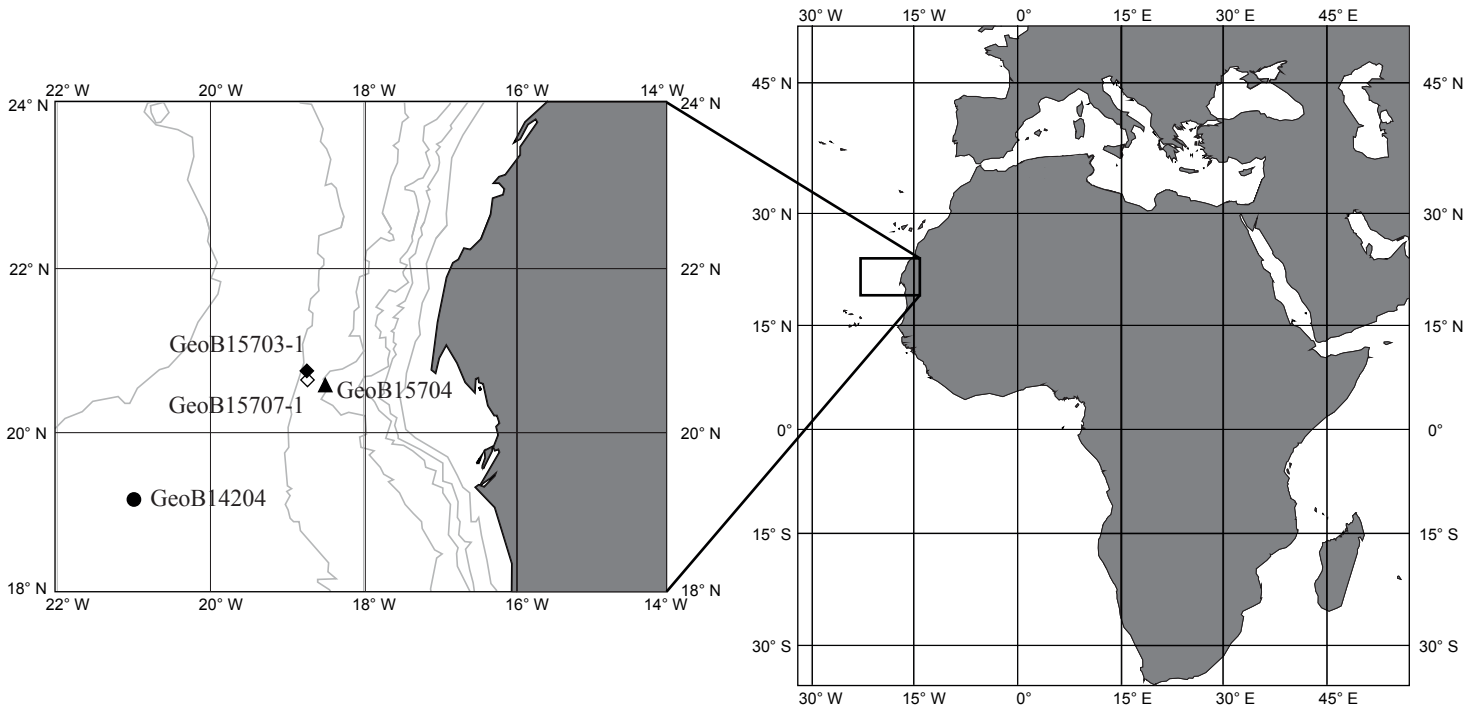
746

747 SUP 1: Scheme of one of the four tubes of a drifting sediment trap. Dashed lines mark
748 water levels.

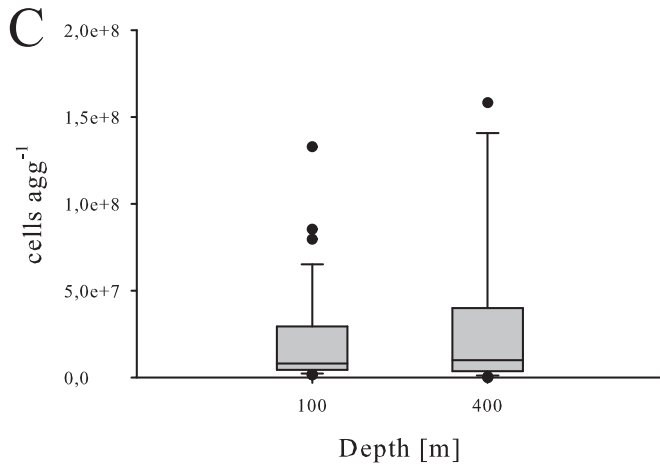
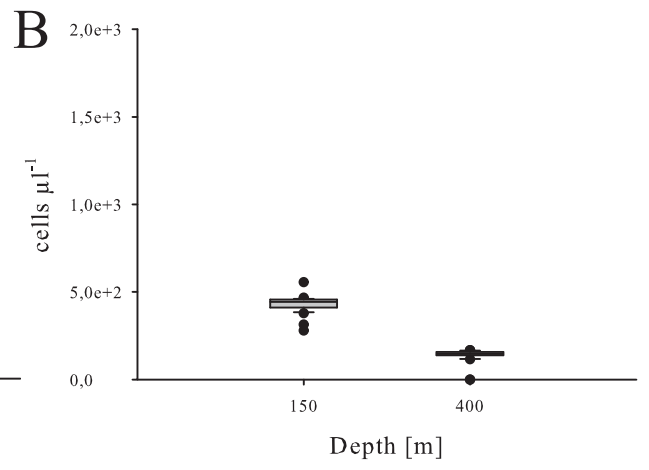
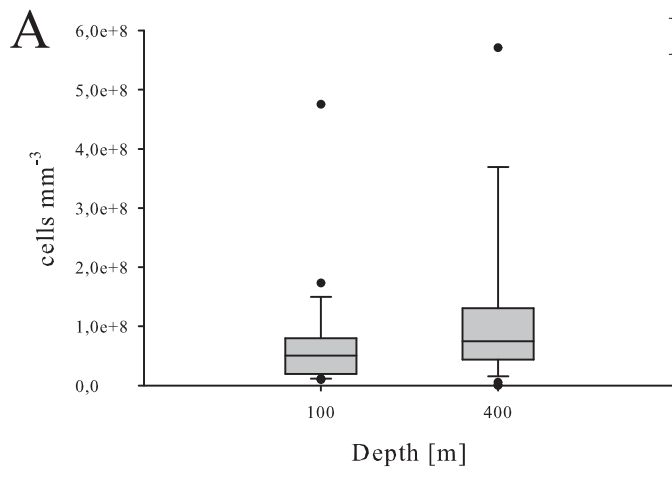
749

750 SUP 2: Workflow of marine snow analyses.

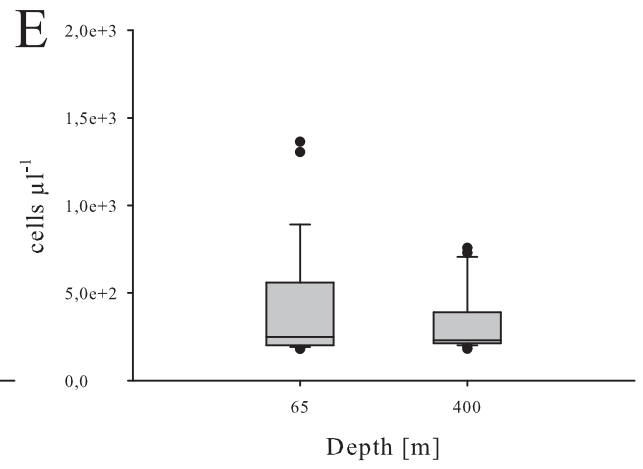
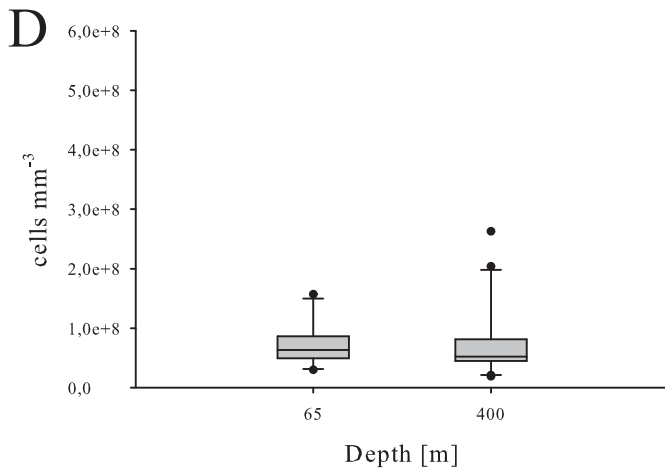
	Target organism	Sequence (5'→3')	<i>E. coli</i> position ^a	FA (%) ^b	Ref.
EUB 338 ^c	Most <i>Bacteria</i>	GCTGCCCTCCCGTAGGAGT	338-355	35	(Amann et al. 1990)
EUB II ^c	<i>Planctomycetales</i>	GCAGCCACCCCGTAGGTGT	338-355	35	(Daims et al. 1999)
EUB III ^c	<i>Verrucomicrobiales</i>	GCTGCCACCCCGTAGGTGT	338-355	35	(Daims et al. 1999)
NON338	Control	ACTCCTAGGGGAGGCAGC	338-355	35	(Wallner et al. 1993)
ARCH915	<i>Archaea</i>	GTGCTCCCCCGCCAAATTCCT	915-934	35	(Stahl & Amann 1991)
CREN554	<i>Thaumarchaeota</i>	TTAGGCCCAATAATCMTCTCT	554-573	0	(Massana et al. 1997)
EURY806	<i>Euryarchaeota</i> marine group II	CACAGCGTTTACACCTAG	806-823	0	(Teira et al. 2004)
SAR11 441	SAR11 clade	AAAAAATACAGTCATTTCTCTCCCCCGAC	441-463	25	(Rappe et al. 2002)
ROSS37	<i>Roseobacter</i> clade	CAACGCTAACCCCTCC	537-553	35	(Eilers et al. 2001)
GAM42a ^b	<i>Gammaproteobacteria</i>	GCCTCCCCACATCGTTT	1027-1043	35	(Manz et al. 1992)
ALT1413	<i>Alteromonas / Cobwellia</i>	TTTGCATCCCCACTCCCAT	1413-1430	40	(Eilers et al. 2000)
PSA184	<i>Pseudoalteromonas</i>	CCCCTTTGGTCCGTAGAC	184-201	30	(Eilers et al. 2000)
SAR324 1412	SAR324-clade	GCCCCGTCAACTCCCAT	1412-1429	35	(Schattenhofer et al. 2009)
CF319a	<i>Bacteroidetes</i>	TGGTCCGTGTCTCAGTAC	319-336	35	(Manz et al. 1996)
PLA46	<i>Planctomycetes</i>	GACTTGCATGCCTAATCC	46-63	30	(Neef et al. 1998)
SYN405	<i>Synechococcus</i>	AGAGGCCCTTCATCCCTCA	405-422	40	(West et al. 2001)
PRO405	<i>Prochlorococcus</i>	AGAGGCCCTTCGTCCCTCA	405-422	40	(West et al. 2001)

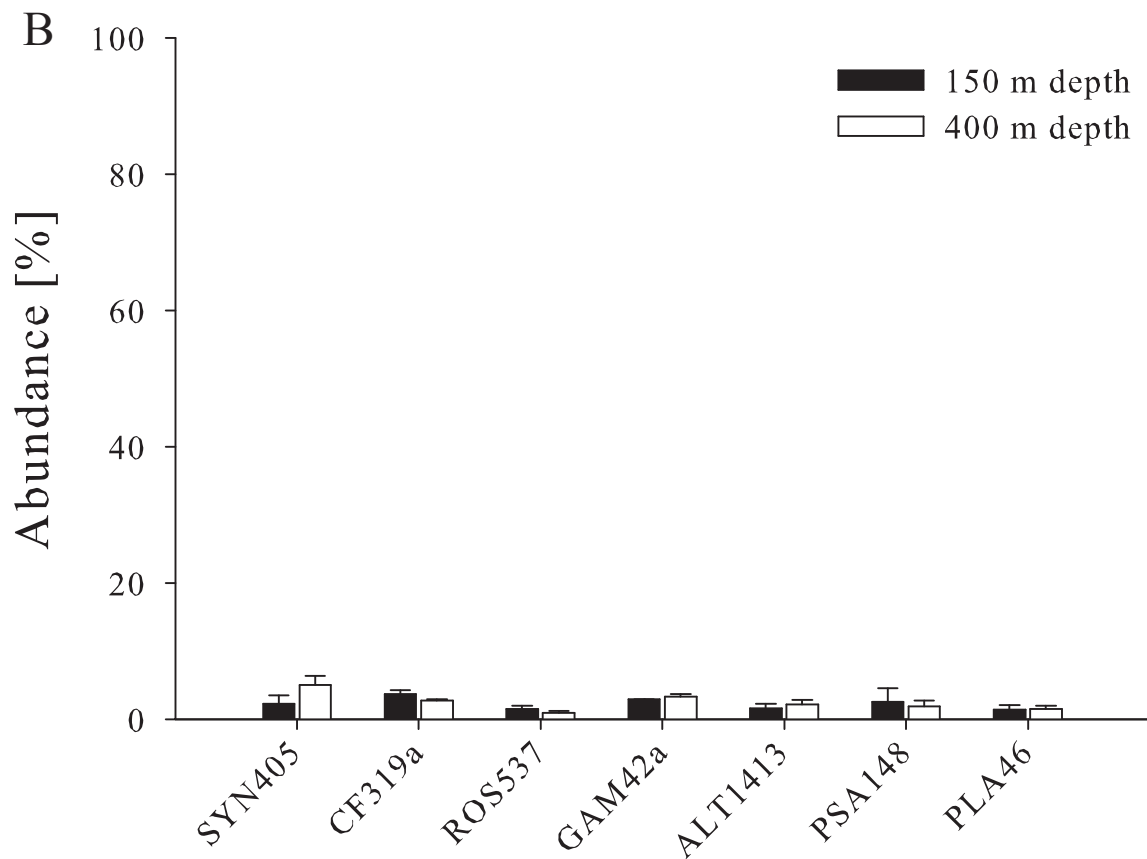
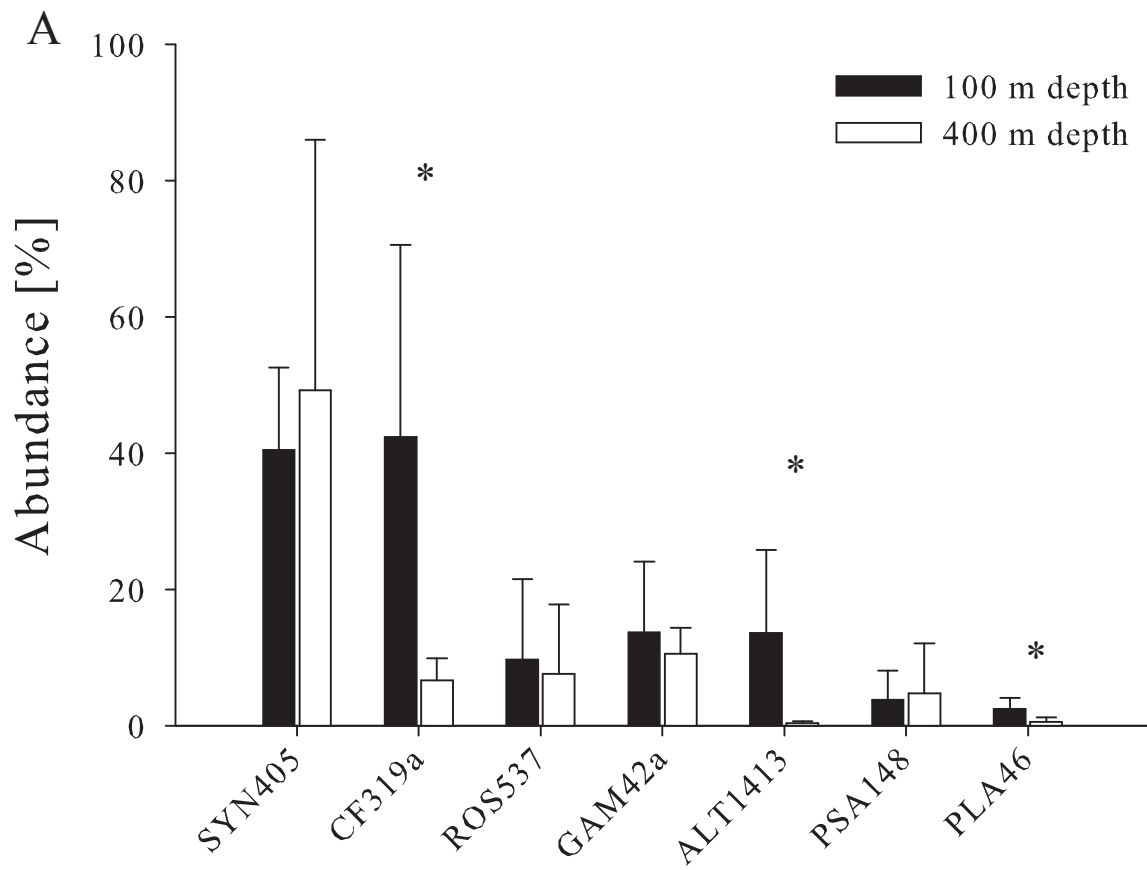


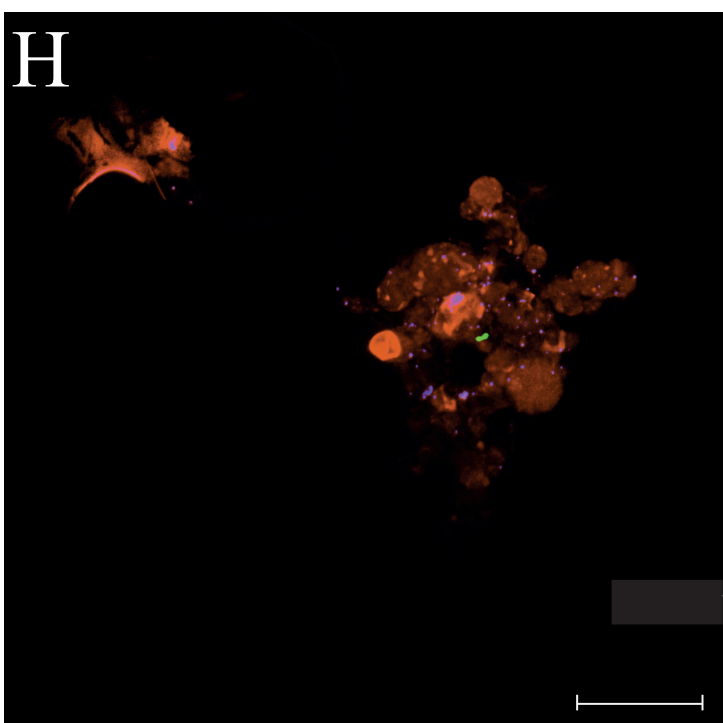
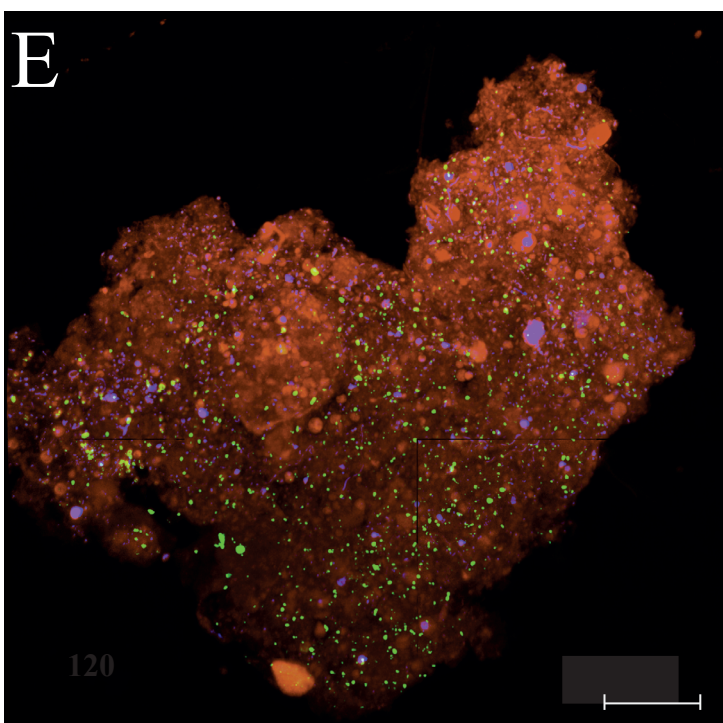
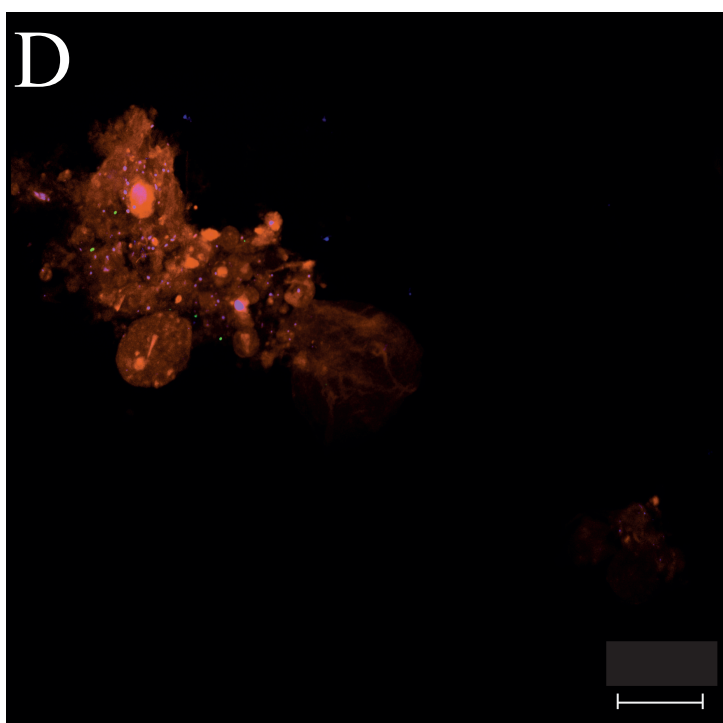
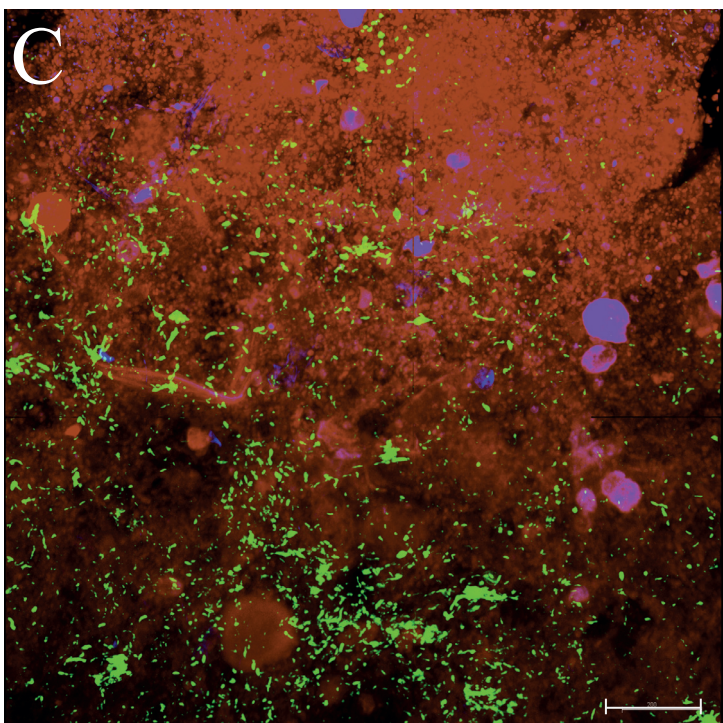
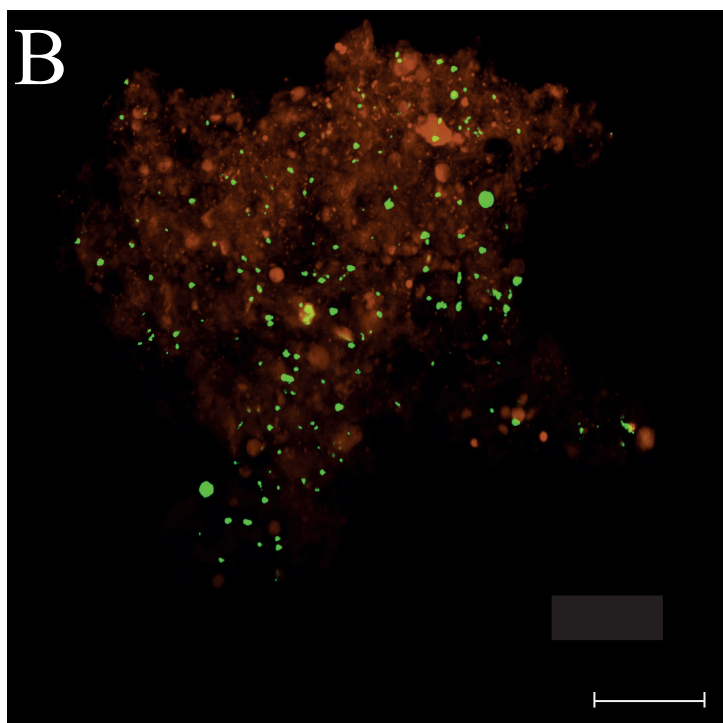
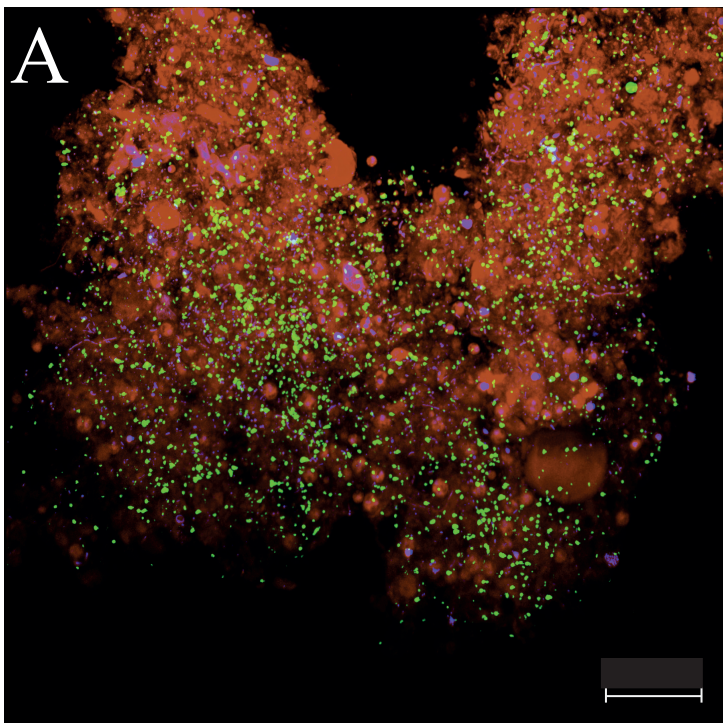
Marine snow aggregates

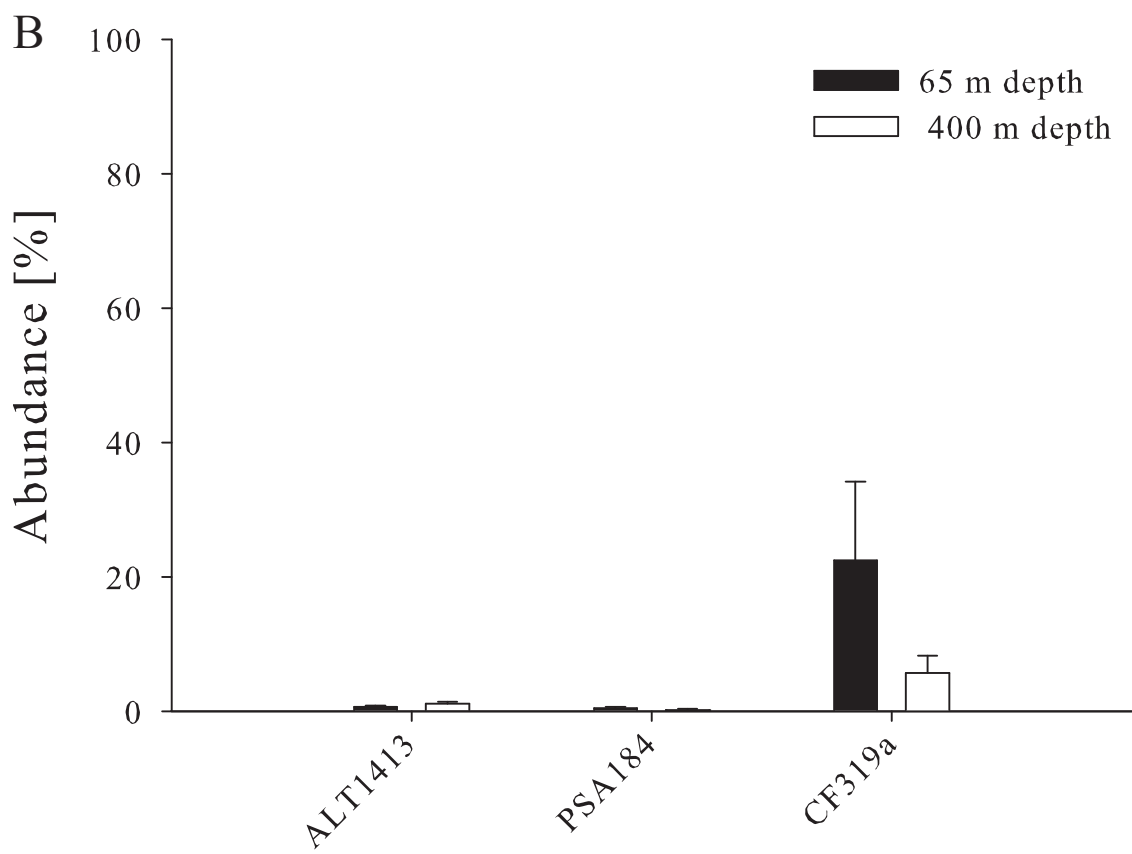
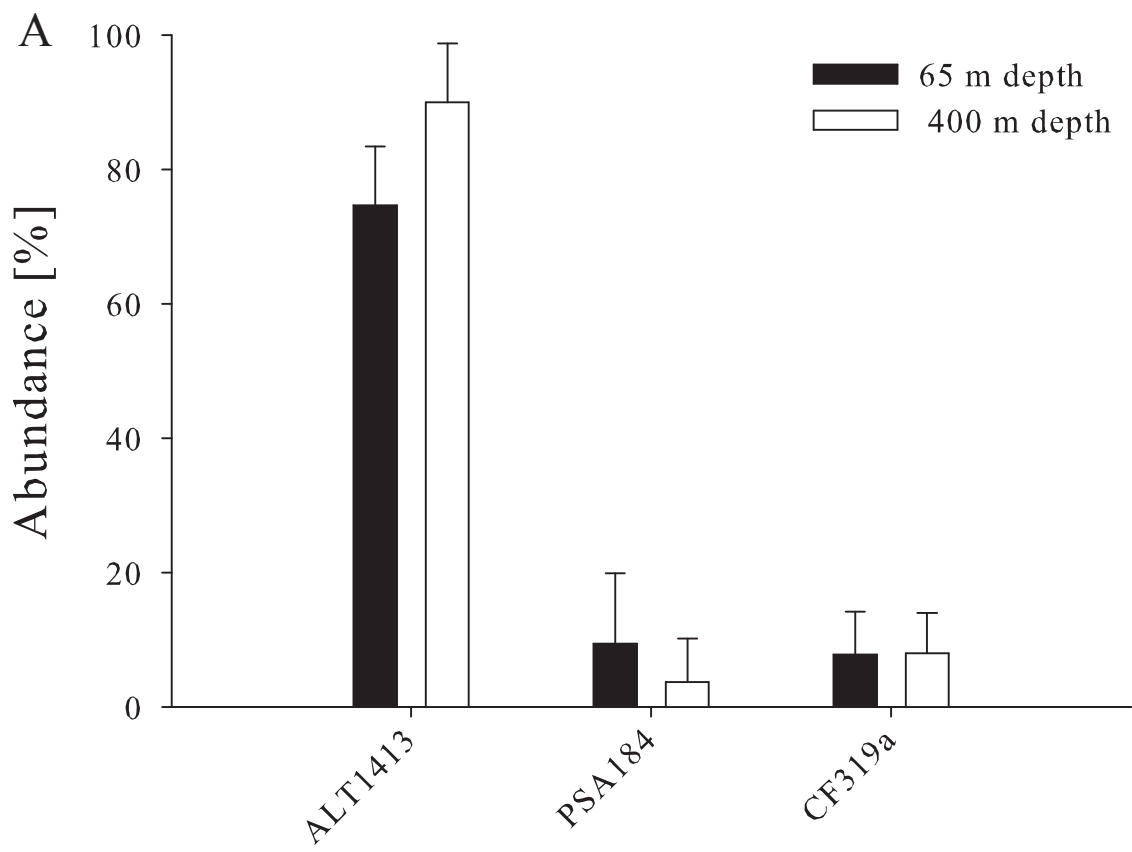


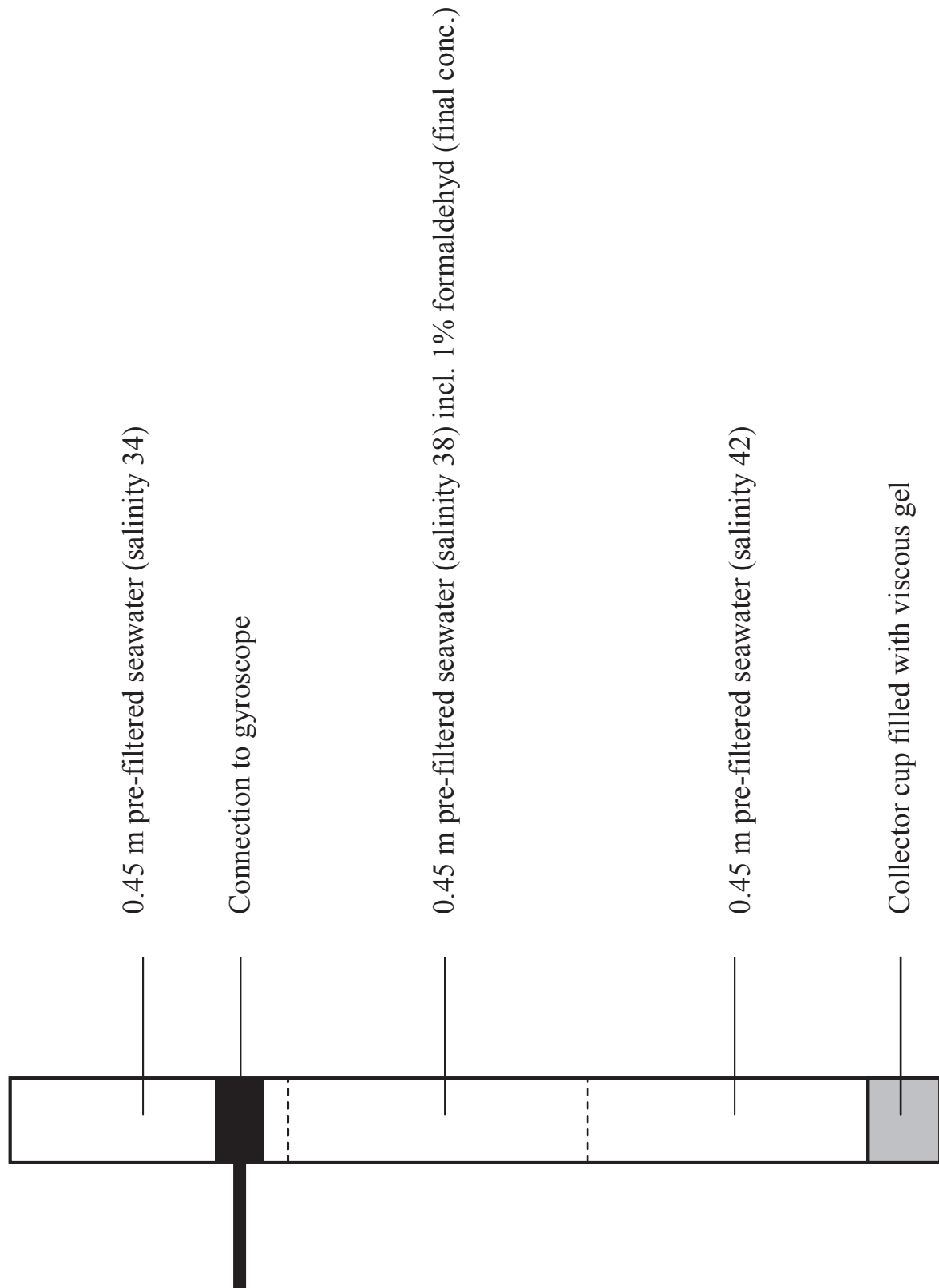
TEP structures

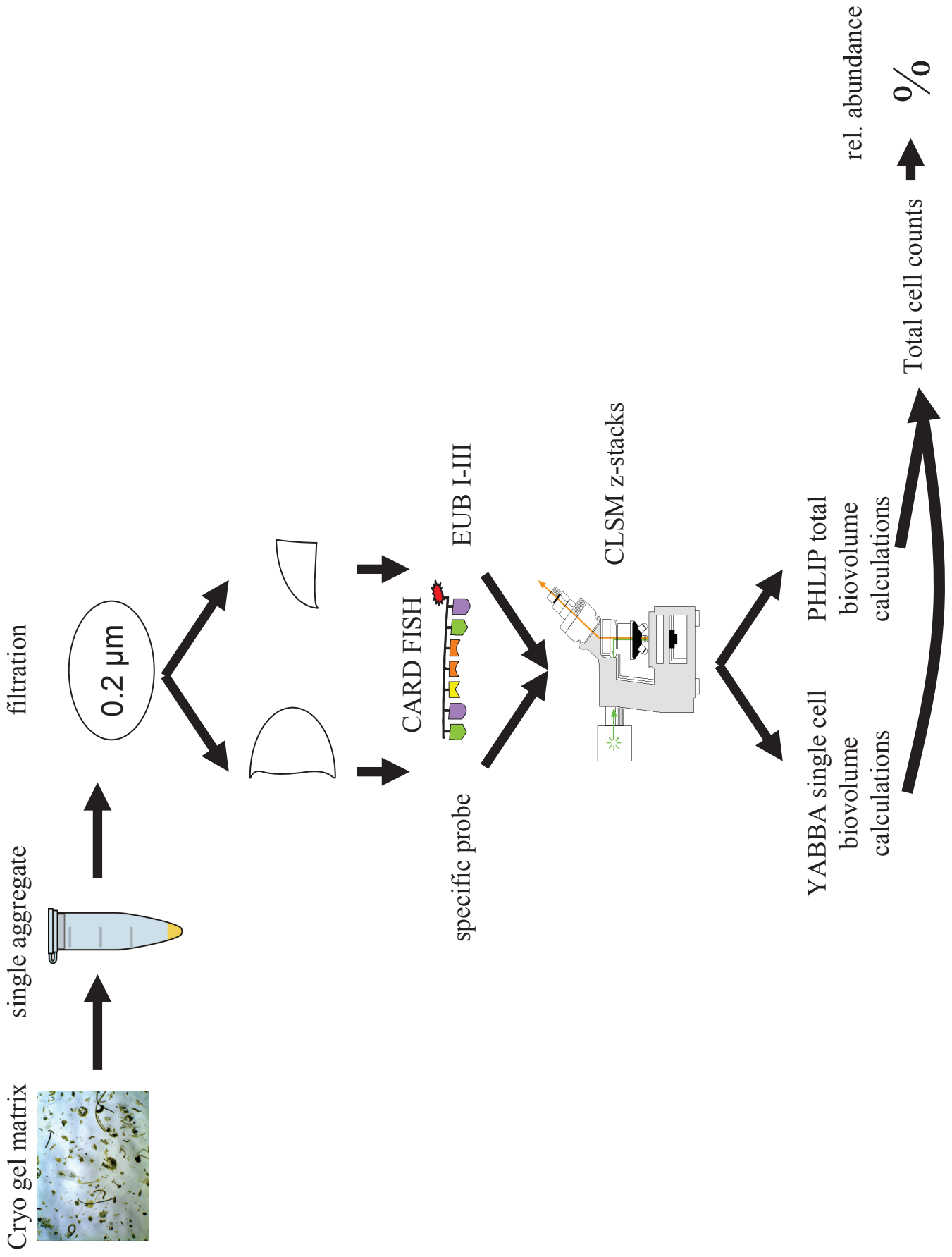












5. General discussion

This doctoral study addresses the role of microorganisms in marine carbon cycling, in particular in the biological carbon pump. The biological carbon pump is highly active in phytoplankton blooms and thus bloom situations provide optimal conditions for the investigation of processes in the biological carbon pump. Naturally, phytoplankton blooms occur mainly in coastal and temporal upwelling areas (Gattuso et al. 1998), as well as in perennial upwelling systems (Aristegui et al. 2004). Artificially, they can be induced by fertilization of HNLC areas with iron (Martin et al. 1994).

5.1. The microbial loop during the LOHAFEX experiment

During the iron fertilization experiment LOHAFEX, a cold core eddy in the South Atlantic was fertilized and a phytoplankton bloom of 300 km² was induced. After five days, chlorophyll a values increased significantly, indicating the induction of a phytoplankton bloom (Manuscript I). This is congruent with increased chlorophyll a concentrations in all previous iron fertilization experiments (deBaar et al. 2005; Peloquin et al. 2011; Smetacek et al. 2012). However, the increase during the LOHAFEX experiment was rather low compared to other iron fertilization experiments (deBaar et al. 2005). During the SOFeX North and the SAGE experiment, similarly low values of below 2 µg l⁻¹ were found (Coale et al. 2004; Peloquin et al. 2011b). All three experiments were conducted in waters with low silicate concentrations (<3 µM), which indicates that silicate is another limiting factor for growth of highly productive phytoplankton blooms (Coale et al. 2004; Peloquin et al. 2011a).

Silicate is an important nutrient to support the growth of diatoms, which form stable and productive blooms, as shown in most iron fertilization experiments (deBaar et al. 2005). The low silicate concentrations during the LOHAFEX experiment are most likely due to a bloom event in the water body, prior to the experiment. The bloom forming diatom species incorporated silicate in their frustules and sequestered it to POM. The resulting depletion of dissolved silica caused unfavourable conditions for diatoms and results in a nano- and picoplankton bloom. Such blooms are formed in low silicate waters (Agawin et al. 2000). Hence, the LOHAFEX bloom consisted mainly from *Phaeocystis* spp. (Manuscript II, Schulz et al. Appendix II), which do not reach the chlorophyll a concentrations of diatom blooms. This also implies that less POC and DOC was

General discussion

produced and consequently bacterial activities were not as high as they might have been in diatom blooms. However, bacterial activities increased after iron fertilization in association with the increase in chlorophyll a values during the LOHAFEX experiment (Manuscript I).

Despite the increasing bacterial activities, the bacterial community was found rather constant. The SAR11 clade and the SAR86 clade dominated the *Alphaproteobacteria* and *Gammaproteobacteria* and constituted for about 70% of the total bacterial community. Both clades are rather small in size and can be found in oligotrophic regions (Pernthaler et al. 2002; Morris et al. 2002).

Stable bacterial communities with elevated bacterial activities could occur when nano- and picoplankton grazers exert strong grazing pressure. During LOHAFEX the bacterial community was most likely controlled by nanoflagellate grazing. Fast growing bacteria, such as *Gammaproteobacteria*, *Roseobacter* and *Bacteroidetes*, are often found to be affected strongly by grazing (Pernthaler 2005). This supports the hypothesis of a pre-bloom prior to the LOHAFEX experiment. Assuming that the waters of the eddy were in the state of an ending bloom, the bloom activated bacterial community should have been instantly exposed to high grazing pressure by nano- and picoplankton, following the law of Lotka-Volterra (Cleven and Weisse 2001; Berryman 2002). This grazer community was most likely at the maximum of the Lotka-Volterra cycle, when iron fertilization induced algal bloom increased bacterial nutrition. Therefore, the increased bacterial activity did not result in a net growth since the bacteria were top down controlled by grazers.

In a next step, we investigated the nano- and picoplankton community during the LOHAFEX experiment. We used samples taken for classical plankton investigations using light microscopy and applied molecular tools. The bloom was dominated by *Phaeocystis* cells (Manuscript II, Schulz et al Appendix II), but only *Micromonas* and *Pelagophyceae* showed an increase in numbers. The peak was of short duration and occurred shortly after the second iron fertilization at day 18. This implies that also on this trophic level, a strong top-down control was exerted by dinoflagellates or ciliate grazers. These grazers might again be top down controlled by copepods, which increased in abundance towards the end of the experiment (Assmy and Smetacek, pers. communication). A subsequent increase of amphipods (Assmy and Smetacek, pers. communication) indicated that grazing was also exerted on the copepod community.

The tight coupling of trophic levels including a pronounced microbial loop resulted in carbon cycling in the surface layer. Consequently, POC export rates measured during LOHAFEX did not significantly differ from those measured outside the fertilized patch (Martin et al. in prep.).

5.1.1. Assessment of molecular tools for nano- and picoplankton analyses

We used samples initially taken for light microscopic studies to assess the community structure and diversity during the iron fertilization experiment LOHAFEX. These samples were fixed with Lugol solution and stored for about 3 years before analyses. Still, we successfully applied CARD FISH to achieve a higher taxonomic resolution for the investigation of the community structure.

As stated in Manuscript II, the traditional way to investigate these organisms is size depended classification based on morphology as assessed by light microscopy (Utermöhl 1958). This provides only a low taxonomic resolution, since shape and size are often similar for many organisms. SEM and marker pigment analyses, which were used for the identification of nano- and picoplankton cells, are also not sufficient for a fast and reliable investigation of these organisms. While SEM provides high resolution pictures and thus might enable a taxonomic classification according to morphological features, it also is solely dependent on these features to identify mostly featureless organisms. The risk of underestimating the diversity due to cryptic species is evident. In addition, SEM is very time consuming and has a relatively low throughput.

Marker pigment analyses using HPLC in combination with identification based on the program CHEMTAX (Mackey et al. 1996) provide a high throughput, but again low taxonomic depth and reliability. Identical marker pigments are found in many phytoplankton clades, and levels of expression of marker pigments may differ. This reduces the accuracy of this method (Schlüter et al. 2000). Therefore, HPLC analyses should always be used in combination with microscopic methods (Irigoien et al. 2004). This shows that classical methods do not provide sufficient taxonomic resolution to investigate the nano- and picoplankton diversity and community structure on a higher taxonomic level.

In contrast to these techniques, molecular methods are widely used for the taxonomic classification of *Bacteria* and *Archaea* and provide taxonomic information independent of the cell morphology. Ribosomal RNA (rRNA) sequences are exceptionally good molecular markers. They, provide a stable framework for taxonomic investigations, due to the features of being ubiquitous in all species and having the same function, providing high information content and

being not affected by horizontal gene transfer (Woese and Fox 1977). In addition, this molecular marker also enables the detection of cryptic species (e.g. Bickford et al. 2007), which cannot be distinguished using classical tools. Methods using rRNA as a molecular marker have been used for the classification of nano- and picoplankton and the investigation of their community structure (Not et al. 2004; Massana et al. 2006).

Next generation sequencing techniques, like 454 tag pyrosequencing (Ronaghi et al. 1996), are now widely used in molecular studies to circumvent the predicament of lacking taxonomic information (Stoeck et al. 2010; Cheung et al. 2010). The resulting sequences allow for the analysis of the community composition, richness, and diversity with a higher resolution compared to other fingerprinting methods. Although 454 tag pyrosequencing provides an outstanding fingerprinting tool, it does not allow for quantitative analyses of community structures due to primer discrimination bias (Farris and Olson 2007) and possible multiple copy numbers of the SSU rRNA gene (Zhu et al. 2006).

Fluorescence *in situ* hybridization (FISH) based on 16S rRNA sequences (Amann et al. 1995) is widely used for the investigation of microorganisms in complex environmental samples. Fluorescently labeled oligonucleotide probes targeting the SSU rRNA of specific taxonomic groups combined with epifluorescence microscopy are used to investigate nano- and picoplankton communities (Beardsley et al. 2005; Massana et al. 2006). FISH based methods allow for the *in situ* quantification of the target groups, localization of the cells in complex samples, and, in comparison to light microscopic quantification, provide in depth information about the community composition.

All of the microscope based techniques are dependent on sample fixation. Thus, fixation is a crucial step for the preservation of cells, but could alter the total cell counts due to shrinkage and cell disruption caused by the fixative (Choi and Stoecker 1989). Since different fixation methods were used for different counting methods during the investigation of the LOHAFEX nano- and picoplankton community, an effect of the fixative on cell abundance could have resulted in differences in total cell counts.

Another explanation for lower cell counts after CARD FISH in comparison to light microscopy and flow cytometric counts might be the inclusion of a filtration step in the CARD FISH procedure. Small picoplankton cells might slip through filter pores, especially of polycarbonate filters, and thus alter the total cell counts (Cynar et al. 1985; Gasol and Morn 1999). However, FISH techniques allow *in situ* quantifications of different taxonomic groups of these

morphologically uniform organisms and make it a valuable tool for the investigation of the nano- and picoplankton community.

We were able to successfully apply molecular tools on these samples and could show that CARD FISH combined with 454 tag pyrosequencing is a valuable method to investigate the nano- and picoplankton community. Still, the “black box” of the nano- and picoplankton community is poorly understood and needs further investigation for the application, improvement and development of molecular tools.

5.2. The bacterial community on marine snow aggregates at different depth

Year round phytoplankton blooms with high primary production are known for the Canary Current Upwelling (Aristegui et al. 2009). Thus the area provides optimal conditions to investigate the bacterial community involved in aggregate degradation. As we could show, the dominant groups on marine snow aggregates are *Synechococcus*, *Bacteroidetes*, and *Alteromonas*, whereas *Alteromonas* was also found dominant on TEP structures (Manuscript III). This community was different to the community found in the free living fraction.

The abundance of *Bacteroidetes* and *Gammaproteobacteria* on marine snow aggregates was shown as early as 1993 (DeLong et al. 1993) and confirmed by more detailed studies very recently (Bizic-Ionescu, pers. communication). We were able to show on *in situ* sampled marine snow aggregates, that the community changes with depth. *Bacteroidetes* and *Alteromonas* decreased significantly from 100 m to 400 m depth. This change is possibly due to the change in nutrient quality on the marine snow aggregate, in conjunction with temperature decrease, pressure increase, and possible interactions with bacterial colonizers from the deeper water layers and protozoan grazing. However, the community structure on the TEP did not change, possibly due to the stable carbon compound quality in the TEP structures.

Since the major part of the aggregate degradation occurs in the upper few hundred meters of the water column, but varies across the global ocean (Martin et al. 1987; Buesseler et al. 2007; Iversen et al. 2010), our finding suggest a major role of *Alteromonas* and selected *Bacteroidetes*, like the members of the AGG 58 clade, found on marine snow by comparative rRNA sequence analysis (DeLong et al. 1993), for the degradation of POC. This would imply that these two bacterial groups are responsible for a major fraction of the release of DIC and DOC from the aggregates and hence counteract the biological carbon pump. Therefore, the role of these groups

in marine carbon cycling might have been underestimated and needs to be addressed in future research.

5.2.1. A novel approach to investigate bacterial communities on aggregates

Investigations of bacterial communities on aggregates are challenging due to the three dimensional structure of the aggregates, their fragility and the difficulties in sampling. In Manuscript III we provide a new approach to investigate the bacterial and archaeal community on aggregates. Using a drifting sediment trap with a viscous gel matrix in the collector cups, we were able to sample marine snow aggregates *in situ* without a need for “re-assembly” in roller tanks due to fragmentation of the fragile aggregates during Niskin bottle sampling. Analyses using the still intact 3D structure of the aggregate were not yet possible, since FISH investigations require a filtration step that leads to the destruction of the aggregates true 3D structure.

Marine snow aggregates on filters are still three dimensional and therefore difficult to assess. Bacterial cells or cell signals from the fluorescent staining in close vicinity may overlap, which proved to be a major challenge in bacterial cell number estimations on 3D objects, in particular marine snow aggregates. Furthermore, autofluorescence from the aggregate material may be strong and overshadow cells. So far, three approaches have been used to investigate marine snow aggregates directly, using (i) manual epifluorescence microscopy (Alldredge et al. 1986), (ii) automated z-stack acquisition using an epifluorescence microscope and subsequent 2D stack mapping in combination with automated cell counting (Bizic-Ionescu, pers. communication), and (iii) z-stack acquisition using confocal laser scanning microscopy (CLSM) and subsequent biovolume measurements (Manuscript III). Manual counting of bacterial cells is most prone to underestimations due to cell signal merging, due to the manually moved microscope stage, and due to the relatively weak discrimination possibilities between autofluorescence and cell signals. Automated image acquisition provides a good vertical resolution, but subsequent 2D image reconstruction only enhances signal overlapping and does not prevent autofluorescent masking of cells.

We used CLSM, which provides 3D information by taking pictures of overlapping confocal planes and subsequent 3D reconstruction. Therefore, underestimations from overlapping bacterial cells can be circumvented. CLSM scanning provides spatial resolution and allows, though still

limited due to the necessary filtration, 3D reconstruction of the aggregate. Another advantage of this technique is the precision of the excitation of the fluorescent dyes used in FISH techniques and the precise detection of the emitted light. Photomultipliers can be tuned to detect the emitted light in a range as narrow as 3 nm and thus autofluorescence of the organic material of the aggregate does not interfere with the positive FISH signal of the cell. This can be a problem in manual cell counting, since the organic material can have high background signals throughout the whole visible light spectrum, which increases the difficulties in FISH signal detection of all fluorochrome labels.

On the other hand, this CLSM technique inherits methodological problems. Due to the measurement of biovolumes and the subsequent calculations of cell numbers, the method provides no direct counts from the aggregates. Again, the close vicinity of the bacterial cells prevents direct counts, since suitable software to separate overlapping signals is not yet available. In addition, many steps of the calculation process introduce errors which add to the inaccuracy of the estimations. Autofluorescence of organic particles may be impossible to exclude and thus lead to overestimations of the cell numbers, as faced during the investigations of the TEP structure communities. However, the methods used in Manuscript III provide useful tools for the investigation of tree dimensional objects and are already widely applied in biological research other than marine snow aggregates (e.g. Solovei et al. 2002; Halary et al. 2008).

Additional to the proposal of a new method to investigate the bacterial community on aggregates, we assessed the changes of the community composition during incubation experiments in roller tanks. Bottle effects due to different physical, chemical and biological factors are well known during incubation experiments (Eilers et al. 2000). We investigated the change in the community composition during roller tank incubations and found a significant shift of the free living bacterial community towards higher abundances of *Alteromonas*. The strength of the bottle effect in roller tanks and the consequences for the bacterial abundances e.g. on TEP structures remains yet unknown, since findings of very small, invisible TEP structures with attached *Alteromonas* cells were found and may lead to an overestimation of the free living *Alteromonas* population (Simon et al. 2002). Although we did not investigate the attached fraction, this shift indicates that results from incubation experiments should be treated carefully.

5.3. Implications for the carbon pump

These findings imply that the microbial loop and consequently the carbon cycle in the surface layer are strong in nano- and picoplankton dominated blooms. A cascade of tight coupled trophic levels dominates these systems and carbon is transformed rapidly within this food web. Consequently, the carbon export rates and the efficiency of the biological carbon pump are low. Another factor counteracting the efficient sequestration of carbon to deeper water layers is the degradation of aggregates which mediate the carbon transfer.

This shows the pivotal role of microbial communities in marine carbon cycling and emphasises the need for further investigation of the microbial processes in carbon cycling. Profound knowledge of processes mediated by microorganisms may enable better prediction about carbon fluxes and subsequently would aid budgeting attempts, which are urgently needed to understand fluxes in global carbon cycling.

6. Outlook

6.1. Next generation iron fertilization

In the last two decades since IronEx I, iron fertilization experiments have become valuable tools to investigate the response of an ecosystem without laboratory artefacts. Still, the response of ecosystems to iron fertilization is not fully understood and future iron fertilization experiments still offer opportunities. Here I propose a new iron fertilization experiment to investigate the role of the microbial loop within artificially induced blooms and the role of the microbial community in the biological carbon pump.

The past experiments, especially LOHAFEX, have shown that careful experimental design is necessary to provide the environmental conditions needed to achieve the aims of the study. LOHAFEX aimed for a stable diatom bloom with high primary production and subsequent high POC export. Due to silicate limitation in the fertilized eddy, the bloom was dominated by nano- and picoplankton with lower net primary production and high carbon cycling in the surface layer. This shows that the choice of the right experimental area is of great importance. Optimally two water bodies, only differentiated by their different silicate concentrations, will be chosen, similar to the SOFEE experiment (Coale et al. 2004). This would provide suitable conditions to answer a broad range of questions.

The overall aim of such a new study would be to understand the ecosystem of induced phytoplankton blooms and elucidate the carbon fluxes within the bloom. The hypothesis that phytoplankton blooms can be induced by iron was verified and the type of induced bloom can be predicted based on nutrient concentrations. In case of diatom blooms, the bloom forming organism is relatively well studied. Nutrient, iron and chlorophyll *a* values have also been in the focus of investigations (deBaar et al. 2005; Peloquin et al. 2011b; Smetacek et al. 2012). Therefore, the major focus of a new study will be laid on processes within the biological carbon pump, in particular the microbial loop and POC formation, sinking and degradation. The main aims of the study are:

- Inducing 2 different phytoplankton blooms, one diatom bloom in silicate rich waters, one nano- and picoplankton bloom in silicate poor waters and monitor the blooms prior to fertilization, during the bloom phase and beyond the decay of the bloom.

Outlook

- Investigate the physicochemical setting of both blooms
- Investigate the ecosystem response on various biological levels
- Investigate the full microbial loop in a silicate limited bloom
- Investigate the biological processes related to aggregate degradation in the silicate rich bloom
- Investigate and compare the ecosystem response and carbon fluxes in both blooms

6.2. Experimental setting

From the three large HNLC areas, the Southern Ocean is the area of choice. Successful carbon export was shown for the North East Pacific (Tsuda et al. 2003) and the Southern Ocean (Smetacek et al. 2012). Along the Antarctic convergence, many eddies are formed in which suitable conditions can be found. Two eddies from water bodies of the Southern Ocean with similar physical, chemical (besides silicate concentrations) and biological parameters will be chosen for fertilization. One eddy contains sufficient silicate concentrations to support a stable diatom bloom, while the second eddy is silicate limited ($<2 \mu\text{M}$). Suitable stable eddies will be found using satellite based altimetry and monitored during the experiment using drifter buoys and salinity, temperature, depth, and acoustic current Doppler profiler measurements (Cisewski et al. 2008).

The fertilization experiment will be conducted in a long time frame. Since the initiation of a phytoplankton bloom was shown in every previous fertilization experiment (deBaar et al. 2005; Peloquin et al. 2011b; Smetacek et al. 2012), the ending of the bloom and the post bloom situation are the focus of this experiment. The monitoring of the fertilized areas during and after the decay of the bloom is important for the correct estimation of export rates. Particle sinking rates are dependent on sinking velocity and accurate measurements can only be done after the main export event of marine snow aggregates has stopped after the bloom. It was furthermore shown, that bacterial succession continues after the decay of a bloom (Teeling et al. 2012) and thus sampling needs to be done until a stable bacterial community is re-established.

After initial sampling, patches of the same size will be fertilized with the same amount of iron sulfate (including the tracer sulfur hexafluoride (SF_6)) in both eddies. The induced blooms will be monitored closely using Chlorophyll a concentrations, SF_6 tracer concentrations and photosynthetic efficiency index (F_v / F_m) measurements of the surface water with fast repetition

rate fluorometry (FRRF). Both fertilized patches will be followed and samplings will be done in short frequencies (ideally 2-3 days) including control stations outside the induced bloom but inside the eddy.

Within both fertilizations, the physicochemical parameters (temperature, salinity, pH, turbidity, wind velocity, and light intensity) will be measured. Nutrient profiles of the major nutrients (nitrate, nitrite, ammonia, sulfate, DIC/ DOC, phosphate, and silicate) will be done at each station. In addition, the iron concentration will be measured in the photic zone and profiles of the chlorophyll a concentration will be done at each station.

The pCO₂ concentration will be measured at several depths within the surface layer over the course of the experiment. After the decay of the induced bloom, buoys will be deployed to continue these measurements. The pCO₂ concentration is of interest, since the blooms would deplete the surface layer DIC pool, which is replenished by atmospheric CO₂. The gradient of the pCO₂ concentration in the surface layer will be used to calculate absorption of atmospheric CO₂ and gives a first estimation of the efficiency of the experiment in carbon uptake from the atmosphere. The long time frame of the measurements is necessary, since previous experiments have shown the slow replenishment of the pCO₂ pool from the atmosphere (deBaar et al. 2005).

6.2.1 The microbial loop in a nano- and picoplankton bloom

Within the silicate limited eddy, the creation of a phytoplankton bloom based on nano- and picophytoplankton, such as *Phaeocystis* spp., is expected. Within the bloom, a strong microbial loop will lead to enhanced carbon cycling in the surface layer and carbon sequestration rates will be minute (Martin et al. in prep.; Peloquin et al. 2011b; Manuscript I, II). Therefore, the aim of this study is the investigation of processes within the microbial loop, including the carbon fluxes. Experimental procedures will be outlined below.

- The main focus of this experiment is on the microbial loop. Within the loop, the nano- and picoplankton community is a key group for carbon fluxes. This group is still considered the “black box” in marine carbon cycling and therefore we lay the focus of the experiment on this group. We will monitor the nano- and picoplankton community closely over the course of the experiment, using flow cytometry, 454 tag pyrosequencing and FISH techniques for quantification, similar to investigations during the LOHAFEX

experiment (Manuscript II). Clone libraries will be done to support the tag sequencing results and can be used for further probe design for FISH investigations. We hypothesize a shift in the community towards one or few major autotrophic bloom formers and an increase of predatory species.

- In combination with the identification of the nano- and picoplankton community, the carbon fluxes of the major groups will be estimated using stable isotope probing for the autotrophic community. Since these autotrophs are expected to be the main bloom forming organisms, most of the solved atmospheric CO₂ will be incorporated in the biomass of this group. Measurements of respiration rates of the heterotrophic nano- and picoplankton community will be done to investigate the replenishment of the DIC pool by these organisms, while grazing rates will be estimated from ship board grazing experiments using stable isotope labelled bacterial cells and with subsequent mass spectrometer analyses, such as halogen *in situ* hybridization (HISH) in combination with nanoSIMS (Musat et al. 2008).
- Mixotrophy of nano- and picoplankton was recently found to be a major factor for nutrient cycling in oligotrophic waters (Zubkov and Tarran 2008). Therefore, investigations of these organisms using cultivation approaches after cell sorting using autofluorescence as a marker will be done. Subsequent grazing experiments could be used to identify major mixotrophs and stable isotope probing using ¹³CO₂, and bacterial prey labelled with either ¹³CO₂ or ¹³C acetate will be used to give first estimates of the carbon fluxes within this group.
- The bacterial and archaeal response to iron fertilization in low silicate water was rather sparse (Manuscript I). We hypothesize a similarly stable community structure and therefore, we use 454 tag pyrosequencing as an initial fingerprinting tool to follow the bacterial community over the course of the experiment. If a succession is indicated by the results of the tag sequencing, FISH techniques will be used for further quantification. Carbon uptake rates will be measured using stable isotope probing. Special focus will be laid on the photoheterotrophic bacteria, such as members of the *Roseobacter* clade, which may contribute significantly to DOC consumption and DIC production (Shiba 1991).
- Viruses can play major roles in the succession of the bacterial community in response to increasing nutrient availabilities, by “killing the winner” (Thingstad and Lignell 1997). This behaviour can lead to a fast decrease of a particular bacterial species after reaching a

specific population size and thus lead to succession patterns of the bacterial community. Hence the abundance of total viruses will be investigated using flow cytometry for virus enumeration (Stoffel et al. 2005), and the specificity of the infection will be investigated using the novel phageFISH technique (Allers et al. in press).

- Top predators within the microbial loop are dinoflagellates and ciliates. Due to the expected dominance of nano- and picoplankton, the community of autotrophic dinoflagellates can be expected minute (Peloquin et al. 2011b). In contrast, the community of dinoflagellates grazers and ciliates is expected to peak at the end of the bloom and it therefore interesting for the determination of carbon fluxes. These protozoa will be identified and quantified based on their morphology using light microscopy, 454 tag pyrosequencing and FISH techniques. Furthermore, stable isotope measurements will be applied as described above.
- The major focus of the study is on the microbial loop and higher levels of the classical food chain will be addressed only briefly. Zooplankton species, such as copepods and amphipods will be counted and the main species will be determined by microscopic investigations. The biomass will be calculated and used for estimations of the carbon flux which is channelled into the classic food chain from the microbial loop.
- The expected tight coupling of the microbial loop results in high carbon cycling and low export rates. Therefore, a quantification of the carbon fluxes from atmospheric CO₂ within the microbial loop would be of interest. To investigate this, cultures of the bloom forming autotroph are fed with ¹³C₂. After incorporation of the label into the biomass, the cultures are transferred in eukaryote free water and lysed in the presence of the bacterial and archaeal community. This bacterial and archaeal community incorporates the ¹³C labelled DOC and POC from the lysed phytoplankton cells, and is subsequently transferred into water containing the nano- and picoplankton community of the ambient water. The ¹³C enriched bacterial and archaeal cells are grazed and the stable isotope labelled biomass is transferred to the next higher trophic level. The nano- and picoplankton community is inoculated with the dinoflagellates and ciliate community and again grazing leads to a transfer of a fraction of the stable isotope to the next trophic level. Isotope uptake rates and isotope concentrations in the ambient DIC of the experiments are measured at all stages to estimate carbon fluxes through the microbial loop can be estimated.

6.2.2. Investigation of POC in a diatom bloom

Within the silicate rich eddy, we expect iron fertilization to create a diatom bloom, e.g. *Pseudo-nitzschia* spp. or *Fragilariopsis kerguelensis* (deBaar et al. 2005) and a weak carbon cycling with high POC export can be expected (Smetacek et al. 2012). However, former experiments not always showed high POC exports (deBaar et al. 2005), giving rise to the hypothesis of POC degradation during the sequestration process. Therefore, the aim of this study is the investigation of biological mineralization processes on aggregates, including the carbon fluxes during the sinking process. Experimental procedures will be outline below.

- Diatoms, as the main bloom forming and POC producing group, will be investigated using light microscopy, SEM and 454 tag pyrosequencing for species identification and quantification. If a substantial amount of cryptic species occurs, FISH techniques will be applied for quantification accordingly. Furthermore, the chemical composition of cells of the bloom forming organism will be investigated to deduce the complex chemical composition of the aggregates formed from these organisms. DOM released from the cells by cell lysis will be investigated using Fourier-transform ion cyclotron resonance mass spectrometer (FT-ICR-MS), which allows the investigation of single molecules within the complex mixture of DOM with ultra high resolution (e.g. D'Andrilli et al. 2010). Raman microscopy could be used to investigate the larger POM structures.
- Investigations of processes on aggregates need appropriate sampling techniques to achieve aggregates in the necessary conditions. Therefore we will use a broad array of sampling techniques. Drifting sediment traps with collector cups filled with viscous gel will be used for the examinations of the bacterial and nanoplankton community on the collected aggregates. This sampling technique enables the sampling of aggregates in their natural structure and can enable a 3D reconstruction of the aggregate and the spatial distribution of the attached living organisms. Unfortunately, no DNA extraction from these samples was possible so far, thus further method development is needed. Roller tank and flow chamber experiments will be used for the measurements of degradation rates, respiration rates, enzyme activity and bacterial colonization. Therefore, aggregates will be re-assembled from water sampled with standard Niskin bottle sampling. Although, a

bottle effect due to the incubation within the roller tanks might occur, re-assembly of aggregates is one of the few methods available to achieve living marine snow aggregates. Another method to achieve living aggregates is *in situ* sampling using a remote operated vehicle (ROV) to catch sinking aggregates in small incubation chambers. Since pressure may play a major role for the bacterial activity on aggregates, sampling and incubation devices ensuring ambient pressure will be used for experiment with living aggregates (Tamburini et al. 2002; Grossart and Gust 2009).

- The complex chemical composition of the achieved aggregates will be investigated as described for DOC/POC above. We hypothesise that due to the degradation during the sinking process, the composition of carbon compounds will change and the ratio of labile carbon to refractory carbon will decrease.
- The major parts of the aggregates are degraded in the first few hundred meters of the water column (Martin et al. 1987; Buesseler et al. 2007; Iversen et al. 2010), therefore the samplings will concentrate on this zone with additional samplings over the water column to close to the sea floor. This sampling strategy, with additional ^{234}Th measurements and $\text{O}_2:\text{Ar}$ based estimations of net community production as described by Martin and co-worker (Martin et al. in prep.), will allow for a good estimation of carbon fluxes during the sinking process and the efficiency of the biological carbon pump.
- *Bacteria*, most likely *Bacteroidetes* and *Gammaproteobacteria*, are the major POM degrader (reviewed in Simon et al. 2002). Therefore the changes of the bacterial community with increasing depth will be monitored using the methods described in Manuscript III. In addition, the major degrader will be identified by stable isotope probing. Therefore, the bloom forming organism will be cultivated and the culture will be incubated with $^{13}\text{CO}_2$. The resulting labelled biomass from the culture will be used to form aggregates in roller tanks with water including the ambient bacterial and archaeal community. After aggregate formation, aggregates and surrounding water will successively be sampled over several days. POM and DOM quality will be estimated as described above. Both, the attached and free living bacterial and archaeal community in the roller tanks will be monitored using CARD FISH and will be separated into labelled and unlabelled fraction using ultracentrifugation. The labelled fraction will be used for clone library construction to identify major carbon degrader. Although this experiment might be influenced by a bottle effect, still important information about main carbon

degrader could be achieved by combining the results with investigations of the community structure on *in situ* sampled aggregates. HISH and nanoSIMS analyses, as well as metagenomics, aiming for genes of carbon active enzymes, and proteomics for enzyme quantification, can further be used to determine uptake rates and potential carbon compounds used by the different organisms. In combination with active enzyme assays, the carbon recycling rate of the major POC degrader will be determined and linked to the identity of the organisms.

- Several iron fertilization experiments successfully induced diatom blooms and investigations of the phytoplankton communities were done (deBaar et al. 2005). Therefore, viruses, nano- and picoplankton, dinoflagellates and ciliates, as well as zooplankton, will be investigated only briefly, using flow cytometry, 454 tag pyrosequencing as fingerprinting tool and light microscopic counting for larger organisms (as described above). The identity of major groups or species will be identified and the total biomass will be calculated and compared.
- In contrast to the phytoplankton community, the bacterial and archaeal community was not investigated sufficiently and will be investigated following the approach described in Manuscript I. We hypothesize a succession similar to one found in coastal waters with major fluctuation within the *Gammaproteobacteria* and *Bacteroidetes* (Teeling et al. 2012). Therefore, we use not only broad oligonucleotide probes but also species or genus specific probes for important clades, like *Alteromonas* or *Polaribacter*. If a succession is found, additional investigation of the genetic potential will be done, to gain insights into the possible carbon cycling within the surface layer. This will be done using metagenomics and proteomics with a focus on the detection of genes for carbohydrate active enzymes.

6.3. Future perspectives in iron fertilization

The aim of the proposed study is to investigate processes in marine carbon cycling in a true Lagrangian experiment. Results from these experiments will shed light on the microbial loop in iron induced phytoplankton blooms, the main organisms responsible for carbon cycling in the loop, and their succession patterns during the bloom. This will lead to a better understanding of phytoplankton bloom dynamics and marine carbon cycling. Furthermore, investigations of the

main organisms involved in marine snow aggregate degradation will allow better predictions about carbon export rates into the deep sea. Both processes are important for the efficiency of the biological carbon pump. Thus, the results from the proposed study can be used for estimations of the efficiency of the biological carbon pump in iron fertilization experiments and their use in carbon sequestration. This is of particular interest, since iron fertilization is discussed as a mean of geoengineering to lower the atmospheric CO₂ concentration and to attenuate the effects of global warming by carbon sequestration in the deep sea (e.g. Lenton and Vaughan 2009). A high efficiency of the biological carbon pump with high carbon export rates was so far only found in silicate rich waters during the SEEDS and EIFEX experiments (Tsuda et al. 2003; Smetacek et al. 2012). Thus, only silicate rich waters which can support stable diatom blooms are suitable for carbon sequestration and measurements of silicate concentrations can not be done remotely. Therefore, industrial iron fertilization bears a high risk for companies due to possible low silicate concentrations and the resulting inefficiency of the biological carbon pump, like during the LOHAFEX experiment. Furthermore, the long term effects on the ecosystem are not investigated yet. Induction of vast phytoplankton blooms may favour certain species over other and lead to shifts in the ecosystem, e.g. towards toxic diatom species (Trick et al. 2010). This is particularly dangerous in HNLC areas close to coastal zones. Furthermore, the long term effect of the induced phytoplankton bloom on the underlying sea floor is uncertain. High carbon influx on the sediment might lead to high oxygen consumption and subsequently to anoxia with deleterious effects on the sea floor ecosystem. Therefore, iron fertilization provides a good opportunity to investigate phytoplankton blooms, and to achieve information to understand and model the global carbon cycle, but should not be used for industrial carbon sequestration to mitigate global warming.

7. References

- Acinas, S., J. Antón, and F. Rodríguez-Valera. 1999. Diversity of free-living and attached bacteria in offshore Western Mediterranean waters as depicted by analysis of genes encoding 16S rRNA. *Appl. Environ. Microbiol.* **65**: 514–522
- Agawin, N. S., C. M. Duarte, and S. Agustí. 2000. Nutrient and temperature control of the contribution of picoplankton to phytoplankton biomass and production. *Limnol. Oceanogr.* **45**: 591–600
- Alderkamp, A.-C., M. Van Rijssel, and H. Bolhuis. 2007. Characterization of marine bacteria and the activity of their enzyme systems involved in degradation of the algal storage glucan laminarin. *FEMS Microbiol. Ecol.* **59**: 108–117
- Allredge, A., J. Cole, and D. Caron. 1986. Production of heterotrophic bacteria inhabiting macroscopic organic aggregates (marine snow) from surface waters. *Limnol. Oceanogr.* **31**: 68–78
- Allredge, A. L., T. C. Granata, C. C. Gotschalk, and T. D. Dickey. 1990. The physical strength of marine snow and its implications for particle disaggregation in the ocean. *Limnol. Oceanogr.* **35**: 1415–1428
- Allredge, A. L., U. Passow, and B. E. Logan. 1993. The abundance and significance of a class of large, transparent organic particles in the ocean. *Deep-Sea Res. Pt. I* **40**: 1131–1140
- Allredge, A. L., and M. W. Silver. 1988. Characteristics, dynamics and significance of marine snow. *Prog. Oceanogr.* **20**: 41–82
- Allers, E., C. Moraru, M. B. Duhaime, E. Beneze, N. Solonenko, J. Barrero-Canosa, R. Amann, and M. B. Sullivan. in press. Single-cell and population level viral infection dynamics

References

- revealed by phageFISH, a method to visualize intracellular and free viruses. *Environ. Microbiol.*
- Amann, R. I., W. Ludwig, and K. H. Schleifer. 1995. Phylogenetic identification and in situ detection of individual microbial cells without cultivation. *Microbiol. Rev.* **59**: 143–169
- Anderson, D. M., A. D. Cembella, and G. M. Hallegraeff. 2012. Progress in understanding harmful algal blooms: paradigm shifts and new technologies for research, monitoring, and management. *Ann. Rev. Mar. Sci.* **4**: 143–176
- Andreae, M. O., and P. Merlet. 2001. Emission of trace gases and aerosols from biomass burning. *Global Biogeochem. Cy.* **15**: 955–966
- Aristegui, J., E. D. Barton, X. A. Álvarez-Salgado, A. M. P. Santos, F. G. Figueiras, S. Kifani, S. Hernández-León, E. Mason, E. Machú, and H. Demarcq. 2009. Sub-regional ecosystem variability in the Canary Current upwelling. *Prog. Oceanogr.* **83**: 33–48
- Aristegui, J., E. D. Barton, P. Tett, M. F. Montero, M. García-Muñoz, G. Basterretxea, A.-S. Cussatlegras, A. Ojeda, and D. de Armas. 2004. Variability in plankton community structure, metabolism, and vertical carbon fluxes along an upwelling filament (Cape Juby, NW Africa). *Prog. Oceanogr.* **62**: 95–113
- Armbrust, E. V., J. A. Berges, C. Bowler, B. R. Green, D. Martinez, N. H. Putnam, S. Zhou, A. E. Allen, K. E. Apt, M. Bechner, M. A. Brzezinski, B. K. Chaal, A. Chiovitti, A. K. Davis, M. S. Demarest, J. C. Detter, T. Glavina, D. Goodstein, M. Z. Hadi, U. Hellsten, M. Hildebrand, B. D. Jenkins, J. Jurka, V. V. Kapitonov, N. Kröger, W. W. Y. Lau, T. W. Lane, F. W. Larimer, J. C. Lippmeier, S. Lucas, M. Medina, A. Montsant, M. Obornik, M. S. Parker, B. Palenik, G. J. Pazour, P. M. Richardson, T. A. Rynearson, M. A. Saito, D. C. Schwartz, K. Thamatrakoln, K. Valentin, A. Vardi, F. P. Wilkerson, and D. S. Rokhsar.

2004. The genome of the diatom *Thalassiosira pseudonana*: ecology, evolution, and metabolism. *Science* **306**: 79–86
- Armstrong, R. A., C. Lee, J. I. Hedges, S. Honjo, and S. G. Wakeham. 2001. A new, mechanistic model for organic carbon fluxes in the ocean based on the quantitative association of POC with ballast minerals. *Deep-Sea Res. Pt. II* **49**: 219–236
- Arrieta, J. M., M. G. Weinbauer, C. Lute, and G. J. Herndl. 2004. Response of bacterioplankton to iron fertilization in the southern ocean. *Limnol. Oceanogr.* **49**: 799–808
- Artolozaga, I., E. Santamaría, A. López, B. Ayo, and J. Iriberrí. 1997. Succession of bacterivorous protists on laboratory-made marine snow. *J. Plankton Res.* **19**: 1429–1440
- Assmy, P., J. Henjes, C. Klaas, and V. Smetacek. 2007. Mechanisms determining species dominance in a phytoplankton bloom induced by the iron fertilization experiment EisenEx in the Southern Ocean. *Deep-Sea Res. Pt. I* **54**: 340–362
- Azam, F., T. Fenchel, J. Field, J. Gray, L. Meyer-Reil, and F. Thingstad. 1983. The ecological role of water-column microbes in the sea. *Mar. Ecol. Prog. Ser.* **10**: 257–263
- Azam, F., and F. Malfatti. 2007. Microbial structuring of marine ecosystems. *Nat. Rev. Microbiol.* **5**: 782–791
- Baldauf, S. L. 2008. An overview of the phylogeny and diversity of eukaryotes. *J. Syst. Evol.* **46**: 263–273
- Bauer, M., M. Kube, H. Teeling, M. Richter, T. Lombardot, E. Allers, C. A. Würdemann, C. Quast, H. Kuhl, F. Knaust, D. Woebken, K. Bischof, M. Mussmann, J. V. Choudhuri, F. Meyer, R. Reinhardt, R. I. Amann, and F. O. Glöckner. 2006. Whole genome analysis of the marine Bacteroidetes “*Gramella forsetii*” reveals adaptations to degradation of polymeric organic matter. *Environ. Microbiol.* **8**: 2201–2213

References

- Beardsley, C., K. Knittel, R. Amann, and J. Pernthaler. 2005. Quantification and distinction of aplastidic and plastidic marine nanoplankton by fluorescence in situ hybridization. *Aquat. Microb. Ecol.* **41**: 163–169
- Behrenfeld, M., and P. Falkowski. 1997. Photosynthetic rates derived from satellite-based chlorophyll concentration. *Limnol. Oceanogr.* **42**: 1–20
- Béjà, O., L. Aravind, E. V. Koonin, M. T. Suzuki, A. Hadd, L. P. Nguyen, S. B. Jovanovich, C. M. Gates, R. A. Feldman, J. L. Spudich, E. N. Spudich, and E. F. DeLong. 2000. Bacterial rhodopsin: evidence for a new type of phototrophy in the sea. *Science* **289**: 1902–1906
- Bekki, S., K. S. Law, and J. A. Pyle. 1994. Effect of ozone depletion on atmospheric CH₄ and CO concentrations. *Nature* **371**: 595–597
- Bergh, Ø., K. Y. Børsheim, G. Bratbak, and M. Heldal. 1989. High abundance of viruses found in aquatic environments. *Nature* **340**: 467–468
- Berglund, J., K. Jrgens, I. Bruchmller, M. Wedin, and A. Andersson. 2005. Use of group-specific PCR primers for identification of chrysophytes by denaturing gradient gel electrophoresis. *Aquat. Microb. Ecol.* **39**: 171–182
- Berryman, A. 2002. *Population cycles: the case for trophic interactions*, Oxford University Press.
- Bickford, D., D. J. Lohman, N. S. Sodhi, P. K. L. Ng, R. Meier, K. Winker, K. K. Ingram, and I. Das. 2007. Cryptic species as a window on diversity and conservation. *Trends Ecol. Evol.* **22**: 148–155
- Bochdansky, A. B., and G. J. Herndl. 1992. Ecology of amorphous aggregations (marine snow) in the Northern Adriatic Sea. III. *Mar. Ecol. Prog. Ser.* **87**: 135–146
- Böckelmann, U., W. Manz, T. R. Neu, and U. Szewzyk. 2000. Characterization of the microbial community of lotic organic aggregates (“river snow”) in the Elbe River of Germany by cultivation and molecular methods. *FEMS Microbiol. Ecol.* **33**: 157–170

- Boetius, A., S. Albrecht, K. Bakker, C. Bienhold, J. Felden, M. Fernández-Méndez, S. Hendricks, C. Katlein, C. Lalande, T. Krumpfen, M. Nicolaus, I. Peeken, B. Rabe, A. Rogacheva, E. Rybakova, R. Somavilla, and F. Wenzhöfer. 2013. Export of algal biomass from the melting arctic sea ice. *Science* **339**: 1430–1432
- Boyd, P., J. A. Berges, and P. J. Harrison. 1998. In vitro iron enrichment experiments at iron-rich and -poor sites in the NE subarctic Pacific. *J. Exp. Mar. Biol. Ecol.* **227**: 133–151
- Boyd, P. W., C. S. Law, C. S. Wong, Y. Nojiri, A. Tsuda, M. Levasseur, S. Takeda, R. Rivkin, P. J. Harrison, R. Strzepek, J. Gower, R. M. McKay, E. Abraham, M. Artychuk, J. Barwell-Clarke, W. Crawford, D. Crawford, M. Hale, K. Harada, K. Johnson, H. Kiyosawa, I. Kudo, A. Marchetti, W. Miller, J. Needoba, J. Nishioka, H. Ogawa, J. Page, M. Robert, H. Saito, A. Sastri, N. Sherry, T. Soutar, N. Sutherland, Y. Taira, F. Whitney, S.-K. E. Wong, and T. Yoshimura. 2004. The decline and fate of an iron-induced subarctic phytoplankton bloom. *Nature* **428**: 549–553
- Boyd, P. W., A. J. Watson, C. S. Law, E. R. Abraham, T. Trull, R. Murdoch, D. C. E. Bakker, A. R. Bowie, K. O. Buesseler, H. Chang, M. Charette, P. Croot, K. Downing, R. Frew, M. Gall, M. Hadfield, J. Hall, M. Harvey, G. Jameson, J. LaRoche, M. Liddicoat, R. Ling, M. T. Maldonado, R. M. McKay, S. Nodder, S. Pickmere, R. Pridmore, S. Rintoul, K. Safi, P. Sutton, R. Strzepek, K. Tanneberger, S. Turner, A. Waite, and J. Zeldis. 2000. A mesoscale phytoplankton bloom in the polar Southern Ocean stimulated by iron fertilization. *Nature* **407**: 695–702
- Broecker, W. S. 1997. Thermohaline circulation, the Achilles heel of our climate system: will man-made CO₂ upset the current balance? *Science* **278**: 1582–1588
- Bruland, K. W., E. L. Rue, and G. J. Smith. 2001. Iron and macronutrients in California coastal upwelling regimes: Implications for diatom blooms. *Limnol. Oceanogr.* **46**: 1661–1674

References

- Buesseler, K. O., J. E. Andrews, S. M. Pike, and M. A. Charette. 2004. The effects of iron fertilization on carbon sequestration in the Southern Ocean. *Science* **304**: 414–417
- Buesseler, K. O., C. H. Lamborg, P. W. Boyd, P. J. Lam, T. W. Trull, R. R. Bidigare, J. K. B. Bishop, K. L. Casciotti, F. Dehairs, M. Elskens, M. Honda, D. M. Karl, D. A. Siegel, M. W. Silver, D. K. Steinberg, J. Valdes, B. V. Mooy, and S. Wilson. 2007. Revisiting carbon flux through the ocean's twilight zone. *Science* **316**: 567–570
- Burkhardt, S., G. Amoroso, U. Riebesell, and D. Sultemeyer. 2001. CO₂ and HCO₃⁻ Uptake in marine diatoms acclimated to different CO₂ concentrations. *Limnol. Oceanogr.* **46**: 1378–1391
- Cambon-Bonavita, M.-A., G. Raguénès, J. Jean, P. Vincent, and J. Guezennec. 2002. A novel polymer produced by a bacterium isolated from a deep-sea hydrothermal vent polychaete annelid. *J. Appl. Microbiol.* **93**: 310–315
- Campbell, L., and D. Vault. 1993. Photosynthetic picoplankton community structure in the subtropical North Pacific Ocean near Hawaii (station ALOHA). *Deep-Sea Res. Pt. I* **40**: 2043–2060
- Carr, M.-E. 2001. Estimation of potential productivity in Eastern Boundary Currents using remote sensing. *Deep-Sea Res. Pt. II* **49**: 59–80
- Carr, M.-E., and E. J. Kearns. 2003. Production regimes in four Eastern Boundary Current systems. *Deep-Sea Res. Pt. II* **50**: 3199–3221
- Chavez, F. P., and R. T. Barber. 1987. An estimate of new production in the equatorial Pacific. *Deep-Sea Res. Pt. I* **34**: 1229–1243
- Chavez, F. P., K. R. Buck, S. K. Service, J. Newton, and R. T. Barber. 1996. Phytoplankton variability in the central and eastern tropical Pacific. *Deep-Sea Res. Pt. II* **43**: 835–870

- Chavez, F. P., and M. Messié. 2009. A comparison of Eastern Boundary Upwelling Ecosystems. *Prog. Oceanogr.* **83**: 80–96
- Cheung, M. K., C. H. Au, K. H. Chu, H. S. Kwan, and C. K. Wong. 2010. Composition and genetic diversity of picoeukaryotes in subtropical coastal waters as revealed by 454 pyrosequencing. *ISME J.* **4**: 1053–1059
- Chin, W.-C., M. V. Orellana, I. Quesada, and P. Verdugo. 2004. Secretion in unicellular marine phytoplankton: demonstration of regulated exocytosis in *Phaeocystis globosa*. *Plant Cell Physiol.* **45**: 535–542
- Chisholm, S. W., R. J. Olson, E. R. Zettler, R. Goericke, J. B. Waterbury, and N. A. Welschmeyer. 1988. A novel free-living prochlorophyte abundant in the oceanic euphotic zone. *Nature* **334**: 340–343
- Choi, J. W., and D. K. Stoecker. 1989. Effects of fixation on cell volume of marine planktonic protozoa. *Appl. Environ. Microbiol.* **55**: 1761–1765
- Christaki, U., S. Jacquet, J. R. Dolan, D. Vaultot, and F. Rassoulzadegan. 1999. Growth and grazing on *Prochlorococcus* and *Synechococcus* by two marine ciliates. *Limnol. Oceanogr.* **44**: 52–61
- Cisewski, B., V. H. Strass, M. Losch, and H. Prandke. 2008. Mixed layer analysis of a mesoscale eddy in the Antarctic Polar Front zone. *J. Geophys. Res.* **113**: C05017
- Cleven, E.-J., and T. Weisse. 2001. Seasonal succession and taxon-specific bacterial grazing rates of heterotrophic nanoflagellates in Lake Constance. *Aquat. Microb. Ecol.* **23**: 147–161
- Cloern, J. E. 1996. Phytoplankton bloom dynamics in coastal ecosystems: A review with some general lessons from sustained investigation of San Francisco Bay, California. *Rev. Geophys.* **34**: 127–168

References

- Coale, K. H., K. S. Johnson, F. P. Chavez, K. O. Buesseler, R. T. Barber, M. A. Brzezinski, W. P. Cochlan, F. J. Millero, P. G. Falkowski, J. E. Bauer, R. H. Wanninkhof, R. M. Kudela, M. A. Altabet, B. E. Hales, T. Takahashi, M. R. Landry, R. R. Bidigare, X. Wang, Z. Chase, P. G. Strutton, G. E. Friederich, M. Y. Gorbunov, V. P. Lance, A. K. Hilting, M. R. Hiscock, M. Demarest, W. T. Hiscock, K. F. Sullivan, S. J. Tanner, R. M. Gordon, C. N. Hunter, V. A. Elrod, S. E. Fitzwater, J. L. Jones, S. Tozzi, M. Koblizek, A. E. Roberts, J. Herndon, J. Brewster, N. Ladizinsky, G. Smith, D. Cooper, D. Timothy, S. L. Brown, K. E. Selph, C. C. Sheridan, B. S. Twining, and Z. I. Johnson. 2004. Southern Ocean iron enrichment experiment: Carbon cycling in high- and low-Si waters. *Science* **304**: 408–414
- Cochlan, W. P. 2001. The heterotrophic bacterial response during a mesoscale iron enrichment experiment (IronEx II) in the eastern Equatorial Pacific Ocean. *Limnol. Oceanogr.* **46**: 428–435
- Cottrell, M. T., and D. L. Kirchman. 2000. Natural assemblages of marine proteobacteria and members of the *Cytophaga-Flavobacter* cluster consuming low- and high-molecular-weight dissolved organic matter. *Appl. Environ. Microbiol.* **66**: 1692–1697
- Cox, P. M., R. A. Betts, C. D. Jones, S. A. Spall, and I. J. Totterdell. 2000. Acceleration of global warming due to carbon-cycle feedbacks in a coupled climate model. *Nature* **408**: 184–187
- Crump, B. C., E. V. Armbrust, and J. A. Baross. 1999. Phylogenetic analysis of particle-attached and free-living bacterial communities in the Columbia River, its estuary, and the adjacent coastal ocean. *Appl. Environ. Microbiol.* **65**: 3192–3204
- Cynar, F. J., K. W. Estep, and J. M. Sieburth. 1985. The detection and characterization of bacteria-sized protists in “protist-free” filtrates and their potential impact on experimental marine ecology. *Microbial Ecol.* **11**: 281–288

- D'Andrilli, J., T. Dittmar, B. P. Koch, J. M. Purcell, A. G. Marshall, and W. T. Cooper. 2010. Comprehensive characterization of marine dissolved organic matter by Fourier transform ion cyclotron resonance mass spectrometry with electrospray and atmospheric pressure photoionization. *Rapid Commun. Mass Spectrom.* **24**: 643–650
- deBaar, H. J. W., P. W. Boyd, K. H. Coale, M. R. Landry, A. Tsuda, P. Assmy, D. C. E. Bakker, Y. Bozec, R. T. Barber, M. A. Brzezinski, K. O. Buesseler, M. Boyé, P. L. Croot, F. Gervais, M. Y. Gorbunov, P. J. Harrison, W. T. Hiscock, P. Laan, C. Lancelot, C. S. Law, M. Levasseur, A. Marchetti, F. J. Millero, J. Nishioka, Y. Nojiri, T. van Oijen, U. Riebesell, M. J. A. Rijkenberg, H. Saito, S. Takeda, K. R. Timmermans, M. J. W. Veldhuis, A. M. Waite, and C.-S. Wong. 2005. Synthesis of iron fertilization experiments: From the iron age in the age of enlightenment. *J. Geophys. Res.* **110**: 1–24
- DeLong, E. F., D. G. Franks, and A. L. Alldredge. 1993. Phylogenetic diversity of aggregate-attached vs. free-living marine bacterial assemblages. *Limnol. Oceanogr.* **38**: 924–934
- DeVries, T., F. Primeau, and C. Deutsch. in press. The sequestration efficiency of the biological pump. *Geophys. Res. Lett.* **39**
- Dilling, L., and A. L. Alldredge. 2000. Fragmentation of marine snow by swimming macrozooplankton: A new process impacting carbon cycling in the sea. *Deep-Sea Res. Pt. I* **47**: 1227–1245
- Duce, R. A., and N. W. Tindale. 1991. Atmospheric transport of iron and its deposition in the ocean. *Limnol. Oceanogr.* **36**: 1715–1726
- Ducklow, H. W., and C. A. Carlson. 1992. Oceanic bacterial production. *Adv. Microb. Ecol.* **12**: 113–181
- Ducklow, H. W., D. K. Steinberg, and K. O. Buesseler. 2001. Upper ocean carbon export and the biological pump. *Oceanography* **14**: 50–58.

References

- Eilers, H., J. Pernthaler, and R. Amann. 2000. Succession of pelagic marine bacteria during enrichment: a close look at cultivation-induced shifts. *Appl. Environ. Microbiol.* **66**: 4634–4640.
- Eisma, D. 1993. *Suspended matter in the aquatic environment*, Springer-Verlag.
- Falkowski, P. G., R. T. Barber, and V. Smetacek. 1998. Biogeochemical controls and feedbacks on ocean primary production. *Science* **281**: 200–206
- Falkowski, P., R. J. Scholes, E. Boyle, J. Canadell, D. Canfield, J. Elser, N. Gruber, K. Hibbard, P. Högberg, S. Linder, F. T. Mackenzie, B. M. Iii, T. Pedersen, Y. Rosenthal, S. Seitzinger, V. Smetacek, and W. Steffen. 2000. The global carbon cycle: A test of our knowledge of earth as a system. *Science* **290**: 291–296
- Fandino, L. B., L. Riemann, G. F. Steward, R. A. Long, and F. Azam. 2001. Variations in bacterial community structure during a dinoflagellate bloom analyzed by DGGE and 16S rDNA sequencing. *Aquat. Microb. Ecol.* **23**: 119–130
- Farris, M. H., and J. B. Olson. 2007. Detection of *Actinobacteria* cultivated from environmental samples reveals bias in universal primers. *Lett. Appl. Microbiol.* **45**: 376–381
- Fenchel, T. 2008. The microbial loop – 25 years later. *J. Exp. Mar. Biol. Ecol.* **366**: 99–103
- Field, C. B., M. J. Behrenfeld, J. T. Randerson, and P. Falkowski. 1998. Primary production of the biosphere: integrating terrestrial and oceanic components. *Science* **281**: 237–240
- Figuères, G., J. M. Martin, and M. Meybeck. 1978. Iron behaviour in the Zaire estuary. *Neth. J. Sea Res.* **12**: 329–337
- Fischer, G., and G. Karakaş. 2009. Sinking rates and ballast composition of particles in the Atlantic Ocean: implications for the organic carbon fluxes to the deep ocean. *Biogeosciences* **6**: 85–102

- Fischer, G., C. Reuter, G. Karakas, N. Nowald, and G. Wefer. 2009. Offshore advection of particles within the Cape Blanc filament, Mauritania: Results from observational and modelling studies. *Prog. Oceanogr.* **83**: 322–330
- Flores, J.-A., E. Colmenero-Hidalgo, A. E. Mejía-Molina, K.-H. Baumann, J. Henderiks, K. Larsson, C. N. Prabhu, F. J. Sierro, and T. Rodrigues. 2010. Distribution of large *Emiliania huxleyi* in the Central and Northeast Atlantic as a tracer of surface ocean dynamics during the last 25,000 years. *Mar. Micropaleontol.* **76**: 53–66
- Forster, P., V. Ramaswamy, P. Artaxo, T. Berntsen, R. Betts, D. W. Fahey, J. Haywood, J. Lean, D. C. Lowe, G. Myhre, J. Nganga, R. Prinn, G. Raga, M. Schulz, R. van Dorland, G. Bodeker, O. Boucher, W. D. Collins, T. J. Conway, E. Dlugokencky, J. W. Elkins, D. Etheridge, P. Foukal, P. Fraser, M. Geller, F. Joos, C. D. Keeling, S. Kinne, K. Lassey, U. Lohmann, A. C. Manning, S. Montzka, D. Oram, K. O’Shaughnessy, S. Piper, G.-K. Plattner, M. Ponater, N. Ramankutty, G. Reid, D. Rind, K. Rosenlof, R. Sausen, D. Schwarzkopf, S. K. Solanki, G. Stenchikov, N. Stuber, T. Takemura, C. Textor, R. Wang, R. Weiss, and T. Whorf. 2007. Changes in atmospheric constituents and in radiative forcing, p. 131–234. *In* T. Nakajima and V. Ramanathan [eds.], *Climate Change 2007: The Physical Science Basis. Contribution of Working Group I to the 4th Assessment Report of the Intergovernmental Panel on Climate Change*. University Press, Cambridge (UK), New York (USA).
- Francois, R., S. Honjo, R. Krishfield, and S. Manganini. 2002. Factors controlling the flux of organic carbon to the bathypelagic zone of the ocean. *Global Biogeochem. Cy.* **16**: 1–20
- Frias-Lopez, J., A. Thompson, J. Waldbauer, and S. W. Chisholm. 2009. Use of stable isotope-labelled cells to identify active grazers of picocyanobacteria in ocean surface waters. *Environ. Microbiol.* **11**: 512–525

References

- Fuhrman, J. A., and F. Azam. 1980. Bacterioplankton secondary production estimates for coastal waters of British Columbia, Antarctica, and California. *Appl. Environ. Microbiol.* **39**: 1085–1095
- Furnas, M. J. 1990. In situ growth rates of marine phytoplankton: approaches to measurement, community and species growth rates. *J. Plankton Res.* **12**: 1117–1151
- Gall, M. P., P. W. Boyd, J. Hall, K. A. Safi, and H. Chang. 2001. Phytoplankton processes. Part 1: Community structure during the Southern Ocean Iron RElease Experiment (SOIREE). *Deep-Sea Res. Pt. II* **48**: 2551–2570
- Gärdes, A., M. H. Iversen, H.-P. Grossart, U. Passow, and M. S. Ullrich. 2011. Diatom-associated bacteria are required for aggregation of *Thalassiosira weissflogii*. *ISME J.* **5**: 436–445
- Gasol, J. M., and X. A. G. Morn. 1999. Effects of filtration on bacterial activity and picoplankton community structure as assessed by flow cytometry. *Aquat. Microb. Ecol.* **16**: 251–264
- Gattuso, J.-P., M. Frankignoulle, and R. Wollast. 1998. Carbon and carbonate metabolism in coastal aquatic ecosystems. *Annu. Rev. Ecol. Syst.* **29**: 405–434
- Gerlach, T. 2011. Volcanic versus anthropogenic carbon dioxide. *Eos* **92**: 201–202
- Gerlach, T. M. 1991. Present-day CO₂ emissions from volcanos. *Eos* **72**: 249–255
- Gerritsen, J., and S. W. Bradley. 1987. Electrophoretic mobility of natural particles and cultured organisms in freshwaters. *Limnol. Oceanogr.* **32**: 1049–1058
- Gibbs, R. J. 1983. Effect of natural organic coatings on the coagulation of particles. *Environ. Sci. Technol.* **17**: 237–40
- Del Giorgio, P. A., and C. M. Duarte. 2002. Respiration in the open ocean. *Nature* **420**: 379–384

- Glöckner, F. O., B. M. Fuchs, and R. Amann. 1999. Bacterioplankton compositions of lakes and oceans: a first comparison based on fluorescence in situ hybridization. *Appl. Environ. Microbiol.* **65**: 3721–3726
- Glover, H. E., B. B. Prézelin, L. Campbell, M. Campbell, and C. Garside. 1988. A nitrate-dependent *Synechococcus* bloom in surface Sargasso Sea water. *Nature* **331**: 161–163
- Goldthwait, S., J. Yen, J. Brown, and A. Alldredge. 2004. Quantification of marine snow fragmentation by swimming euphausiids. *Limnol. Oceanogr.* **49**: 940–952
- Gómez-Pereira, P. R., M. Schüler, B. M. Fuchs, C. Bennke, H. Teeling, J. Waldmann, M. Richter, V. Barbe, E. Bataille, F. O. Glöckner, and R. Amann. 2012. Genomic content of uncultured *Bacteroidetes* from contrasting oceanic provinces in the North Atlantic Ocean. *Environ. Microbiol.* **14**: 52–66
- Gram, L., H.-P. Grossart, A. Schlingloff, and T. Kiørboe. 2002. Possible quorum sensing in marine snow bacteria: production of acylated Homoserine Lactones by *Roseobacter* strains isolated from marine snow. *Appl. Environ. Microbiol.* **68**: 4111–4116
- Grossart, H.-P., and G. Gust. 2009. Hydrostatic pressure affects physiology and community structure of marine bacteria during settling to 4000 m: an experimental approach. *Mar. Ecol. Prog. Ser.* **390**: 97–104
- Grossart, H.-P., T. Kiørboe, K. Tang, and H. Ploug. 2003. Bacterial colonization of particles: growth and interactions. *Appl. Environ. Microbiol.* **69**: 3500–3509
- Grossart, H.-P., T. Kirboe, K. W. Tang, M. Allgaier, E. M. Yam, and H. Ploug. 2006. Interactions between marine snow and heterotrophic bacteria: aggregate formation and microbial dynamics. *Aquat. Microb. Ecol.* **42**: 19–26
- Grossart, H.-P., and H. Ploug. 2000. Bacterial production and growth efficiencies: Direct measurements on riverine aggregates. *Limnol. Oceanogr.* **45**: 436–445

References

- Grossart, H.-P., A. Schlingloff, M. Bernhard, M. Simon, and T. Brinkhoff. 2004. Antagonistic activity of bacteria isolated from organic aggregates of the German Wadden Sea. *FEMS Microbiol. Ecol.* **47**: 387–396
- Grossart, H.-P., and M. Simon. 1998. Bacterial colonization and microbial decomposition of limnic organic aggregates (lake snow). *Aquat. Microb. Ecol.* **15**: 127–140
- Halary, S., V. Riou, F. Gaill, T. Boudier, and S. Duperron. 2008. 3D FISH for the quantification of methane- and sulphur-oxidizing endosymbionts in bacteriocytes of the hydrothermal vent mussel *Bathymodiolus azoricus*. *ISME J.* **2**: 284–292
- Hall, J. A., and K. Safi. 2001. The impact of in situ Fe fertilisation on the microbial food web in the Southern Ocean. *Deep-Sea Res. Pt. II* **48**: 2591–2613
- Hallegraeff, G. M. 1993. A review of harmful algal blooms and their apparent global increase. *Phycologia* **32**: 79–99
- Hamm, C. 2002. Interactive aggregation and sedimentation of diatoms and clay-sized lithogenic material. *Limnol. Oceanogr.* **47**: 1790–1795
- Harvey, M. J., C. S. Law, M. J. Smith, J. A. Hall, E. R. Abraham, C. L. Stevens, M. G. Hadfield, D. T. Ho, B. Ward, S. D. Archer, J. M. Cainey, K. I. Currie, D. Devries, M. J. Ellwood, P. Hill, G. B. Jones, D. Katz, J. Kuparinen, B. Macaskill, W. Main, A. Marriner, J. McGregor, C. McNeil, P. J. Minnett, S. D. Nodder, J. Peloquin, S. Pickmere, M. H. Pinkerton, K. A. Safi, R. Thompson, M. Walkington, S. W. Wright, and L. A. Ziolkowski. 2011. The SOLAS air–sea gas exchange experiment (SAGE) 2004. *Deep-Sea Res. Pt. II* **58**: 753–763
- Heissenberger, A., G. G. Leppard, and G. J. Herndl. 1996. Ultrastructure of marine snow. II. Microbiological considerations. *Mar. Ecol. Prog. Ser.* **135**: 299–308

- Herndl, G. J., J. M. Arrieta, and K. Stoderegger. 1999. Interaction between specific hydrological and microbial activity leading to extensive mucilage formation in the northern Adriatic Sea. *Ann. Ist. Super. Sanita* **35**: 405–409
- Hirose, M., T. Katano, and S.-I. Nakano. 2008. Growth and grazing mortality rates of *Prochlorococcus*, *Synechococcus* and eukaryotic picophytoplankton in a bay of the Uwa Sea, Japan. *J. Plankton Res.* **30**: 241–250
- Houghton, R. A. 2003. Revised estimates of the annual net flux of carbon to the atmosphere from changes in land use and land management 1850–2000. *Tellus B* **55**: 378–390
- Irigoin, X., B. Meyer, R. Harris, and D. Harbour. 2004. Using HPLC pigment analysis to investigate phytoplankton taxonomy: the importance of knowing your species. *Helgoland Mar. Res.* **58**: 77–82
- Iversen, M. H., N. Nowald, H. Ploug, G. A. Jackson, and G. Fischer. 2010. High resolution profiles of vertical particulate organic matter export off Cape Blanc, Mauritania: Degradation processes and ballasting effects. *Deep-Sea Res. Pt. I* **57**: 771–784
- Iversen, M. H., and H. Ploug. 2010. Ballast minerals and the sinking carbon flux in the ocean: carbon-specific respiration rates and sinking velocities of macroscopic organic aggregates (marine snow). *Biogeosciences Discuss.* **7**: 3335–3364
- Iversen, M. H., and H. Ploug. 2013. Temperature effects on carbon-specific respiration rate and sinking velocity of diatom aggregates – potential implications for deep ocean export processes. *Biogeosciences Discuss.* **10**: 371–399
- Iversen, M. H., and L. K. Poulsen. 2007. Coprorhexy, coprophagy, and coprochaly in the copepods *Calanus helgolandicus*, *Pseudocalanus elongatus*, and *Oithona similis*. *Mar. Ecol. Prog. Ser.* **350**: 79–89

References

- Jackson, G. A. 1990. A model of the formation of marine algal flocs by physical coagulation processes. *Deep-Sea Res. Pt. I* 1197–1211
- Jannasch, H. W., B. D. Honeyman, and J. W. Murray. 1996. Marine scavenging: The relative importance of mass transfer and reaction rates. *Limnol. Oceanogr.* **41**: 82–88
- Jeffrey, S., and S. Wright. 2006. Photosynthetic pigments in marine microalgae: insights from cultures and the sea, p. 33–90. *In* D.V.S. Rao [ed.], *Algal cultures, Analogues of blooms and applications*. Science Publisher, Enfield (UK).
- Jickells, T. D., Z. S. An, K. K. Andersen, A. R. Baker, G. Bergametti, N. Brooks, J. J. Cao, P. W. Boyd, R. A. Duce, K. A. Hunter, H. Kawahata, N. Kubilay, J. laRoche, P. S. Liss, N. Mahowald, J. M. Prospero, A. J. Ridgwell, I. Tegen, and R. Torres. 2005. Global iron connections between desert dust, ocean biogeochemistry, and climate. *Science* **308**: 67–71
- Johnson, C. P., X. Li, and B. E. Logan. 1996. Settling velocities of fractal aggregates. *Environ. Sci. Technol.* **30**: 1911–1918
- Kepkay, P. E. 1994. Particle aggregation and the biological reactivity of colloids. *Mar. Ecol. Prog. Ser.* **109**: 293–293
- Kiene, R. P., L. J. Linn, and J. A. Bruton. 2000. New and important roles for DMSP in marine microbial communities. *J. Sea Res.* **43**: 209–224
- Kindler, K., A. Khalili, and R. Stocker. 2010. Diffusion-limited retention of porous particles at density interfaces. *Proc. Natl. Acad. Sci. USA* **107**: 22163–22168
- Kjørboe, T. 1993. Turbulence, phytoplankton cell size, and the structure of pelagic food webs, p. 1–72. *In* J.H.S. Blaxter and A.J. Southward [eds.], *Advances in Marine Biology*. Academic Press, Inc., London (UK).
- Kjørboe, T. 2000. Colonization of marine snow aggregates by invertebrate zooplankton: Abundance, scaling, and possible role. *Limnol. Oceanogr.* 479–484

- Kiørboe, T., H.-P. Grossart, H. Ploug, and K. Tang. 2002. Mechanisms and rates of bacterial colonization of sinking aggregates. *Appl. Environ. Microbiol.* **68**: 3996–4006
- Kiørboe, T., and G. A. Jackson. 2001. Marine snow, organic solute plumes, and optimal chemosensory behavior of bacteria. *Limnol. Oceanogr.* **46**: 1309–1318
- Kiørboe, T., K. Tang, H.-P. Grossart, and H. Ploug. 2003. Dynamics of microbial communities on marine snow aggregates: colonization, growth, detachment, and grazing mortality of attached bacteria. *Appl. Environ. Microbiol.* **69**: 3036–3047
- Kirchman, D. L., E. K'nees, and R. Hodson. 1985. Leucine incorporation and its potential as a measure of protein synthesis by bacteria in natural aquatic systems. *Appl. Environ. Microbiol.* **49**: 599–607
- Klaas, C., and D. E. Archer. 2002. Association of sinking organic matter with various types of mineral ballast in the deep sea: Implications for the rain ratio. *Global Biogeochem. Cy.* **16**: 1–14
- Klochko, V., L. Zelena, S. Ivoychuk, and A. Ostapchuk. 2012. Peculiarities of *Alteromonas macleodii* strains reflects their deep/surface habitation rather than geographical distribution. *J. Gen. Appl. Microbiol.* **58**: 129–135
- Knittel, K., and A. Boetius. 2009. Anaerobic oxidation of methane: progress with an unknown process. *Annu. Rev. Microbiol.* **63**: 311–334
- Lachkar, Z., and N. Gruber. 2011. A comparative study of biological production in eastern boundary upwelling systems using an artificial neural network. *Biogeosciences Discuss.* **8**: 9901–9941
- Lampitt, R. S., T. Noji, and B. von Bodungen. 1990. What happens to zooplankton faecal pellets? Implications for material flux. *Mar. Biol.* **104**: 15–23

References

- Lau, W. W. Y., R. G. Keil, and E. V. Armbrust. 2007. Succession and diel transcriptional response of the glycolate-utilizing component of the bacterial community during a spring phytoplankton bloom. *Appl. Environ. Microbiol.* **73**: 2440–2450
- Law, K. L., S. Morét-Ferguson, N. A. Maximenko, G. Proskurowski, E. E. Peacock, J. Hafner, and C. M. Reddy. 2010. Plastic accumulation in the North Atlantic subtropical gyre. *Science* **329**: 1185–1188
- Lenton, T. M., and N. E. Vaughan. 2009. The radiative forcing potential of different climate geoengineering options. *Atmos. Chem. Phys.* **9**: 5539–5561
- Long, R. A., and F. Azam. 2001. Antagonistic interactions among marine pelagic bacteria. *Appl. Environ. Microbiol.* **67**: 4975–4983
- Macintyre, S., A. L. Alldredge, and C. C. Gottschalk. 1995. Accumulation of marine snow at density discontinuities in the water column. *Limnol. Oceanogr.* **40**: 449–468
- Mackey, M., D. Mackey, H. Higgins, and S. Wright. 1996. CHEMTAX - a program for estimating class abundances from chemical markers: application to HPLC measurements of phytoplankton. *Mar. Ecol. Prog. Ser.* **144**: 265–283
- Marchetti, A., N. D. Sherry, H. Kiyosawa, A. Tsuda, and P. J. Harrison. 2006. Phytoplankton processes during a mesoscale iron enrichment in the NE subarctic Pacific: Part I - Biomass and assemblage. *Deep-Sea Res. Pt. II* **53**: 2095–2113
- Mari, X. 1999. Carbon content and C:N ratio of transparent exopolymeric particles (TEP) produced by bubbling exudates of diatoms. *Marine Ecology-Progress Series* **183**: 59–71
- Martin, J. H. 1990. Glacial-interglacial CO₂ change: The iron hypothesis. *Paleoceanography* **5**: 1–13
- Martin, J. H., K. H. Coale, K. S. Johnson, S. E. Fitzwater, R. M. Gordon, S. J. Tanner, C. N. Hunter, V. A. Elrod, J. L. Nowicki, T. L. Coley, R. T. Barber, S. Lindley, A. J. Watson, K.

- Van Scoy, C. S. Law, M. I. Liddicoat, R. Ling, T. Stanton, J. Stockel, C. Collins, A. Anderson, R. Bidigare, M. Ondrusek, M. Latasa, F. J. Millero, K. Lee, W. Yao, J. Z. Zhang, G. Friederich, C. Sakamoto, F. Chavez, K. Buck, Z. Kolber, R. Greene, P. Falkowski, S. W. Chisholm, F. Hoge, R. Swift, J. Yungel, S. Turner, P. Nightingale, A. Hatton, P. Liss, and N. W. Tindale. 1994. Testing the iron hypothesis in ecosystems of the equatorial Pacific Ocean. *Nature* **371**: 123–129
- Martin, J. H., G. A. Knauer, D. M. Karl, and W. W. Broenkow. 1987. VERTEX: carbon cycling in the northeast Pacific. *Deep-Sea Res. Pt. I* **34**: 267–285
- Martin, P., M. Rutgers v.d. Loeff, N. Cassar, P. Vandromme, F. d' Ovidio, R. Rengarajan, M. Soares, H. E. Gonzales, F. Ebersbach, R. S. Lampitt, R. Sanders, B. A. Barnett, V. S. Smetacek, and W. A. Naqvi. in prep. Net community production and downward particle export during the LOHAFEX artificial iron fertilization experiment.
- Marty, B., and I. N. Tolstikhin. 1998. CO₂ fluxes from mid-ocean ridges, arcs and plumes. *Chem. Geol.* **145**: 233–248
- Mary, I., D. G. Cummings, I. C. Biegala, P. H. Burkill, S. D. Archer, and M. V. Zubkov. 2006. Seasonal dynamics of bacterioplankton community structure at a coastal station in the western English Channel. *Aquat. Microb. Ecol.* **42**: 119–126
- Massana, R., R. Terrado, I. Forn, C. Lovejoy, and C. Pedrós-Alió. 2006. Distribution and abundance of uncultured heterotrophic flagellates in the world oceans. *Environ. Microbiol.* **8**: 1515–1522
- McCarren, J., J. W. Becker, D. J. Repeta, Y. Shi, C. R. Young, R. R. Malmstrom, S. W. Chisholm, and E. F. DeLong. 2010. Microbial community transcriptomes reveal microbes and metabolic pathways associated with dissolved organic matter turnover in the sea. *Proc. Natl. Acad. Sci. USA* **107**: 16420–16427

References

- Middelburg, J. J., and F. J. R. Meysman. 2007. Burial at sea. *Science* **316**: 1294–1295
- Moeseneder, M. M., C. Winter, and G. J. Herndl. 2001. Horizontal and vertical complexity of attached and free-living bacteria of the eastern Mediterranean Sea, determined by 16S rDNA and 16S rRNA fingerprints. *Limnol. Oceanogr.* **46**: 95–107
- Morris, R. M., M. S. Rappe, S. A. Connon, K. L. Vergin, W. A. Siebold, C. A. Carlson, and S. J. Giovannoni. 2002. SAR11 clade dominates ocean surface bacterioplankton communities. *Nature* **420**: 806–810
- Morrissey, J., and C. Bowler. 2012. Iron utilization in marine cyanobacteria and eukaryotic algae. *Front. Microbiol.* **3**: 1–13
- Mueller, L. N., J. F. C. de Brouwer, J. S. Almeida, L. J. Stal, and J. B. Xavier. 2006. Analysis of a marine phototrophic biofilm by confocal laser scanning microscopy using the new image quantification software PHLIP. *BMC Ecol.* **6**: 1
- Musat, N., H. Halm, B. Winterholler, P. Hoppe, S. Peduzzi, F. Hillion, F. Horreard, R. Amann, B. B. Jørgensen, and M. M. M. Kuypers. 2008. A single-cell view on the ecophysiology of anaerobic phototrophic bacteria. *Proc. Natl. Acad. Sci. USA* **105**: 17861–17866
- Nodder, S. D., and A. M. Waite. 2001. Is Southern Ocean organic carbon and biogenic silica export enhanced by iron-stimulated increases in biological production? Sediment trap results from SOIREE. *Deep-Sea Res. Pt. II* **48**: 2681–2701
- Not, F., M. Latasa, D. Marie, T. Cariou, D. Vaultot, and N. Simon. 2004. A single species, *Micromonas pusilla* (*Prasinophyceae*), dominates the eukaryotic picoplankton in the western English Channel. *Appl. Environ. Microbiol.* **70**: 4064–4072
- O’Kelly, C. J., M. E. Sieracki, E. C. Thier, and I. C. Hobson. 2003. A transient bloom of *Ostreococcus* (*Chlorophyta*, *Prasinophyceae*) in West Neck Bay, Long Island, New York. *J. Phycol.* **39**: 850–854

- Okada, H., and S. Honjo. 1973. The distribution of oceanic coccolithophorids in the Pacific. *Deep Sea Res. Oceanogr. Abstr.* **20**: 355–374
- Okada, H., and A. McIntyre. 1979. Seasonal distribution of modern coccolithophores in the western North Atlantic Ocean. *Mar. Biol.* **54**: 319–328
- Oliver, J. L., R. T. Barber, W. O. Smith, and H. W. Ducklow. 2004. The heterotrophic bacterial response during the Southern Ocean Iron Experiment (SOFeX). *Limnol. Oceanogr.* **49**: 2129–2140
- Olson, R. J., S. W. Chisholm, E. R. Zettler, and E. V. Armbrust. 1988. Analysis of *Synechococcus* pigment types in the sea using single and dual beam flow cytometry. *Deep-Sea Res. Pt. I* **35**: 425–440
- Olson, R. J., S. W. Chisholm, E. R. Zettler, and E. V. Armbrust. 1990. Pigments, size, and distributions of *Synechococcus* in the North Atlantic and Pacific Oceans. *Limnol. Oceanogr.* **35**: 45–58
- Partensky, F., W. R. Hess, and D. Vaultot. 1999. *Prochlorococcus*, a marine Photosynthetic prokaryote of global significance. *Microbiol. Mol. Biol. Rev.* **63**: 106–127
- Passow, U. 2000. Formation of transparent exopolymer particles, TEP, from dissolved precursor material. *Mar. Ecol. Prog. Ser.* **192**: 1–11
- Passow, U., and C. L. De La Rocha. 2006. Accumulation of mineral ballast on organic aggregates. *Global Biogeochemical Cycles* **20**: 1–7
- Peloquin, J., J. Hall, K. Safi, M. Ellwood, C. S. Law, K. Thompson, J. Kuparinen, M. Harvey, and S. Pickmere. 2011a. Control of the phytoplankton response during the SAGE experiment: A synthesis. *Deep-Sea Res. Pt. II* **58**: 824–838

References

- Peloquin, J., J. Hall, K. Safi, W. O. Smith Jr., S. Wright, and R. van den Enden. 2011b. The response of phytoplankton to iron enrichment in Sub-Antarctic HNLC waters: Results from the SAGE experiment. *Deep-Sea Res. Pt. II* **58**: 808–823
- Pernthaler, A., J. Pernthaler, and R. Amann. 2002. Fluorescence in situ hybridization and catalyzed reporter deposition for the identification of marine bacteria. *Appl. Environ. Microbiol.* **68**: 3094–3101
- Pernthaler, J. 2005. Predation on prokaryotes in the water column and its ecological implications. *Nat. Rev. Micro.* **3**: 537–546
- Pernthaler, J., A. Pernthaler, and R. Amann. 2003. Automated enumeration of groups of marine picoplankton after fluorescence in situ hybridization. *Appl. Environ. Microbiol.* **69**: 2631–2637
- Pinhassi, J., F. Azam, J. Hemphälä, R. A. Long, J. Martinez, U. L. Zweifel, and Å. Hagström. 1999. Coupling between bacterioplankton species composition, population dynamics, and organic matter degradation. *Aquat. Microb. Ecol.* **17**: 13–26
- Pinhassi, J., M. M. Sala, H. Havskum, F. Peters, Ò. Guadayol, A. Malits, and C. Marrasé. 2004. Changes in bacterioplankton composition under different phytoplankton regimens. *Appl. Environ. Microbiol.* **70**: 6753–6766
- Pizzetti, I., B. M. Fuchs, G. Gerdt, A. Wichels, K. H. Wiltshire, and R. Amann. 2011. Temporal Variability of Coastal Planctomycetes Clades at Kabeltonne Station, North Sea. *Appl. Environ. Microbiol.* **77**: 5009–5017
- Ploug, H., and H.-P. Grossart. 2000. Bacterial growth and grazing on diatom aggregates: Respiratory carbon turnover as a function of aggregate size and sinking velocity. *Limnol. Oceanogr.* **45**: 1467–1475

- Ploug, H., H.-P. Grossart, F. Azam, and B. B. Jørgensen. 1999. Photosynthesis, respiration, and carbon turnover in sinking marine snow from surface waters of Southern California Bight: implications for the carbon cycle in the ocean. *Mar. Ecol. Prog. Ser.* **179**: 1–11
- Ploug, H., S. Hietanen, and J. Kuparinen. 2002. Diffusion and advection within and around sinking, porous diatom aggregates. *Limnol. Oceanogr.* **47**: 1129–1136.
- Ploug, H., M. H. Iversen, and G. Fischer. 2008a. Ballast, sinking velocity, and apparent diffusivity within marine snow and zooplankton fecal pellets: Implications for substrate turnover by attached bacteria. *Limnol. Oceanogr.* **53**: 1878–1886
- Ploug, H., M. H. Iversen, M. Koski, and E. T. Buitenhuis. 2008b. Production, oxygen respiration rates, and sinking velocity of copepod fecal pellets: Direct measurements of ballasting by opal and calcite. *Limnol. Oceanogr.* **53**: 469–476
- Proctor, L. M., and J. A. Fuhrman. 1990. Viral mortality of marine bacteria and cyanobacteria. *Nature* **343**: 60–62
- Puddu, A., A. Zoppini, S. Fazi, M. Rosati, S. Amalfitano, and E. Magaletti. 2003. Bacterial uptake of DOM released from P-limited phytoplankton. *FEMS Microbiol. Ecol.* **46**: 257–268
- Raiswell, R., L. G. Benning, M. Tranter, and S. Tulaczyk. 2008. Bioavailable iron in the Southern Ocean: the significance of the iceberg conveyor belt. *Geochem. Trans.* **9**: 7
- Rath, J., K. Ying Wu, G. J. Herndl, and E. F. DeLong. 1998. High phylogenetic diversity in a marine-snow-associated bacterial assemblage. *Aquat. Microb. Ecol.* **14**: 261–269
- Raven, J. A., and P. G. Falkowski. 1999. Oceanic sinks for atmospheric CO₂. *Plant Cell Environ.* **22**: 741–755
- Reeburgh, W. S. 2007. Oceanic methane biogeochemistry. *Chem. Rev.* **107**: 486–513

References

- Riebesell, U. 1991. Particle aggregation during a diatom bloom. II. Biological aspects. *Mar. Ecol. Prog. Ser.* **69**: 281–291
- Riebesell, U. 1992. The formation of large marine snow and its sustained residence in surface waters. *Limnol. Oceanogr.* **37**: 63–76
- Riemann, L., G. F. Steward, and F. Azam. 2000. Dynamics of bacterial community composition and activity during a mesocosm diatom bloom. *Appl. Environ. Microbiol.* **66**: 578–587
- Rines, J. E. B., and E. C. Theriot. 2003. Systematics of *Chaetocerotaceae* (*Bacillariophyceae*). I. A phylogenetic analysis of the family. *Phycol. Res.* **51**: 83–98
- Rogerson, A., and J. Laybourn-Parry. 1992. Aggregate dwelling protozooplankton communities in estuaries. *Arch. Hydrobiol.* **125**: 411–422
- Ronaghi, M., S. Karamohamed, B. Pettersson, M. Uhlén, and P. Nyren. 1996. Real-Time DNA sequencing using Detection of pyrophosphate release. *Analyt. Biochem.* **242**: 84–89
- Rooney-Varga, J. N., M. W. Giewat, M. C. Savin, S. Sood, M. LeGresley, and J. L. Martin. 2005. Links between phytoplankton and bacterial community dynamics in a coastal marine environment. *Microb. Ecol.* **49**: 163–175
- Sage, R. F. 1995. Was low atmospheric CO₂ during the Pleistocene a limiting factor for the origin of agriculture? *Glob. Change Biol.* **1**: 93–106
- Sarmiento, J. L., and C. L. Quéré. 1996. Oceanic carbon dioxide uptake in a model of century-scale global warming. *Science* **274**: 1346–1350
- Scanlan, D. J. 2003. Physiological diversity and niche adaptation in marine *Synechococcus*. *Adv. Microb. Physiol.* **47**: 1–64.
- Schimel, D., D. Alves, I. Enting, M. Heimann, F. Joos, D. Raynaud, T. Wigley, and J. A. Lakeman. 1995. *Climate Change 1995 - The science of climate change; Contribution of*

- WGI to the Second Assessment Report of the Intergovernmental Panel on Climate Change, University Press, Cambridge (UK).
- Schlüter, L., F. Møhlenberg, H. Havskum, and S. Larsen. 2000. The use of phytoplankton pigments for identifying and quantifying phytoplankton groups in coastal areas: testing the influence of light and nutrients on pigment/chlorophyll a ratios. *Mar. Ecol. Prog. Ser.* **192**: 49–63
- Schoemann, V., S. Becquevort, J. Stefels, V. Rousseau, and C. Lancelot. 2005. *Phaeocystis* blooms in the global ocean and their controlling mechanisms: a review. *J. Sea Res.* **53**: 43–66
- Schweitzer, B., I. Huber, R. Amann, W. Ludwig, and M. Simon. 2001. *Alpha-* and *beta-Proteobacteria* control the consumption and release of amino acids on lake snow aggregates. *Appl. Environ. Microbiol.* **67**: 632–645
- Shanks, A. L., and E. W. Edmondson. 1989. Laboratory-made artificial marine snow: a biological model of the real thing. *Mar. Biol.* **101**: 463–470
- Shiba, T. 1991. *Roseobacter litoralis* gen. nov., sp. nov., and *Roseobacter denitrificans* sp. nov., aerobic pink-pigmented bacteria which contain bacteriochlorophyll a. *Syst. Appl. Microbiol.* **14**: 140–145
- Silver, M. W., S. L. Coale, C. H. Pilskaln, and D. R. Steinberg. 1998. Giant aggregates: Importance as microbial centers and agents of material flux in the mesopelagic zone. *Limnol. Oceanogr.* **43**: 498–507
- Simon, M., H.-P. Grossart, B. Schweitzer, and H. Ploug. 2002. Microbial ecology of organic aggregates in aquatic ecosystems. *Aquat. Microb. Ecol.* **28**: 175–211
- Smetacek, V., C. Klaas, V. H. Strass, P. Assmy, M. Montresor, B. Cisewski, N. Savoye, A. Webb, F. d' Ovidio, J. M. Arrieta, U. Bathmann, R. Bellerby, G. M. Berg, P. Croot, S. Gonzalez,

References

- J. Henjes, G. J. Herndl, L. J. Hoffmann, H. Leach, M. Losch, M. M. Mills, C. Neill, I. Peeken, R. Röttgers, O. Sachs, E. Sauter, M. M. Schmidt, J. Schwarz, A. Terbrüggen, and D. Wolf-Gladrow. 2012. Deep carbon export from a Southern Ocean iron-fertilized diatom bloom. *Nature* **487**: 313–319
- Smith, D. C., G. F. Steward, R. A. Long, and F. Azam. 1995. Bacterial mediation of carbon fluxes during a diatom bloom in a mesocosm. *Deep-Sea Res. Pt. II* **42**: 75–97
- Smith, K. L., B. H. Robison, J. J. Helly, R. S. Kaufmann, H. A. Ruhl, T. J. Shaw, B. S. Twining, and M. Vernet. 2007. Free-drifting icebergs: hot spots of chemical and biological enrichment in the Weddell Sea. *Science* **317**: 478–482
- Solovei, I., A. Cavallo, L. Schermelleh, F. Jaunin, C. Scasselati, D. Cmarko, C. Cremer, S. Fakan, and T. Cremer. 2002. Spatial preservation of nuclear chromatin architecture during three-dimensional fluorescence in situ hybridization (3D-FISH). *Exp. Cell Res.* **276**: 10–23
- Stoeck, T., D. Bass, M. Nebel, R. Christen, M. D. M. Jones, H.-W. Breiner, and T. A. Richards. 2010. Multiple marker parallel tag environmental DNA sequencing reveals a highly complex eukaryotic community in marine anoxic water. *Mol. Ecol.* **19**: 21–31
- Stoffel, C. L., R. F. Kathy, and K. L. Rowlen. 2005. Design and characterization of a compact dual channel virus counter. *Cytometry* **65A**: 140–147
- Suttle, C. A. 2005. Viruses in the sea. *Nature* **437**: 356–361
- Suttle, C. A., A. M. Chan, and M. T. Cottrell. 1990. Infection of phytoplankton by viruses and reduction of primary productivity. *Nature* **347**: 467–469
- Suzuki, K., A. Hinuma, H. Saito, H. Kiyosawa, H. Liu, T. Saino, and A. Tsuda. 2005. Responses of phytoplankton and heterotrophic bacteria in the northwest subarctic Pacific to in situ iron fertilization as estimated by HPLC pigment analysis and flow cytometry. *Prog. Oceanogr.* **64**: 167–187

- Suzuki, K., H. Saito, T. Isada, A. Hattori-Saito, H. Kiyosawa, J. Nishioka, R. M. L. McKay, A. Kuwata, and A. Tsuda. 2009. Community structure and photosynthetic physiology of phytoplankton in the northwest subarctic Pacific during an in situ iron fertilization experiment (SEEDS-II). *Deep-Sea Res. Pt. II* **56**: 2733–2744
- Takahashi, T., S. C. Sutherland, C. Sweeney, A. Poisson, N. Metzl, B. Tilbrook, N. Bates, R. Wanninkhof, R. A. Feely, C. Sabine, J. Olafsson, and Y. Nojiri. 2002. Global sea–air CO₂ flux based on climatological surface ocean pCO₂, and seasonal biological and temperature effects. *Deep-Sea Res. Pt. II* **49**: 1601–1622
- Tamburini, C., J. Garcin, M. Ragot, and A. Bianchi. 2002. Biopolymer hydrolysis and bacterial production under ambient hydrostatic pressure through a 2000m water column in the NW Mediterranean. *Deep-Sea Res. Pt. II* **49**: 2109–2123
- Tamburini, C., M. Goutx, C. Guigue, M. Garel, D. Lefèvre, B. Charrière, R. Sempéré, S. Pepa, M. L. Peterson, S. Wakeham, and C. Lee. 2009. Effects of hydrostatic pressure on microbial alteration of sinking fecal pellets. *Deep-Sea Res. Pt. II* **56**: 1533–1546
- Tang, K.-H., Y. J. Tang, and R. E. Blankenship. 2011. Carbon metabolic pathways in phototrophic bacteria and their broader evolutionary implications. *Front. Microbiol.* **2**: 1–23
- Taylor, F. J. R., M. Hoppenrath, and J. F. Saldarriaga. 2008. Dinoflagellate diversity and distribution. *Biodivers. Conserv.* **17**: 407–418
- Teeling, H., B. M. Fuchs, D. Becher, C. Klockow, A. Gardebrecht, C. M. Bennke, M. Kassabgy, S. Huang, A. J. Mann, J. Waldmann, M. Weber, A. Klindworth, A. Otto, J. Lange, J. Bernhardt, C. Reinsch, M. Hecker, J. Peplies, F. D. Bockelmann, U. Callies, G. Gerds, A. Wichels, K. H. Wiltshire, F. O. Glöckner, T. Schweder, and R. Amann. 2012. Substrate-

References

- controlled succession of marine bacterioplankton populations induced by a phytoplankton bloom. *Science* **336**: 608–611
- Thauer, R. K., A.-K. Kaster, H. Seedorf, W. Buckel, and R. Hedderich. 2008. Methanogenic archaea: ecologically relevant differences in energy conservation. *Nat. Rev. Microbiol.* **6**: 579–591
- Thingstad, T. F., and R. Lignell. 1997. Theoretical models for the control of bacterial growth rate, abundance, diversity and carbon demand. *Aquat. Microb. Ecol.* **13**: 19–27
- Trainer, V. L., S. S. Bates, N. Lundholm, A. E. Thessen, W. P. Cochlan, N. G. Adams, and C. G. Trick. 2012. *Pseudo-nitzschia* physiological ecology, phylogeny, toxicity, monitoring and impacts on ecosystem health. *Harmful Algae* **14**: 271–300
- Trick, C. G., B. D. Bill, W. P. Cochlan, M. L. Wells, V. L. Trainer, and L. D. Pickell. 2010. Iron enrichment stimulates toxic diatom production in high-nitrate, low-chlorophyll areas. *Proc. Natl. Acad. Sci. USA* **107**: 5887–5892
- Tsuda, A., H. Kiyosawa, A. Kuwata, M. Mochizuki, N. Shiga, H. Saito, S. Chiba, K. Imai, J. Nishioka, and T. Ono. 2005. Responses of diatoms to iron-enrichment (SEEDS) in the western subarctic Pacific, temporal and spatial comparisons. *Prog. Oceanograph.* **64**: 189–205
- Tsuda, A., S. Takeda, H. Saito, J. Nishioka, Y. Nojiri, I. Kudo, H. Kiyosawa, A. Shiimoto, K. Imai, T. Ono, A. Shimamoto, D. Tsumune, T. Yoshimura, T. Aono, A. Hinuma, M. Kinugasa, K. Suzuki, Y. Sohrin, Y. Noiri, H. Tani, Y. Deguchi, N. Tsurushima, H. Ogawa, K. Fukami, K. Kuma, and T. Saino. 2003. A mesoscale iron enrichment in the western subarctic Pacific induces a large centric diatom bloom. *Science* **300**: 958–961
- Tsuyoshi Fukao, K. K. 2012. Production of transparent exopolymer particles by four diatom species. *Fisheries Sci.* **76**: 755–760

- Turner, J. T. 2002. Zooplankton fecal pellets, marine snow and sinking phytoplankton blooms. *Aquat. Microb. Ecol.* **27**: 57–102
- Utermöhl, H. 1958. Zur Vervollkommnung der quantitativen Phytoplankton-Methodik. *Mitt. int. Ver. theor. angew. Limnol.* **9**: 1–38
- Vanucci, S., A. Dell’Anno, A. Pusceddu, M. Fabiano, R. S. Lampitt, and R. Danovaro. 2001. Microbial assemblages associated with sinking particles in the Porcupine Abyssal Plain (NE Atlantic Ocean). *Prog. Oceanogr.* **50**: 105–121
- Volk, T., and M. I. Hoffert. 1985. Ocean carbon pumps: Analysis of relative strengths and efficiencies in ocean-driven atmospheric CO₂ changes, p. 99–110. *In* E.T. Sundquist and W.S. Broecker [eds.], *Geophysical Monograph Series*, American Geophysical Union, Washington DC (USA).
- Vørs, N., K. R. Buck, F. P. Chavez, W. Eikrem, L. E. Hansen, J. B. Østergaard, and H. A. Thomsen. 1995. Nanoplankton of the equatorial Pacific with emphasis on the heterotrophic protists. *Deep-Sea Res. Pt. II* **42**: 585–602
- Waterbury, J. B., S. W. Watson, R. R. L. Guillard, and L. E. Brand. 1979. Widespread occurrence of a unicellular, marine, planktonic, cyanobacterium. *Nature* **277**: 293–294
- Van der Werf, G. R., J. T. Randerson, G. J. Collatz, L. Giglio, P. S. Kasibhatla, A. F. Arellano, S. C. Olsen, and E. S. Kasischke. 2004. Continental-scale partitioning of fire emissions during the 1997 to 2001 El Niño/La Niña period. *Science* **303**: 73–76
- West, N. J., I. Obernosterer, O. Zemb, and P. Lebaron. 2008. Major differences of bacterial diversity and activity inside and outside of a natural iron-fertilized phytoplankton bloom in the Southern Ocean. *Environ. Microbiol.* **10**: 738–756
- Wilhelm, S. W., and C. A. Suttle. 1999. Viruses and nutrient cycles in the sea. *Bioscience* **49**: 781–788

References

- Willey, J. M., and J. B. Waterbury. 1989. Chemotaxis toward Nitrogenous Compounds by Swimming Strains of Marine *Synechococcus* spp. *Appl. Environ. Microbiol.* **55**: 1888–1894
- Woese, C. R., and G. E. Fox. 1977. Phylogenetic structure of the prokaryotic domain: the primary kingdoms. *Proc. Natl. Acad. Sci. USA* **74**: 5088–5090
- Wolf, C., S. Frickenhaus, E. S. Kiliyas, M. Lunau, I. Peeken, and K. Metfies. in prep. Oceanographic fronts in the Southern Ocean determine biogeographic differences in eukaryotic protist communities – new insights based on 454-pyrosequencing.
- Wolf, C., S. Frickenhaus, E. S. Kiliyas, I. Peeken, and K. Metfies. in press. Regional variability in eukaryotic protist communities in the Amundsen Sea. *Antarctic Science*.
- Yoon, W., S. Kim, and K. Han. 2001. Morphology and sinking velocities of fecal pellets of copepod, molluscan, euphausiid, and salp taxa in the northeastern tropical Atlantic. *Mar. Biol.* **139**: 923–928
- Zhou, J., K. Mopper, and U. Passow. 1998. The role of surface-active carbohydrates in the formation of transparent exopolymer particles by bubble adsorption of seawater. *Limnol. Oceanogr.* **43**: 1860–1871
- Zhu, F., R. Massana, F. Not, D. Marie, and D. Vaultot. 2006. Mapping of picoeucaryotes in marine ecosystems with quantitative PCR of the 18S rRNA gene. *FEMS Microbiol. Ecol.* **52**: 79–92
- Zimmermann-Timm, H., H. Holst, and S. Müller. 1998. Seasonal dynamics of aggregates and their typical biocoenosis in the Elbe Estuary. *Estuaries* **21**: 613–621
- Zingone, A., M.-J. Chretiennot-Dinet, M. Lange, and L. Medlin. 1999. Morphological and genetic characterization of *Phaeocystis cordata* and *P. jahnii* (*Prymnesiophyceae*), two new species from the Mediterranean Sea. *J. Phycol.* 1322–1337

- Zubkov, M. V., B. M. Fuchs, S. D. Archer, R. P. Kiene, R. Amann, and P. H. Burkill. 2001. Linking the composition of bacterioplankton to rapid turnover of dissolved dimethylsulphoniopropionate in an algal bloom in the North Sea. *Environ. Microbiol.* **3**: 304–311
- Zubkov, M. V., and G. A. Tarran. 2008. High bacterivory by the smallest phytoplankton in the North Atlantic Ocean. *Nature* **455**: 224–226

Appendix

A. Identification of Microorganisms Using the Ribosomal RNA Approach and Fluorescence *In situ* Hybridization

Stefan Thiele, Bernhard M. Fuchs, Rudolf Amann

Published 2011 in Peter Wilderer (ed.) *Treatise on Water Science*, 3: 171–189, Academic Press, Oxford (UK).

The manuscript was written by S.T. with editorial assistance from B.M.F. and R.A.

B. Response of a flagellate dominated plankton community to artificial iron fertilization in the Southern Ocean

Isabelle Schulz, Philipp Assmy, Rajdeep Roy, Mangesh Gauns, Amit Sakar, **Stefan Thiele**, Christian Wolf, Sina Wolzenburg, Christine Klaas, Victor Smetacek

In preparation

Idea: I.S., P.A., M.G., C.K. and V.S.; Research designed by I.S., P.A., M.G., and V.S.; Sampling was done by P.A., C.K., R.R., M.G. and Bernhard M. Fuchs.; Experimental work was done by I.S., R.R., A.S., S.T., C.W., and S.W.; The manuscript was written by I.S. with editorial assistance from P.A., C.K. and V.S.

C. Controlling factors for the efficiency of the biological pump: the role of microbial degradation versus flux feeding on the export of particulate organic matter

Morten H. Iversen, **Stefan Thiele**, Andreas Basse, Nicolas Nowald, Marco Klann., Götz Ruland, George A. Jackson, Gerhard Fischer

In preparation

Idea: M.H.I. and G.F.; Research design by M.H.I.; sampling was done by M.H.I., S.T., A.B., N.N. and M.K.; Experimental work was done by M.H.I., N.N. and M.K.; Programming work was done by M.H.I. and G.A.J.; The manuscript was written by M.H.I. with editorial assistance from G.F.

Appendix A

Identification of Microorganisms Using the Ribosomal RNA Approach and Fluorescence *In situ* Hybridization

Stefan Thiele, Bernhard M. Fuchs, Rudolf Amann

Published 2011 in Peter Wilderer (ed.) *Treatise on Water Science*, 3: 171–189, Academic Press,
Oxford (UK).

The pdf-document of this publication is not displayed due to copyright reasons. The publication can be accessed at: <http://www.sciencedirect.com/science/article/pii/B9780444531995000567>; DOI: 10.1016/B978-0-444-53199-5.00056-7.

Appendix B

Response of a flagellate dominated plankton community to artificial iron fertilization in the Southern Ocean

Isabelle Schulz, Philipp Assmy, Rajdeep Roy, Mangesh Gauns, Amit Sakar, Stefan Thiele, Christian Wolf, Sina Wolzenburg, Christine Klaas, Victor Smetacek

Manuscript in preparation. Intended as article in *Deep-Sea Research Part II: Topical Studies in Oceanography*

Response of a flagellate dominated plankton community to artificial iron fertilization in the Southern Ocean

Isabelle Schulz^{1,2}, Philipp Assmy³, Rajdeep Roy⁴, Mangesh Gauns⁴, Amit Sakar⁴, Stefan Thiele⁶, Christian Wolf¹, Sina Wolzenburg¹, Christine Klaas¹, Victor Smetacek^{1,4,#}

¹ Alfred Wegener Institute Helmholtz Center for Polar and Marine Research, 27570 Bremerhaven, Germany,

² MARUM – Center for Marine Environmental Sciences, University of Bremen, Leobener Str., 28359 Bremen

³ Norwegian Polar Institute, Fram Centre, Hjalmar Johansens gt. 14, 9296 Tromsø, Norway

⁴ National Institute of Oceanography, Dona Paula-Goa, 403 004 India

⁵ Stazione Zoologica Anton Dohrn, Villa Comunale, 80121 Naples, Italy

⁶ Max Planck Institute for Marine Microbiology, Celsiusstr. 1, 28359 Bremen, Germany

Ocean iron fertilization (OIF) experiments carried out in the Southern Ocean (SO) have all induced phytoplankton blooms dominated by diatoms, because silicate required by diatoms was in sufficient supply. However, low silicate concentrations were measured in the northern half of the SO where a different response of non-diatom phytoplankton to OIF can be expected. The Indo-German OIF experiment LOHAFEX was carried out in the core of an oceanic eddy with extremely low silicic acid concentrations ($<2 \mu\text{M}$). The effect of iron input on the composition and abundance of the various components of the pelagic ecosystem, from bacteria to macrozooplankton, was monitored at regular intervals over 39 days inside and outside the fertilized patch using standard methods and state of the art molecular techniques. The phytoplankton community, characterized by various species of mixotrophic (auto- and phagotrophic) prymnesiophytes and prasinophytes, responded rapidly to the iron addition. Chlorophyll concentrations in the 60 m layer doubled to $1.5 \text{ mg Chl } a \text{ m}^{-3}$ within two weeks but stabilized thereafter, although rates of primary production remained high ($> 1.0 \text{ g C m}^{-2} \text{ d}^{-1}$). The composition of the fertilized plankton did not differ from outside water implying that iron input stimulated the entire community. Biomass of bacteria but also phyto- and protozooplankton was apparently stabilized by their grazers, phagotrophic nanoflagellates and copepods respectively. Trophic cascading effects channeled primary production to higher trophic levels and to the dissolved organic carbon pool. Grazing pressure of the copepod populations was similar to that prevailing in other experiments, indicating that diatoms are

able to accumulate biomass over many weeks because they are better protected against grazing than other phylogenetic lineages in the plankton.

Appendix C

Controlling factors for the efficiency of the biological pump: the role of microbial degradation versus flux feeding on the export of particulate organic matter

Morten H. Iversen, Stefan Thiele, Andreas Basse, Nicolas Nowald, Marco Klann., Götz Ruland,
George A. Jackson, Gerhard Fischer

Manuscript in preparation. Intended as article in *Deep-Sea Research Part II: Topical Studies in Oceanography*

Controlling factors for the efficiency of the biological pump: the role of microbial degradation versus flux feeding on the export of particulate organic matter

Iversen M. H.^{1,*}, Thiele S.², Basse A.^{1,3}, Nowald N.¹, Klann, M.¹, Ruland G.¹, Jackson G. A.⁴, Fischer G.¹

¹Faculty of Geosciences and MARUM, University of Bremen, Klagenfurter and Leobener Strasse, 28359 Bremen, Germany

²Max Planck Institute for Marine Microbiology, 28359 Bremen, Germany

³Alfred Wegener Institute for Polar and Marine Research, Am Handelshafen 12, 27570 Bremerhaven, Germany

⁴Department of Oceanography, Texas A&M University, College Station, Texas 77843

This study presents new findings of the relative vertical importance of microbes and flux feeders for POC flux attenuation. Using high resolution *in situ* imaging and deep-ocean sediment traps and free-drifting mesopelagic traps, carbon-specific degradation rates and *in situ* size-specific sinking speed of organic aggregates were calculated in different depth layers off Cape Blanc, Mauritania. Three depth layers with distinct degradation mechanisms of settling aggregates were identified; i) dominance of flux feeding during night in the upper 130 m, ii) dominance of microbial degradation between 130 and 250 m during night and in the upper 250 m during day, and iii) low microbial degradation at depths below 250 m. The low degradation rates below 250 m were comparable to previous measured degradation rates at 4 °C, suggesting temperature limitation on aggregate associated microbial activity in the deep ocean. The *in situ* carbon-specific degradation rates of settling aggregates within different depth layers presented here provide new quantitative support to the general observation that POC is efficiently removed in the upper mixed layer. Carbon preservation presumably prevails with depth since POC degradation decreases in the cold waters below the mixed layer, and it seems that flux feeders have little influence on carbon attenuation at these depths. Therefore, the magnitude of the flux attenuation depends on the residence time of aggregates within high degradation depth layers in the upper ocean, indicating aggregate sinking speed as a controlling factor for the efficiency of the biological pump.

Acknowledgement

Zuallererst möchte ich meiner Familie danken, die mich auf allen erdenklichen Wegen unterstützt und an mich geglaubt hat. Meinen Eltern Ilse und Heinrich Thiele, meinem Bruder Karsten, meinen Großeltern, meinen Onkeln, Tanten und meinen Cousins.

I would also like to thank Bernhard Fuchs, Morten Iversen and Rudolf Amann for the good cooperation, supervision, and for teaching me the way of science.

I thank Karlheinz Altendorf for believing in me and initially organizing my internship in the MPI Bremen.

I thank all the people in the Molecular Ecology department, in particular the plankton group.

All the collaborators in the LOHAFEX project, especially Victor Smetacek and Wajih Naqvi, the chief scientists.

I also thank the crews of the POS396 and MSM 18-1 cruises, especially the chief scientist Gerhard Fischer and my main collaborator Andreas Basse.

Cheers to all my friends, colleagues, co-workers and fellow MarMic students. You all made the MPI my home and the probably best working environment somebody could hope for. I cannot mention all your names, but you know who you are.

Last but not least I would like to thank all my friends outside the MPI who supported me and gave me the recreational room to withdraw from science from time to time.

Name: ...Stefan Thiele..... Ort, Datum:Bremen, den.....

Anschrift:....Friedrich-Ebert-Strasse 150, 28201 Bremen.....

ERKLÄRUNG

Hiermit erkläre ich, dass ich die Doktorarbeit mit dem Titel:

"The role of specific microbial communities in the biological carbon pump"

selbstständig verfasst und geschrieben habe und außer den angegebenen Quellen keine weiteren Hilfsmittel verwendet habe.

Ebenfalls erkläre ich hiermit, das es sich bei den von mir abgegebenen Arbeiten um 3 identische Exemplare handelt.

.....
(Unterschrift)